

**AEROMAGNETIC AND AIRBORNE RADIOMETRIC DATA INTERPRETATION  
ON CHIRANO AREA OF THE SEFWI GOLD BELT**

**BY**

**DESMOND APPIAH, BSC (HONS)**

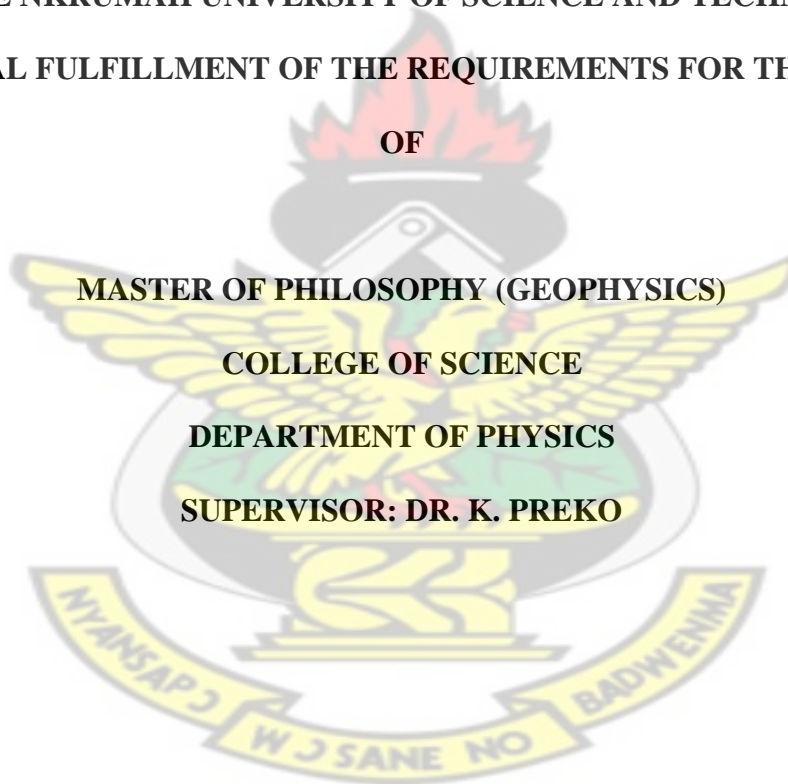
**A THESIS SUBMITTED TO THE DEPARTMENT OF PHYSICS,  
KWAME NKRUMAH UNIVERSITY OF SCIENCE AND TECHNOLOGY  
IN PARTIAL FULFILLMENT OF THE REQUIREMENTS FOR THE DEGREE  
OF**

**MASTER OF PHILOSOPHY (GEOPHYSICS)**

**COLLEGE OF SCIENCE**

**DEPARTMENT OF PHYSICS**

**SUPERVISOR: DR. K. PREKO**



**APRIL 2, 2015**

## DECLARATION

I hereby declare that this submission is my own work towards the MPhil and that, to the best of my knowledge, it contains no material previously published by another person or material that has been accepted for the award of any other degree of the University, except where due acknowledgement has been made in the text.

KNUST

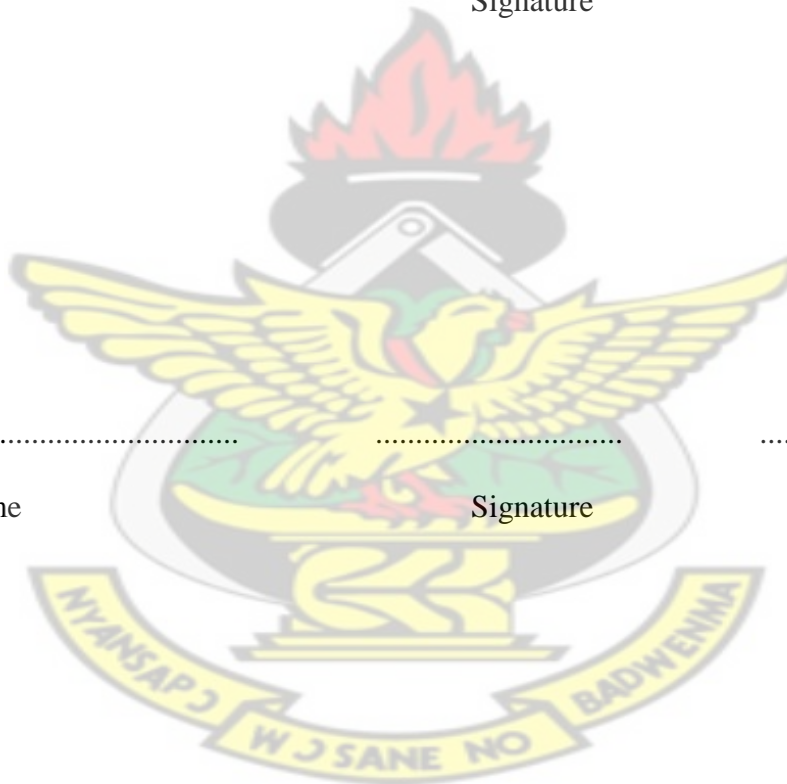
.....

Student Name  
(PG8045612)

Signature

Date

Certified by:



.....

Supervisor Name

Signature

Date

Certified by:

.....

Head of Dept. Name

Signature

Date

## ABSTRACT

The Chirano gold deposit is hosted in Paleoproterozoic rocks within the Sefwi Birimian metavolcanic belt which has been metamorphosed regionally to greenschist facies. Aeromagnetic and airborne radiometric datasets were used to examine the Chirano area. Very important information (lithology and geological features) were acquired from the datasets. These data (aeromagnetic and airborne radiometric) were enhanced to improve on the data quality to help locate the geological boundaries and features which may be of economical importance. First vertical derivative, analytic signal and reduction to the pole were some of the mathematical algorithms used in enhancing the magnetic data. These enhancements aided in locating the folds, fractures and faults which may entrap hydrothermal fluid (deposits). The Birimian metasedimentary and metavolcanic rocks which are eminent in hosting gold mineralization and other metal ores were mapped as well in the Belt. The values recorded from the radiometric survey gave the amount of the uranium (U), potassium (K) and thorium (Th) which were very useful in mapping the Birimian metavolcanics, metasediments, zones of extreme deformation (altered zones) found in the lithology and contact zones between the main geological formations (lithological boundaries). The metasediments and the Belt-type granitoid (B1) were delineated to have high K, Th and U. The high resolution airborne radiometric and magnetic datasets of the study area (Chirano) gave an improved description of the major rock sequences, lithological boundaries and geological structures. This research demonstrates the worth of sets of data from geophysical surveys in mapping the possible geological structures which control the mineralization of hydrothermal gold.

## ACKNOWLEDGMENT

I first thank Almighty God for His special guidance, knowledge and grace throughout this whole period of working on this project. I would like to thank my supervisor for this project Dr. Kwasi Preko (KNUST) earnestly for his useful discussions to improve this work. I am highly grateful to my co-supervisor Dr. D. D. Wemegah for his motivation, encouragement and criticism that has made this work a success. To Mr. Isaac Nkrumah (KNUST Physics Department), I say may God favor you for the encouragement and advice.

I thank all the lecturers who taught me through the geophysics programme and to all my course mates who shared their knowledge on this project especially Mr. Benjamin Boadi.

I am extremely indebted to Mr. Stephen Ahimah and family for all the support and encouragement, I say God bless you.

My final appreciations go to my parents Mr. and Mrs. Appiah for your various ways contributing to my education, Mr. Emmanuel Oppong Konadu, Selina Owusu and all my family members. I am very thankful for your support in all diverse ways. May God bless you all.

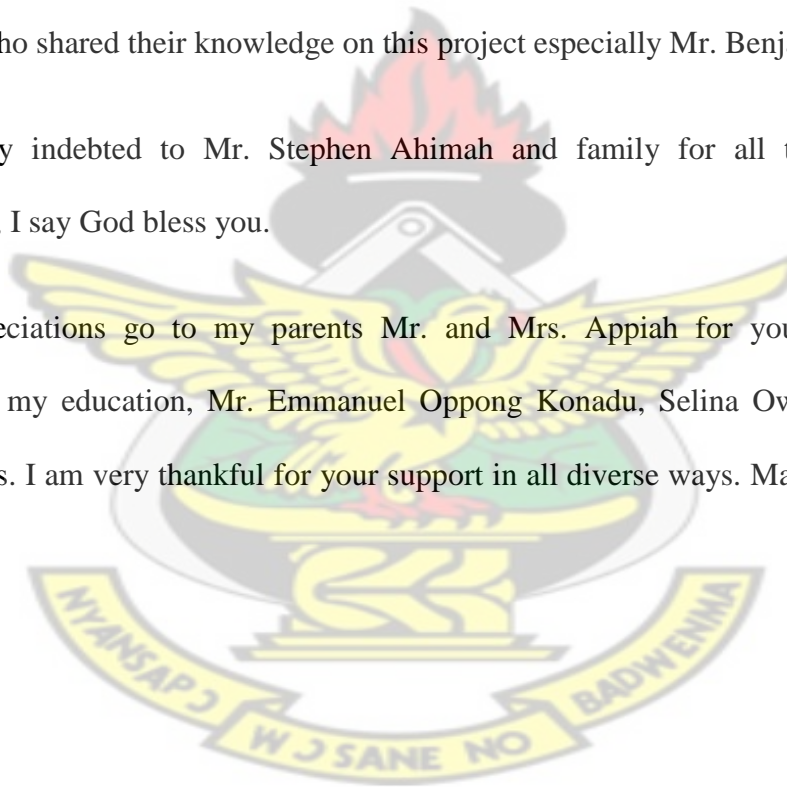


## TABLE OF CONTENTS

<b>DECLARATION</b> .....	<b>ii</b>
<b>ABSTRACT</b> .....	<b>iii</b>
<b>ACKNOWLEDGMENT</b> .....	<b>iv</b>
<b>TABLE OF CONTENTS</b> .....	<b>v</b>
<b>LIST OF TABLES</b> .....	<b>viii</b>
<b>LIST OF FIGURES</b> .....	<b>ix</b>
<b>LIST OF SYMBOLS AND ACRONYMS</b> .....	<b>x</b>
<b>CHAPTER ONE</b> .....	<b>11</b>
<b>INTRODUCTION</b> .....	<b>11</b>
1.1 Research Background .....	11
1.2 Literature Review.....	13
1.3 Problem Statement .....	16
1.4 Objectives of the Research.....	17
1.5 Justification of Objectives.....	18
1.6 Structure of Project .....	18
<b>CHAPTER TWO</b> .....	<b>20</b>
<b>GEOLOGICAL BACKGROUND</b> .....	<b>20</b>
2.1 Regional Geology .....	20
2.1.1 The Birimian System .....	22
2.1.2 Birimian Granitoids .....	23
2.1.3 The Tarkwaian System .....	24
2.2 Local geology.....	25
2.3 Mineralization .....	26
<b>CHAPTER THREE</b> .....	<b>28</b>
<b>THEORETICAL BACKGROUND</b> .....	<b>28</b>
3.1 Magnetism of the Earth.....	28
3.1.1 Nature of the Geomagnetic Field.....	28
3.1.2 The Earth's Magnetic Field .....	29
3.1.3 Maxwell's Equations .....	30
3.2 Magnetism of Rocks and Minerals .....	31
3.2.1 Magnetic Susceptibility .....	33
3.2.2 Remanent and Induced Magnetism.....	34

3.2.3 Magnetization at Low Magnetic Latitudes .....	35
3.3 Rock Alteration .....	36
3.4 Lithology, Structure and Magnetism .....	37
3.5 Enhancement Techniques .....	38
3.5.1 Fourier Transform Filter .....	39
3.5.2 Reduction to the Pole (RTP) .....	39
3.5.3 Analytic Signal.....	40
3.5.4 Vertical Derivative Filter .....	40
3.6 Principles of Radioactivity.....	40
3.6.1 Basic Radioactivity .....	40
3.6.2 Disequilibrium .....	42
3.6.3 Source-Detector Geometry .....	43
3.7 Measurement of Gamma Radiation .....	43
3.8 Mapping Natural Sources of Radiation.....	45
3.8.1 Geochemistry of Radioelements .....	45
3.8.1.1 Potassium .....	45
3.8.1.2 Thorium.....	46
3.8.1.3 Uranium .....	47
3.8.2 Distribution of the Radioelements in Rocks and Soils .....	47
3.8.3 Direct Detection of Mineralization .....	49
<b>CHAPTER FOUR.....</b>	<b>51</b>
<b>MATERIALS AND METHODS .....</b>	<b>51</b>
4.1 Project Site Description .....	51
4.1.1 Location and Accessibility.....	51
4.1.2 Physiography.....	52
4.1.3 Vegetation .....	53
4.1.4 Climatic Conditions and Occupation of Inhabitants .....	53
4.2 Data Acquisition .....	54
4.2.1 Data Specifications .....	55
4.3 Data Processing.....	56
4.4 Aeromagnetic Data .....	57
4.4.1 Reduction to the Pole (RTP) .....	58
4.4.2 First Vertical and Horizontal Derivatives .....	58
4.4.3 Analytic Signal Amplitude .....	59

4.5 Airborne Radiometric Data.....	59
4.5.1 Total Count (TC), Potassium (K), Thorium (Th) and Uranium (U) Channels .....	59
4.5.2 Composite Images and Ratio Maps .....	60
4.6 Interpretation of Airborne Geophysical Data .....	61
<b>CHAPTER FIVE .....</b>	<b>63</b>
<b>RESULTS AND DISCUSSIONS.....</b>	<b>63</b>
5.1 Interpretation of Magnetic Data.....	63
5.1.1 Total Magnetic Intensity (TMI) Image .....	64
5.1.2 Reduction to the Pole (RTP) Map.....	65
5.1.3 Analytic Signal Grid .....	67
5.1.4 Digitized Elevation Map (DEM) .....	68
5.1.5 First Vertical Derivative (1VD) Map.....	70
5.1.6 Tilted Magnetic Filtered (TDR) Map .....	71
5.1.7 Delineated Geological Structures .....	72
5.2 Interpretation of Radiometric Data .....	76
5.2.1 Potassium (K), Thorium (Th) and Uranium (U) Channels .....	77
5.2.2 Ratio Maps of K/U, K/Th and Th/U .....	80
5.2.3 Composite Images (Ternary map) .....	84
5.2.4 The Composite Lithological Map from the Radiometric Datasets .....	86
5.3 Relating Geophysical Datasets to Geology.....	89
5.3.1 Integrated Aeromagnetic and Airborne Radiometric Geological and structural map .....	89
5.3.2 Alteration .....	90
5.3.3 Possible Zones of Mineralization.....	92
<b>CHAPTER SIX .....</b>	<b>93</b>
<b>SUMMARY AND CONCLUSIONS .....</b>	<b>93</b>
6.1 Summary .....	93
6.2 Conclusions.....	93
<b>CHAPTER SEVEN.....</b>	<b>96</b>
<b>OUTLOOK AND RECOMMENDATIONS .....</b>	<b>96</b>
<b>REFERENCES.....</b>	<b>98</b>
<b>APPENDICES .....</b>	<b>109</b>

## LIST OF TABLES

Table 4.1: Airborne Geophysical Survey Equipment (Geological Survey of Ghana, 1998)...55

Table 4.2: Airborne Geophysical Survey Parameters (Geological Survey of Ghana, 1998) ..55

# KNUST



## LIST OF FIGURES

Figure 2.1: Geological map of Ghana with study area marked with black ink (modified after GSD, 1988). .....	22
Figure 2.2: Geological map of the Chirano area (Modified from Giffis et al., 2002) .....	26
Figure 3.1 Vector representation of the geomagnetic field at any place on the Northern Hemisphere (Whitham, 1960).....	30
Figure 3.2: Typical spectrum of the gamma radiations showing the individual peaks (IAEA, 2003). .....	44
Figure 4.1: Accessibility map of study area (Chirano) .....	52
Figure 5.1: TMI Map of the Study Area (Chirano Area).....	65
Figure 5.2: TMI reduced to the magnetic pole with $I = -14.80$ , $D = -5.10$ .....	66
Figure 5.3: Analytic Signal magnetic map .....	68
Figure 5.4: Digitized elevation map of the study area.....	69
Figure 5.5: First order vertical derivative map showing magnetic structures.....	70
Figure 5.6: A Magnetic TDR map in grayscale.....	72
Figure 5.7: Proposed geology map from aeromagnetic data. ....	76
Figure 5.9: Potassium (K) Concentration Map of the Radiometric Data .....	77
Figure 5.10: Thorium (Th) Concentration Map of the Radiometric Data .....	78
Figure 5.11: Uranium (U) Concentration Map of the Radiometric Data.....	80
Figure 5.12: A ratio map of thorium and potassium (K/Th).....	82
Figure 5.13: A ratio map of uranium and potassium (U/K).....	83
Figure 5.14: A ratio map of thorium and uranium (Th/U).....	84
Figure 5.15: Composite (Ternary) Image of the Chirano Area. ....	86
Figure 5.16: Proposed geology map from airborne radiometric data. ....	88
Figure 5.17: Proposed geological and structural map from the aeromagnetic and airborne radiometric data of the study area. ....	90

## LIST OF SYMBOLS AND ACRONYMS

K	Magnetic susceptibility
Fe	The Earth's magnetic field
Ze	Vertical component of the Earth's magnetic field
He	Horizontal component of the Earth's magnetic field
I	Angle of inclination
D	Angle of declination
M	Intensity of magnetization
H	Applied external field
Pi	c.g.s centi gram second
Jr	Remanent magnetization
Ji	Induced magnetization
Q	Königsberger's ratio
Nt	Number of atoms present at time t(s)
No	Number of atoms present at time t=0
$\lambda$	Decay constant
$T_{\frac{1}{2}}$	Half life
U	Uranium
Th	Thorium
K	Potassium

## CHAPTER ONE

### INTRODUCTION

#### 1.1 Research Background

Geophysics is a very potent and vital tool of exploration and consistently used in reconnaissance and surveys. There are a lot of geophysical survey methods which include gravity, magnetic, radiometric, seismic, electrical resistivity etc. Each of the above survey method has a unique operative physical property like density, magnetic susceptibility, radioactivity, propagation or velocity of seismic waves, electrical conductivity etc. of the Earth (Kearey et al., 2002). These methods have been used to investigate the subsurface geology of an area of interest. Some of these methods can still be applied by flying the geophysical equipment namely magnetic, electromagnetic, radiometric and gravity. Airborne geophysics is an effective way for surveying a very large area quickly for regional exploration.

Aeromagnetic survey is the frequent type of airborne geophysical survey and has been recognized as a principal mapping tool for materials that are strongly magnetized (Murthy, 2007). Magnetic method seeks to probe the geology of the particular area due to the differences in the geomagnetic field. These differences are as a result of the magnetic features of the rocks subsurface (Kearey et al., 2002). The most vital magnetic minerals in soils are the iron oxides, such as magnetite. In soils the main source of magnetic minerals is the parent material through the soil formation processes. A general practice to identify the existence and concentration of magnetic minerals is the amount of the magnetic susceptibility in soils. Soil magnetic susceptibility can be related to different terrain topographic attributes such as the slope, elevation and concavity-convexity of the surface terrain to explain the distribution of magnetic minerals within soils (Quijano et al., 2011)

Radiometric data are collected above the ground by flying an airplane with a spectrometer for regional surveys. Gamma rays arising from the decaying of unstable nuclei from the rocks are recorded in the radiometric survey. The entire noticeable gamma radiation from soil minerals occur from the natural breaking down of only three radioactive elements which are thorium, potassium and uranium. Similarly, the aeromagnetic technique is an effective way of identifying and delineating only magnetite rich minerals within the earth, so as the airborne radiometric technique is efficient in the identification of only the existence of Thorium (Th), Uranium (U) and Potassium (K) at the Earth's surface (Urquhart, 2003). Due to the depth of penetration which is only 30 cm, rocks beneath are inferred from the energies of Uranium, Thorium and Potassium released by the parent rock within a specified region.

Over the last few years, the search for radioactive minerals has turn out to be very important because recent need of nuclear energy fuels. Based on this reason, most of the equipments used for radiometric surveys were manufactured with uranium being the main focus until the new applications were found. Radiometric method is used in the mapping for radioactive mineral reserves needed for this purpose, and also for non-radioactive reserves related with radioactive elements. Radiometric method produces exceptional radioactive results in the mapping of the various kinds of geological formations (Kearey et al., 2002; Milsom, 2003).

With this work, the aeromagnetic and airborne radiometric datasets for Chirano were acquired from the Ghana Geological Survey, Accra which were collected in 1997. These datasets were processed and the resulting grids and images were interpreted. These grids and images were interpreted in relation to patterns in geology, and the patterns were deduced with regards to known or supposed relationships between rock types, structure, stratigraphic order and ore mineralisation. Again these patterns helped to delineate and outlined the local geological structures like the shear zones and faults.

## 1.2 Literature Review

Aeromagnetic and radiometric surveys are entrenched ways of bringing out signs of lithologic contrast, faults, folds, and concentrations of ore. The radiometric method has extensively been used in many fields. This method was initially used mainly for the exploration of uranium. Lately, it has been employed as a geological mapping tool in mineral exploration.

Anderson and Nash (1997) interpreted the mine area of Rössing and lower Khan Gorge region of Namibia using airborne geophysical data sets including radiometric and magnetic. The gridded magnetic concentration images and ternary maps from the radioactive elements helped to delineate the different rocks types. The early Palaeozoic alaskitic intrusions causing the fold trending NNE of the type was revealed in the gridded images from both datasets. These intrusions caused severe faults in the NNE direction which are capable of host uranium deposits in the Rössing mine area.

Appel et al. (2000) also reviewed that airborne magnetic datasets acquired by Geosurvey International during the 1970 to 1971 were interpreted to delineate gold mineralization zones in the Ubendian Mobile Belt in Tanzania. The entire landmarks of Tanzania and parts of Zanzibar offshore were surveyed with a nominal line spacing of 1000 m. The aircraft flew 120 m high above the Earth's surface using the Geometrics G803 precession magnetometer for recording the data with a grid spacing of 50 m. A residual magnetic map of 500 m by 500 m was produced using the minimum curvature algorithm.

Airo (2007) used both aeromagnetic and airborne radiometric datasets to delineate the structurally weak zones which have potentially been the pathways for Au-mineralising hydrothermal fluids in Finland around the central Lapland greenstone belt. A strong correlation was observed between potassic alteration of ultramafic rocks, K/Th ratios in

radiometric data and magnetic reduction. The characteristics pointed out are expected to be common to other similar greenstone belts in the world.

In many cases, radiometric survey is perhaps more helpful than every other lone aerogeophysical survey method in giving data which can be interpreted directly in terms of surface geology. Analyzing the potassium, thorium and uranium concentrations intended for delineating the lithology is founded on the finest assumption that different kinds of rocks are made up of different quantity of minerals forming the soil which include the definite radioactive elements contents (Darnley and Ford, 1989).

Integrated aeromagnetic, radiometric and gravity surveys have been extremely helpful in the delineation of numerous epithermal reserves in the Hauraki Goldfield that includes the Karangahake, Waitekauri, Komata, Golden Cross and Maratoto deposits. This was done by Harris et al. (2003). They demonstrated that aeromagnetic survey is appropriate to epithermal mapping since the inflow of hydrothermal fluids readily causes demagnetization. The epithermal deposits always mapped within 'magnetic quiet zones' when there is no post-mineralisation cover. These deposits are normally mapped a number of kilometres across.

The aeromagnetic method is especially potent for delineating epithermal reserves as most of them take place in the highly magnetised volcanic rocks, which have very distinct quiet zones. They also indicated that in the epithermal deposits the host rock is altered to form minerals which importantly raise the potassium concentration within the soil. The radiometric survey method is very useful mapping tool in the exploration of these epithermal deposits.

The soil and the overlying rock lessen the radiations of gamma so ratio maps are very useful for distinguishing the difference lithogological units. The ratio map of potassium to uranium or thorium is extensively useful in identifying regions of potassium enrichment than the potassium map alone. Again, these ratio maps help to identify the regions where uranium and

thorium contents are not strongly affected by alteration. Alteration zones with potassium concentration are mostly associated with mineralization of gold.

Recently, the cardinal resources limited led by Koimtsidis (2013) carried out geophysical surveys in Ghana for potential gold mineralisation zones. Aeromagnetic and airborne radiometric surveys were conducted particularly in the Bolgatanga which is located in NE Bole-Nangodi gold belt and Subranum found in the SW Sefwi gold belt.

At the end of the day here were their findings; the Bolgatanga Project

The results from the aeromagnetic and radiometric data correlate with the two surveys done early by Southern Geoscience which were sponsored by government. The aircraft was flown to an altitude of 400 m with line spacing of 800 m. Potential gold mineralisation zones were identified along the main NE-SW trending shear zones with structures totaling over 100 km striking through the Cardinal tenements.

- Subranum Project

Like the Bolgatanga Project, the aeromagnetic and radiometric results from Subranum Project also agree with the two surveys done early by sponsored by government. The data were recorded with line spacing of 400 m. Potential gold mineralisation targets were delineated along the contact zone trending in NE-SW direction.

Also in 2013, Boadi et al. used these same two methods (*i.e* aeromagnetic and airborne radiometric survey) to interpret the Konongo area which falls within Ashanti gold belt structurally and geologically. They concluded that the main geological structures controlling the gold mineralization within the area includes faults, fractures and shear zone.

### 1.3 Problem Statement

The magnetic field of the Earth is significantly affected by the magnetic minerals in the subsurface.

The magnetic susceptibility values are greatly influenced by the amount of magnetite in the various types of rocks. The highest susceptibilities are usually recorded among rocks which are made up of large amount of iron oxide. Basic and ultra-basic rocks, acid igneous and metamorphic rocks and sedimentary rocks have the highest, moderate and weak magnetic susceptibilities respectively (Reynolds, 1997). The different lithology units in the area is mainly associated with the different distributions in the concentration of the three radioelements uranium, potassium and thorium. Differences in the content of radioelements will possibly demonstrate most important geological procedures that include the processes of metamorphism or mineralizing solutions. Supergene alteration and leaching may also be depicted in secondary geological procedures due to differences in the content of radioelements. The occurrence of uranium and various intrusive associated mineral deposits are detectable in radiometric survey method (Urquhart 2003). Of the three radioactive elements, potassium is the most abundant in rock whereas the mobile uranium and immobile thorium are found in smaller concentration.

The acid content in soils enhances the potassium concentration of the soil also enhances with acidity (Elawadi et al., 2004). Younger felsic intrusive rocks are associated with higher concentration of uranium and thorium whereas mafic rocks lack uranium and thorium concentrations. Sedimentary rocks especially shales produce the highest amount of gamma rays equivalent to the energies of uranium and thorium. The acidity content in rocks greatly affects the concentrations of uranium and thorium.

The area under study is situated within the gold belt of Sefwi in Southwestern part of Ghana underlain by the Birimian Supergroups which comprises of the thick series of the metasediment basin alternating with the mafic metavolcanics formation. The contact zone between these main formations hosts the gold mineralization with the Southwestern Ghana. The problem this work tries to solve is to use the aeromagnetic and airborne radiometric data to interpret possible geological structures (fractures, faults, folds and shear zones) and to map the different lithologic units of the research area. Reimold et al. (2005) explained that traps like the lineaments, fold, faults etc help accumulate economical minerals like gold, bauxite etc. These economical minerals when mined play very important role in Ghana's economy and the world at large.

Geophysical surveys including radiometric and magnetic have been carried out in Ghana to discover different geological structures. The mining industry has contributed immensely to the economy of Ghana, mainly revenue (Aryee, 2000). Also, the mining industry has been a major source of employment especially to the indigenous people. It is however expected that with the current change in using more environmental friendly methods in the search of deposits, the industry would expand more to add up more revenue to the economy of the nation.

#### **1.4 Objectives of the Research**

The area under study is been mined actively for mainly gold. The main objectives are

- interpret the aeromagnetic and airborne radiometric datasets
- map the lithology and the rock types

The specific objectives are

- map the geology and geological structures of the study area
- identify hydrothermal zones with the study area
- identify mark of the known mineral deposits

### **1.5 Justification of Objectives**

Geological bodies can affect the geomagnetic field of a particular region of survey owing to the composition of magnetic mineral within the rock. These magnetic minerals which are mainly iron oxide have concentrations that differ in rocks; hence higher content will give rise to higher magnetic field intensity and vice versa. These magnetic anomalies possibly will come up from concentrated deposits of materials.

Subsurface materials can transform the simple pattern of the geomagnetic field into complex shapes (Grant and Martin, 1966). The study of these patterns can help interpret most of the magnetic geological bodies underground.

Radiometric survey is one of the best exploration tools in the investigation of epithermal deposits (Au, Au-Ag, Ag, Pb, Zn, Cu, Sn) since the deformation of the source rock to form deposits of minerals mostly elevate the rock potassium content (Allis, 1990). The area for the project satisfies this criteria since reserves of gold in the Chirano area in Southwestern Ghana are sourced along the chirano shear zone of the Sefwi belt. Mineralisation of gold within this district is controlled extremely by altered and sheared zones which paved way for the inflow of hydrothermal fluids (Kenworthy et al., 2009)

### **1.6 Structure of Project**

This project work has divided into seven chapters. Each chapter deals with a main heading. Chapter one introduces the whole project and explains the subject matter, bringing out the major objectives of the research work.

Chapter two outlines the geological settings of the study area. It examines both the regional and local geology of the study area.

Chapter three reviews the main theoretical background behind aeromagnetic and airborne radiometric method, taking into consideration some enhancement techniques applicable to magnetic and radiometric data.

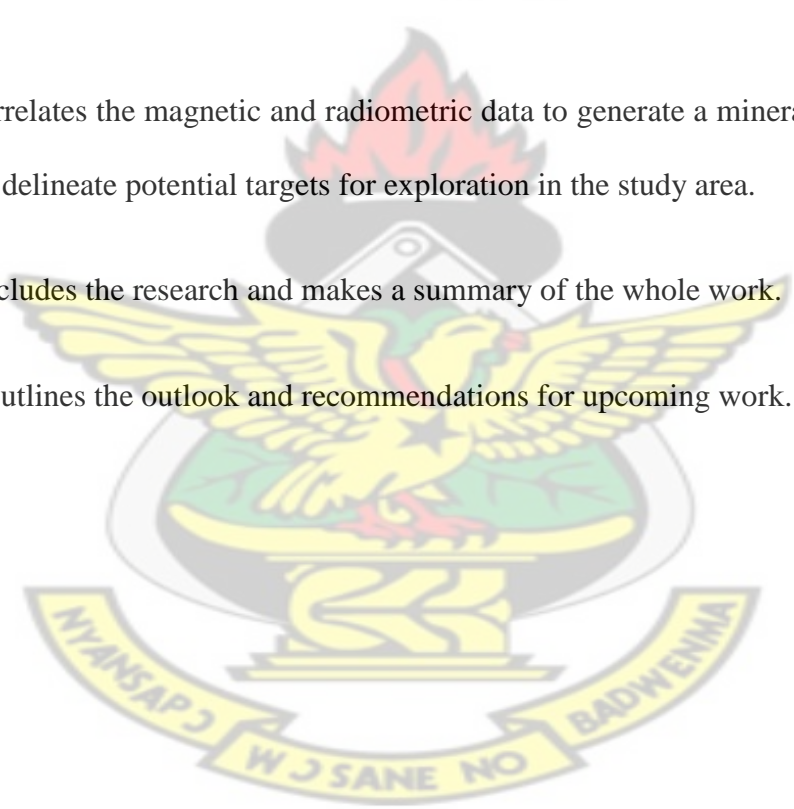
Chapter four deals with the methods used to obtain the data and some available software application for processing the datasets. This chapter also reviews the processing steps employed in the data processing.

Chapter five examines the resulting maps acquired from the radiometric and magnetic datasets.

This chapter correlates the magnetic and radiometric data to generate a mineral potential map that would help delineate potential targets for exploration in the study area.

Chapter six concludes the research and makes a summary of the whole work.

Chapter seven outlines the outlook and recommendations for upcoming work.



## CHAPTER TWO

### GEOLOGICAL BACKGROUND

The geology of the study area (Chirano area) which consists of lithological relationships, geological structures, metamorphism and also mineral potential of the area is analysed in this chapter. The significance of geology in this project should be highlighted. A complete investigation into the geology of Ghana can help locate unknown and possible geological structures of economic importance (Cozens, 1989).

#### 2.1 Regional Geology

The West African Craton which stabilised in the early Proterozoic (2000Ma) during the Eburnean Orogeny is where Ghana can be found. This orogeny also stabilised the Zaire Craton and affected vast parts of Western Africa and neighbouring regions in South America that were conterminous with the Eburnean tectonothermal province. The second largest craton in Africa is the West Africa where lower Proterozoic rocks are extensively preserved with South African craton being the first. These early Proterozoic rocks comprise extensive belts of metamorphosed volcanic and sedimentary rocks exposed in Ghana, Burkina Faso, Niger and Cote d'Ivoire. On the east and west, the Craton is bounded by late Proterozoic mobile belts (700 - 500 Ma) referred to as the Pan African mobile belts (Kesse, 1985; Wright, 1985; Leube et al., 1990).

Vast regions were faulted, metamorphosed and folded during the series of processes of tectonic activity owing to volcanic activities, erosion and sedimentary processes hosting the various belts of gold (Lunt et al., 1995). This gives a good idea of specific mineral and rock resources which are situated in Ghana. Ghana can be divided into several distinct terranes geologically,

- An early Proterozoic terrane (Birimian System) which hosts most of the country's mineral deposits and occupies the western and northernmost part of the country;
- The Tarkwaian System, a distinctive sequence of clastic sediments within the Ashanti, Bui, and Bole-Navrongo Belts
- The Voltaian Basin, in which are preserved the late Precambrian to Paleozoic sediments that mantle the craton
- The Dahomeyan System, occupying the easternmost part of Ghana
- A mobile pan-African belt, the formations of Togo and Buem, separated from the Birimian terrane by a prominent topographic feature known as the Akwapim -Togo range;
- Phanerozoic sedimentary rocks; and
- Intrusive rocks (Kesse, 1985).

Most parts of Ghana comprise mainly metavolcanic Paleoproterozoic Birimian series of rocks and the central west and northern parts are dominated by the clastic Tarkwaian. The eastern Ghana is covered with clastic shallow water sediments of the Neoproterozoic Volta Basin. Occurring along the coast and in the farthest southeastern Ghana is a narrow sequence of Paleozoic and Cretaceous to Tertiary sediments (Van Straaten, 2002). Modern geologists group gold deposits into two general categories (Dzigbodi-Adjimah and Bansah 1995).

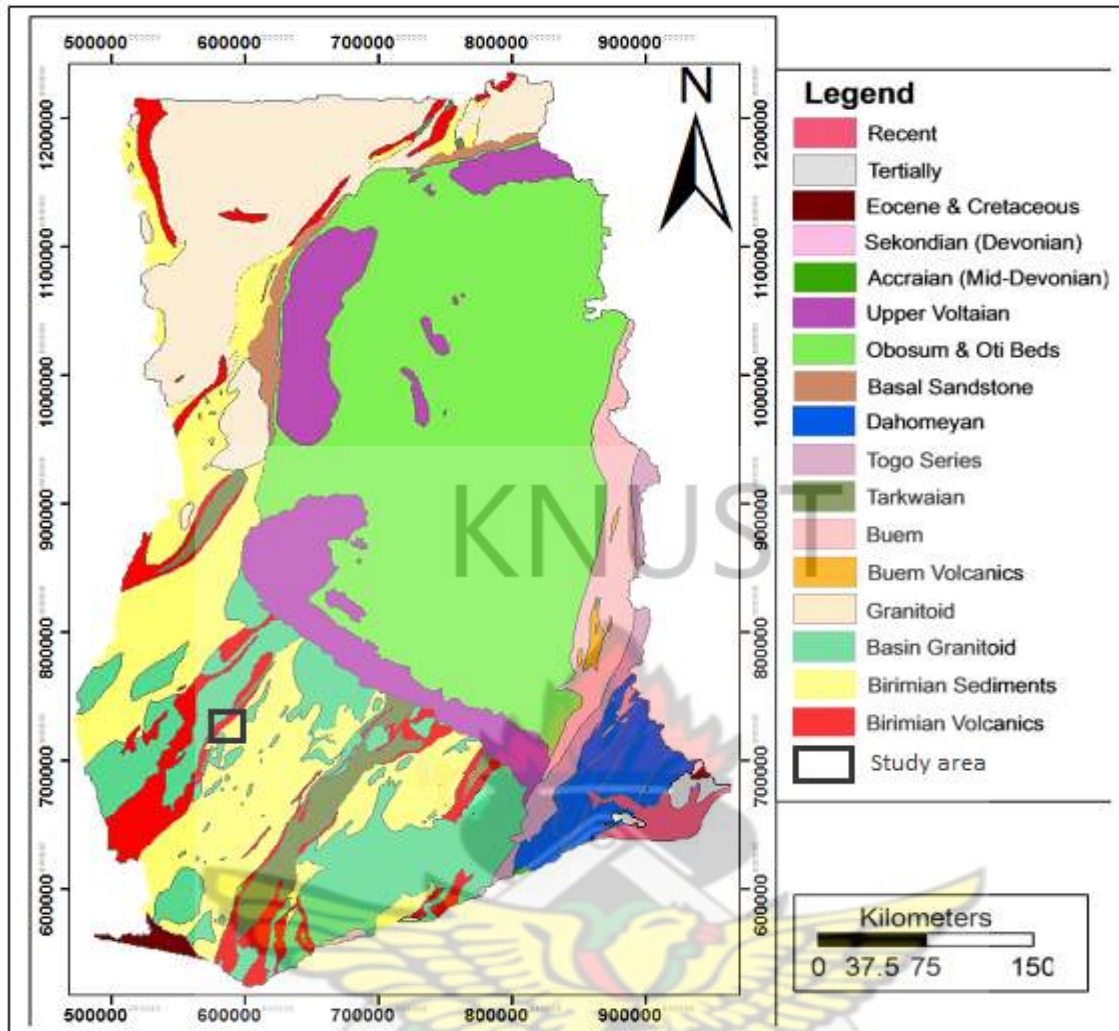


**Figure 2.1:** Geological map of Ghana with study area marked with black ink (modified after GSD, 1988).

### 2.1.1 The Birimian System

The Birimian was first defined by (Kitson, 1928) from outcrops of clastic and metavolcanic rocks in the Birim River valley of southern Ghana. Early Proterozoic Birimian rock series (2100 Ma) constitute the major geologic units in Ghana. They occupy the largest area of Ghana, and which belongs to the craton of West Africa that outcrops extensively in other parts of the subcontinent, including Cote d'Ivoire, Mali and Burkina Faso (Kesse, 1985).

The Birimian is separated into two major units and various granitoid intrusions. The first unit is the older lower unit. This unit comprises mainly sedimentary rocks which have undergone

metamorphism. The younger upper unit which is the second is composed of the volcanic rocks (Hammond, 1997).

The metasediments consist mainly of sediments that include greywackes, tuffaceous phyllites and graphitic schists where as the largely metavolcanics are metamorphosed lava that mainly consist mafic extrusive and intrusive rocks that include basaltic, andesitic and rhyolitic volcanic and tuffs with minor sedimentary intercalations. Both metasediments and metavolcanics are intruded by granites (Smith and Amanor, 2010; Cudjoe, 1961; Pohl, 1998). The metasediments was given a five-fold division of arenaceous and argillaceous units. The metavolcanics was divided into three main volcanic suites; this included an upper Basic Volcanic Sub-series, middle Acid Volcanic Sub-series and a lower Sedimentary-Volcanic Sub-series that included tuaceous greywackes, quartzite, conglomerates and grits (Griffis et al., 2002). The Birimian rock systems mass up about 80% of the most economic important geologic groups such as gold, sulphide mineralization and diamond deposits in Ghana. The northern and western parts of Ghana are mainly dominated by the Birimian supergroups (Kesse, 1985)

### **2.1.2 Birimian Granitoids**

Intrusive granitoids are grouped into two different kinds based on their types. These are the Belt Type granitoid and Basin Type granitoid. Belt type granitoids (ca. 2180 Ma) (Allibone et al., 2004) are metaluminous in nature which are usually tonalite to granodiorite and are limited to Birimian metavolcanic formations (Hirdes and Leube, 1989). These granodiorites are sometimes believed to have formed from gabbros by magmatic activities. This belt forms non-foliated bodies (Kesse, 1985)

The basin-type granitoid are mostly well separated into thin layers which are enriched usually with magmatic potash granitoids which appear in the shape of muscovite biotite granite and

granodiorite, porphyroblastic biotite gneiss, aplites and pegmatites (Kesse, 1985). These belts are described by the existence of many regions of schists and gneisses. Again they have a peraluminous character and higher K as compared to belt type granitoids, are principally granodiorite, and allied within the middle areas of Birimian metasedimentary basins (Hirdes and Leube, 1989).

### **2.1.3 The Tarkwaian System**

The Tarkwaian rock formations are mainly found around the south-western (Tarkwa area) part of Ghana. The coarse clastic debris resulting from the Birimian and granitoid source rocks mainly make up the Tarkwaian formation (Eisenlohr and Hirdes, 1992).

Pohl in 1998 also recognized all such clastic sequences in the Tarkwaian but made them intraformational within the Upper Birimian. Beneath the older Palaeoproterozoic mafic metavolcanics of the Birimian Supergroups are the Tarkwaian clastic fluvial sediments which is part of the West Africa Craton (Leube et al., 1990) interpret the Tarkwaian as fluvial intra-montane basins postdating the Birimian. It was proposed that the Tarkwaian represents a foreland thrust basin resulting from the collision of Birimian volcanic arcs (Pohl, 1998). The zones characterized by the contact between the Birimian and the Tarkwaian are severe deformations which control the most gold mineralization within the area. The Tarkwaian is associated with weaker strength of metamorphism and the high proportions of coarse-grained, younger sedimentary rocks. The widespread minerals found in the Tarkwaian system are chlorite, sericite, zoisite, calcite, quartz, limonite and chloritoid (Junner, 1940) and (Kesse, 1985).

Hirdes and Nunoo (1994) carried out much investigation in finding the age of the Tarkwa system. The system may range from 2096 to 2132 Ma. The age of deposition of the Tarkwa

group can be bracketed by the youngest zircon grain from the lowermost Kawere series and age of the authigenic rutile which formed after deposition.

## **2.2 Local geology**

An Australian company called the Red Back Mining NL which moved to Canada in April 2004, first explored and developed Chirano in 1998. The Chirano concession is centred about 90km in a southwestern direction of Kumasi. The different structural settings along the intensely deformed zone with Paleoproterozoic rocks of the Sefwi belt controls the gold deposits in Chirano (Kenworthy et al., 2009).

The Chirano concession is situated by the side of the mid Sefwi metavolcanic formation. It is estimated to be about 20 km of strike-length of the severely altered zone caused by the contact between the Sefwi metavolcanics and the neighboring Kumasi metasediments and intermediate granitoid batholiths to the east. The western part of the Chirano forms the greater part of the Bibiani Range which is mainly composed of thick series of the mafic metavolcanics and the eastern low lying areas are the metasediments principally composed of argillaceous and volcanoclastic facies (Griffis et al., 2002).

A narrow sliver of Tarkwaian sedimentary rocks divide the Birimian and basin formations. The dolerites, basalts and gabbros with slight tuffaceous sedimentary rocks and felsic lavas and dykes make up the Birimian igneous rocks. Mafic phyllites and fine grained argillaceous sandstones also make up the Birimian sedimentary rocks. Fine to coarse-grained quartz, polymictic conglomerate, and arkosic sandstones, arenites and thin mudstone beds are the main constituents of the Tarkwaian rock formation (Kenworthy et al., 2009).

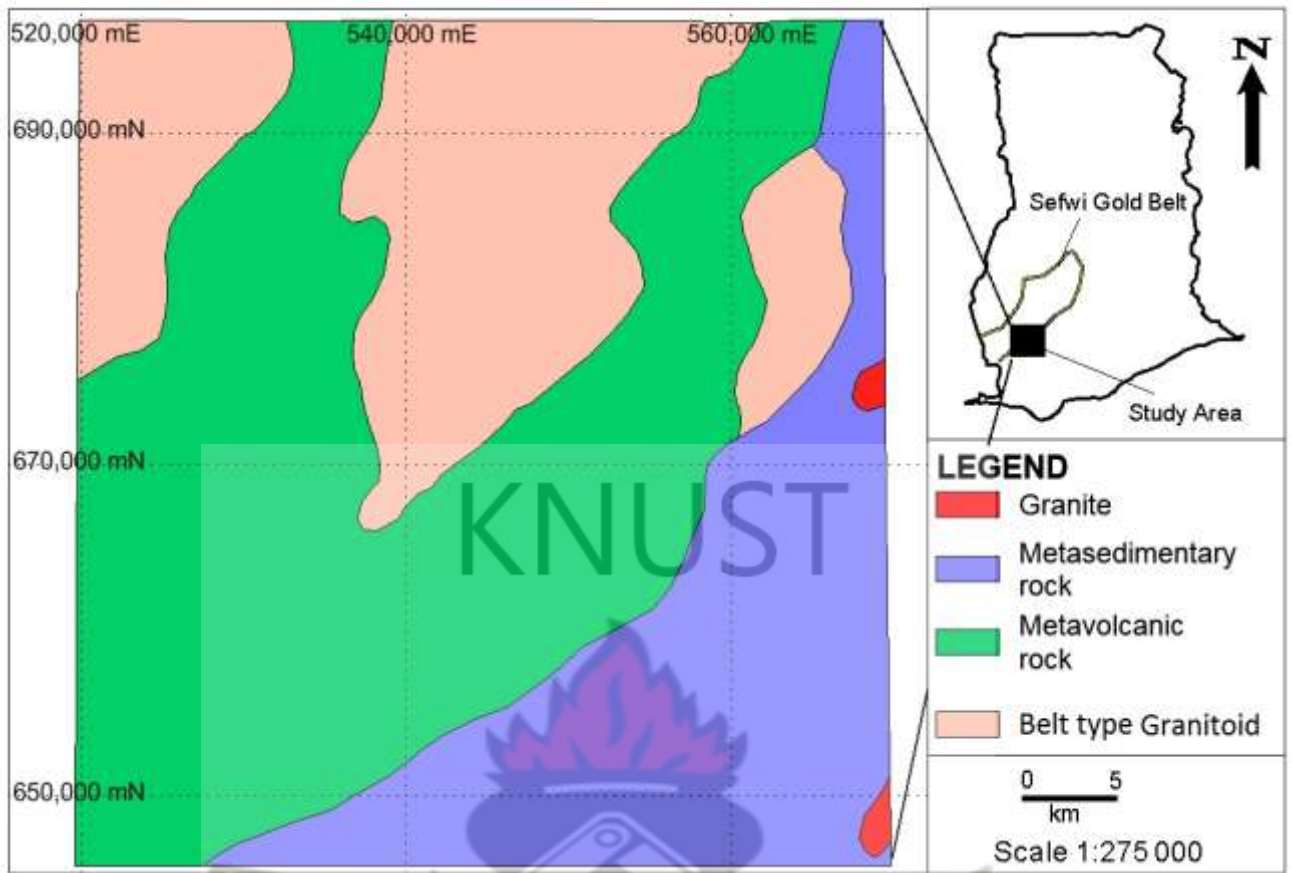


**Figure 2.2:** Geological map of the Chirano area (Modified from Giffis et al., 2002)

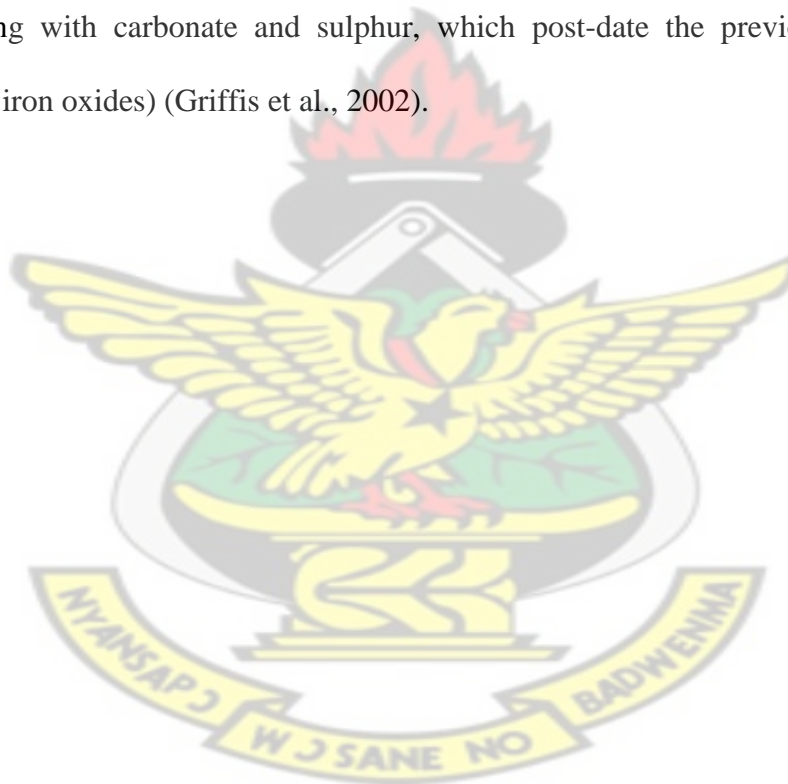
### 2.3 Mineralization

The Chirano shear zone host most of the gold deposits within the study area. Also, some of the deposits are controlled just about 200 m to the west by a parallel structure found within the mafic metavolcanics rocks. Every deposits of gold within are situated within or along the strongly altered regions. *i.e* (the chirano shear zone) and some zones of severe faulting. Hydrothermal zones, small fault splays, veins and foliation host the minerlisation of gold within Chirano (Kenworthy et al., 2009).

The main centers of gold mineralization consist of brittle zones of silica-albite-graphite-pyrite breccias and ankerite-dolomite-albite-pyrite breccias overprinting a central ductile shear zone. Essential host rocks include quartz dolerite and dolerite sills, which intrude finer mafic sequences. A suite of highly oxidized intermediate to felsic intrusive rocks, including tonalite

and quartz porphyry, is spatially and temporally associated with the main mineralizing event (Kenworthy et al., 2009).

The mineralization of gold is strongly characterized with quartz stockwork rocks sourced predominately in granitoids. The gold can be found within the veins and in the adjacent, highly deformed host rock; the high-grade regions are more often than not accompanied by about up to 5% of pyrite. The deformation seems to comprise principally of silica, albite, sericite and iron-rich carbonate, along with fine-grained hematite and magnetite. The gold happens in very fine grains, strongly characterized with pyrite and seems to have been introduced along with carbonate and sulphur, which post-date the previous deformation (silica, sericite, iron oxides) (Griffis et al., 2002).



## CHAPTER THREE

### THEORETICAL BACKGROUND

#### 3.1 Magnetism of the Earth

The Earth may be divided into three parts *i.e* crust, mantle and core. The core of the Earth may also be divided into two parts that is the molten outer core and the solid inner core. The core of the Earth is the main provider of heat energy in the Earth. Inglis (1955) pointed out that, it is impossible at present to determine the types of convective motion in the molten core. Reeve (2010) indicated that the movement of the charged electric particles within the molten core produces a magnetic field around the Earth after several theoretical and experimental studies. This magnetic field enveloping the Earth gives rise to the magnetic features of the various rocks found within or on the surface of the Earth.

The flow of these electrical charges successfully creates a huge electromagnet (Clark and Emerson, 1991).

##### 3.1.1 Nature of the Geomagnetic Field

The Earth's magnetic field within or at the surface of the Earth is produced from the molten outer core (Rivas, 2009). The Earth's magnetic field is made up of three parts (Telford et al., 1990) namely;

- The major field, which differs comparatively gradually and originates within the Earth.
- The minor field (compared to the major field), which differs rather quickly and of external origin.
- The spatial variation of the major field which are usually lesser than the major field, are almost the same in time and place, and are brought by local magnetic anomalies within the Earth's crust. These are the areas of interest in magnetic surveying.

The compass needle aligns itself in the direction of magnetic field of the Earth when hanged freely at any position on the surface of the Earth. This alignment creates an angle between the magnetic and geographic north (Kearey et al., 2002).

Almost 90% of the geomagnetic field can be characterized by the field of a theoretical magnetic dipole at the Earth's centre subtended at an angle of about  $11.5^\circ$  to the rotation axis (Kearey et al., 2002)

### 3.1.2 The Earth's Magnetic Field

If an unmagnetized steel needle could be hung at its centre of gravity, so that it is free to orient itself in any direction, and if other magnetic fields are absent, it would assume the course of the total geomagnetic field, a direction which is usually neither horizontal nor in-line with the geographic meridian (Telford et al., 1990).

The compass needle direction when hanged freely at any position of the Earth gives the direction of the geomagnetic field. The direction can be specified in terms of declination, the angle between the true north and the horizontal and the direction of the total field. The field magnitude is proportional to the maximum torque exerted on the compass needle by the field.

The geomagnetic field to which the compass needle is reacting seems to be caused by complex interactions between the Earth's hot, liquid, metal outer core as it rotates and convection with it, generating circular current at the core-mantle boundary.

The Earth's magnetic field sources vary in nature and place. The dynamo action of the molten core produces the most extreme field recorded at the equator is in the range 30,000 nT while the poles record a range of 60,000 nT (Kono and Schubert, 2007)

Whitham (1960) indicated that the magnetic elements are illustrated in Fig. 3.1. The declination 'D' is taken positive or negative depending on the deviation east or west of the

geographic north. So declination can be defined as the angle the geographic north makes with the magnetic north of the Earth. Following Fig. 3.1 in which the magnetic field is vertical plane, it is passing through the total magnetic force 'T'. Hence, the magnetic field of the Earth at every position on the surface of the Earth 'V' and 'H' are vertical and horizontal components of 'F'.

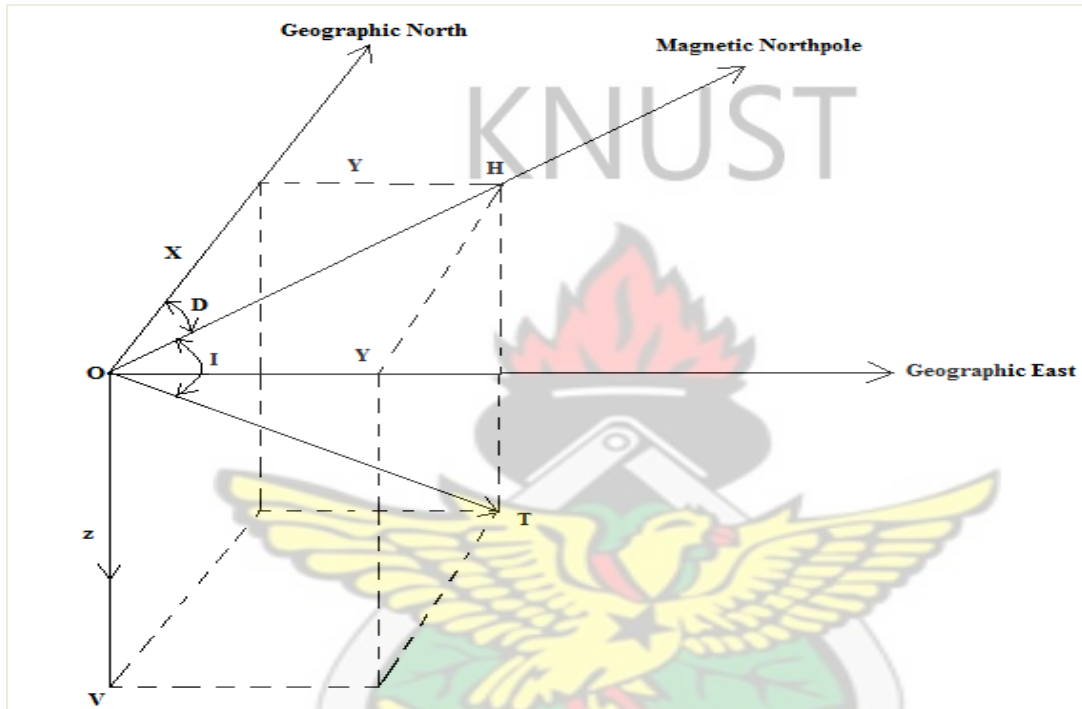


**Figure 3.1** Vector representation of the geomagnetic field at any place on the Northern Hemisphere (Whitham, 1960).

These magnetic elements can be related as follows:

$$H = T \cos I \quad (3.1)$$

$$V = T \sin I \quad (3.2)$$

### 3.1.3 Maxwell's Equations

The universe of classical electrodynamics begins with a vacuum containing matter solely in the form of electric charges, possibly in motion, and electric and magnetic fields. We can detect the presence of these fields by the forces they exert on a moving point charge  $q$ .

Maxwell's equations provide the curl and divergence of the electric fields and magnetic fields in terms of other things.

The universe we are operating in comprises an infinite vacuum containing electrical charges, represented by a local density  $\rho$ , which may be moving, and hence generating electric current, represented by a local current density  $\mathbf{J}$ . The equations in vector form are:

$$\nabla \times \mathbf{E} = -\frac{\partial(\mathbf{B})}{\partial(t)} \quad (3.3)$$

$$\nabla \cdot \mathbf{E} = \frac{\rho}{\epsilon_0} \quad (3.4)$$

$$\nabla \times \mathbf{B} = \mu_0(\mathbf{J} + \epsilon_0 \partial_t \mathbf{E}) \quad (3.5)$$

$$\nabla \cdot \mathbf{B} = 0 \quad (3.6)$$

where  $\rho$  is measured in (coulomb/m<sup>3</sup>),  $\mathbf{J}$  is also measured in (ampere/m<sup>3</sup>),  $\mu_0$  is permeability of vacuum ( $4\pi \times 10^{-7}$  henries/m),  $\epsilon_0$  is capacitivity of vacuum ( $1^{07}/ 4\pi c^2$  farads/m),  $\mathbf{B}$  is in teslas and  $\mathbf{E}$  is in volt/m

### 3.2 Magnetism of Rocks and Minerals

Most rock-forming minerals are non-magnetic. Only a few magnetic minerals, that include magnetite (Fe<sub>3</sub>O<sub>4</sub>), ilmenite (FeTiO<sub>3</sub>) and pyrrhotite (FeS), significantly affect the magnetization field of the particular area. Magnetic rocks contain these minerals, usually in small quantities.

Because subsurface temperatures increase with depth, substantial magnetization can occur only above certain depths. In areas with relatively high geothermal gradients, the maximum depth of magnetization is shallower than it is in areas with lower geothermal gradients.

Most sedimentary rocks contain negligible quantities of magnetic minerals, and are therefore non-magnetic. Most basic igneous rocks, on the other hand, have high magnetic

susceptibilities, while acid igneous rocks and metamorphic rocks can have susceptibilities ranging from negligible to extremely high (Reeves, 1989; Petersen, 1990; Reynolds, 1997).

Below the Curie temperature is when the magnetic features of rocks can exist. This temperature varies for different rock types but ranges from 550°C to 600°C. Present day geothermal studies have indicated that Curie point can be reached at depths 30 to 40 km beneath the Earth. Based on these assumptions, it is estimated that all crustal rocks are very potent to carry magnetic features. Reeves (1989) suggested that the upper part of mantle has no magnetic properties hence the bottom of the Earth's crust may be effective depth where magnetic sources can be found.

Magnetic materials can be grouped on the basis of their behavior when placed in an external field (Telford et al., 1990). Many materials have equal numbers of electrons spinning and orbiting in opposite direction so that, in absence of some external magnetic field, their effects cancel out. If a magnetic field is applied, the electron orbits are very slightly disturbed electromagnetism induction. This very slightly weakens the field inside the material giving a minute magnetic effect called diamagnetism. Diamagnetism is independent of the temperature. Diamagnetic materials include quartz, feldspar, calcite, graphite, salt. The diamagnetic substances have negative magnetic susceptibilities (Reynolds, 1997).

The paramagnetic materials have unbalanced electrons so that the individual atoms or molecules act like very tiny magnets. In the absence of an external magnetic field these molecular magnets are arranged at random, giving no resultant magnetic effect to the material as a whole but if a magnetic field is applied the molecular magnetic becomes partially aligned with it thus increasing its strength. This is small effect is called paramagnetism. With paramagnetic materials which have positive values of magnetic susceptibilities. The total

magnetic intensity will be bigger than the original magnetic field. Examples of such materials include pyroxene, olivine, pyrite, and biotite (Reynolds, 1997).

Strong paramagnetic materials such as iron, nickel and cobalt are said to be ferromagnetic. With ferromagnetic materials, there is almost a perfect arrangement of their domains.

Ferromagnetic materials have all their magnetic dipoles aligned hence there is a magnetization of high effect being produced. With anti-ferromagnetic materials such as hematite its adjacent magnetic dipoles are opposite to the direction of magnetization hence produces zero magnetization effect.

Materials such as magnetite, ilmenite show very strong magnetization effect and its domains align themselves in the direction of applied external field (Reynolds, 1997).

### 3.2.1 Magnetic Susceptibility

The degree to which a material can be magnetized in an applied external field is a physical parameter known as magnetic susceptibility (Dalan, 2006). In geology, magnetic susceptibility is one characteristic of a mineral type. Its measurement gives us information about the type and quantity of minerals present in the sample. The measure of magnetization is solely characterized by the amount and composition (shape and size) of iron oxide in the rocks (Dearing, 1994; Wemegah et al., 2009).

The magnetic susceptibility effectively is the magnetization effect divided by the applied magnetic field. If the magnetic field is  $\mathbf{H}$  (A/m) and the magnetization is  $\mathbf{M}$  (A/m), the magnetic susceptibility is

$$\kappa = x_v = \mathbf{M}/\mathbf{H} \quad (3.7)$$

where  $x_v$  is volume of susceptibility

Although susceptibility has no units, to rationalize its numerical value to be compatible with the SI or rationalized system of units, the value in c.g.s. equivalent units should be multiplied by 4 (Clark, 1997).

Reynolds (1997) indicates that most sedimentary rocks contain negligible quantities of magnetic minerals, and are therefore non-magnetic. Most basic igneous rocks, on the other hand, have high magnetic susceptibilities, while acid igneous rocks and metamorphic rocks can have susceptibilities ranging from negligible to extremely high. Magnetic susceptibility is a trace parameter of rocks, because the percentage of magnetic minerals is usually one percent or less, even in basic igneous rocks. Slight differences in iron oxide content of a mineral can cause large magnetic susceptibility variations. Remke et al. (2004) also pointed out that the amount of iron oxides in rocks are influenced by the parent rock, age of rock and weathering processes.

### **3.2.2 Remanent and Induced Magnetism**

There are two components involved in a rock's magnetization that is remanent magnetism and induced magnetism. Remanent magnetism also known as the permanent magnetism is the type which when the applied field is removed, still remains in the rock. Materials that belong to ferromagnetic and ferromagnetic retain their magnetism even when the external field is taken away. Rock magnetization usually takes place mostly at the shallow depths because there is an increment in temperature towards the centre of the Earth (typically < 50 km depth) (Clark and Emerson, 1991). Furthermore, remanent magnetization can occur when the arrangement of the magnetic domains are locked in the presence of a weak geomagnetic field.

During cooling the magnetic domains are locked up at specific curie points owing to significant change in crystal growth. These thermo, chemical, and detrital remanent magnetizations are little and influence only the most sensitive magnetic sensors (Remke et

al., 2004). Primary remnant magnetization is acquired by the cooling and solidification of an igneous rock from above the Curie point (of the sources of magnetic minerals) to normal surface temperature (TRM) or by detrital remnant magnetization (DRM). Secondary remnant magnetization, such as chemical, viscous or post-depositional remnant magnetization, may be acquired later on in the rock's history (Reynolds, 1997). The magnetization effect,  $M$  divided by the applied effect;  $H$  gives the magnetic susceptibility of the rocks. This explains best induced magnetization (Remke et al., 2004)

### 3.2.3 Magnetization at Low Magnetic Latitudes

Close to the magnetic equator of Earth, the ambient magnetic field is almost horizontally oriented approximately north-south, and has a field intensity of between 25000 and 40000 nT, about one-half the intensity at the magnetic poles. The magnetic equator lies within  $10^\circ$  of the Earth's geographic equator. The decreased equatorial field intensity causes local magnetic anomalies at low latitudes to have smaller magnitudes than those produced by similar structures at high latitudes. The north-south orientation of the horizontal inducing field means that a long north-south striking magnetic structure may show no anomaly at all, except at the south and north termination of the structure (Beard and Goitom, 2000). On the other hand, the outcome can be generally reviewed this way; magnetic readings are high along and near a line that goes through a magnetic object in the direction of the field of the Earth; magnetic readings are low in all other locations. Additionally, at very low latitudes, typically between  $10^\circ$  inclinations, the amplitude correction for north-south trending features unduly intensifies noise and alters difference in the magnetic susceptibilities from originating magnetic sources in different directions from the external field. There are always complications with magnetic dataset interpretations because of the asymmetric anomalies produced by symmetric causative rocks mostly located anywhere on the Earth apart from areas closer to the magnetic poles (Rajagopalan, 2003).

### 3.3 Rock Alteration

Alteration is a deformation of rock when hot fluids moves from high pressure areas to low pressure areas. Along the Earth's surface alteration of rocks may occur during chemical weathering which is the supergene alteration (Appiah, 1991). Shanks (2010) explained that the reaction of hydrothermal liquids and rocks brings about a deformation called hydrothermal alteration. Hydrothermal alteration can occur as results of isochemical activities such as metamorphism, and characterized by mineralogical variations, or it can be metasomatic and result in major element addition or removal.

The deformation of magnetic minerals is significant to remember when it comes to the explanations of magnetic anomalies. Mineral deposits are mainly controlled by wall rock alteration next to hydrothermal veins by the hot liquids (Appiah, 1991).

The alteration may range from simple recrystallization to the addition, removal or rearrangement of chemical components. The nature of the alteration products depend upon, the character of the original rock, the character of the invading fluid, which defines such factors as pH, vapour pressure and the degree of hydrolysis and the temperature and pressure at which the reactions took place (Studemeister, 1983).

The potassic alteration zone associated with oxidized, magnetic felsic intrusions is often magnetite-rich. This is commonly observed for Au-rich porphyry copper systems (Sillitoe, 1979). However, contact metamorphism of hydrothermally altered, demagnetized igneous rocks for instance by dike injection may produce secondary magnetite (Hall and Fisher, 1987). Deformation of the wall rock can bring about recrystallization, color transformations and permeability changes. The edges of a vein or close to an igneous contact are recrystallized to form carbonate rocks. The permeability of the undeformed rocks is lesser than the recrystallized rock signifying that some ores may be transported following a

complex wave of recrystallization. Wall rocks alteration is an important exploration tool, the alteration brings around many deposits which are extensive and much easier to locate than the ore bodies (Appiah, 1991).

### **3.4 Lithology, Structure and Magnetism**

In the natural environment, magnetic minerals are pervasive and occur in every kind of rocks *i.e* rocks, sediments and soils. These magnetic minerals have the magnetic dipoles locked the direction of the Earth's magnetic field during the formation of the rock (Harrison et al., 2007).

Plummer et al. (2001) grouped structures into two. The first is the brittle structures which resulted in the brittle-elastic breakdown of rocks long-ago. Joints and faults formed part of this broad type of structures. The second type is ductile structures which conserves the main viscoplastic alteration of rock all the way through the geological time. Examples of such structures include the folds and metamorphic foliations.

Isolated magnetic anomalies, generally circular or oval in plan and several hundred meters across, and with amplitude of tens to hundreds of nanoteslas, may arise from accumulation of magnetite and pyrrhotite, which may be associated with economic grades of copper, lead, zinc, silver, gold and others (Plummer et al., 2001).

Grant (1985) pointed out that sedimentary rocks are usually non-magnetic. The analysis of geophysical data suggests that sources of magnetic bodies must located beneath the bottom of the sedimentary rocks. Sedimentary rocks like sandstone, dolomite, limestone etc have low magnetic features hence the outcome anomalies of the magnetic values are extremely small in amplitude. Due to this characteristic nature of sedimentary rocks it is sometimes difficult to detect such formations using airborne surveys (Langenheim et al., 2000).

Very little or no magnetic influence is experienced or detected within the Precambrian metasedimentary sequences. The only exemption is a slight lithologic part which is mainly made up of an iron rich metachert. Igneous and plutonic rocks demonstrate a broad range of magnetic features (Plummer et al., 2001). On the other hand, metavolcanic formations, gabbros and several intrusive formations can generate strong magnetic anomalies (Langenheim et al., 2000). The Precambrian metavolcanic formations produce magnetic susceptibility values ranging from 2 for meta-rhyolite to 8000 for metabasalt multiplied by  $10^{-6}$  SI units (Langenheim et al., 2000).

The crust of the Earth is mainly dominated by metamorphic rocks and has a broad range of magnetic susceptibilities. They produce composite sample of magnetic anomalies. The rocks with highest magnetic anomalies are Itabiritics followed by metabasic rocks. On the other hand, regions of felsic dominated rocks such as granitic/gneissic series produce weak magnetic anomalies on a comparatively smooth background (Grant, 1985).

### **3.5 Enhancement Techniques**

Usually, the original total magnetic intensity grid is visually difficult to observe and interpret the various structures. A variety of enhancement techniques when applied to geophysical data tends to improve the data quality on the basis of mathematical principles. Mathematical enhancements filters which include reduction to the pole, analytical signal, vertical derivative, etc are extremely helpful in developing near surface geological features except that their restrictions are based on the value of the data and extra reasons like the angle the Earth's magnetic axis makes with the horizontal.

### 3.5.1 Fourier Transform Filter

Fourier transforms are predominantly helpful in magnetics (Telford et al., 1990) for

- resolution of specific anomalies by downward or upward continuation,
- changing the effective field inclination (pole reduction) or conversion of residual magnetic data to vertical-component data
- calculation of derivatives and
- general filtering-separating anomalies caused by sources of different size and depth and modelling.

A much faster algorithm developed by Cooley and Tukey (1965) called the Fast Fourier Transform (FFT) is a competent mathematical tool used to calculate the Discrete Fourier transform (DFT) and its inverse. FFT algorithms can hence be regularly made into data processing programs so as to analyze spectral lines of the waveforms of geophysical data.

Fourier transformations operate based on the operation of application program like Microsoft Excel for organizing, analyzing and storing data in the form of a table (Kearey et al., 2002).

### 3.5.2 Reduction to the Pole (RTP)

This mathematical filter converts induced magnetic anomalies from near or close to the equator to behave as if the sources were positioned at the magnetic north pole. Pole reduction filter makes explanations of the magnetic data like faults much easier because it changes their asymmetric anomalies to symmetric and anti-symmetric forms (Mendonça and Silva, 1993).

Reduction-to-the-pole (RTP) is a useful and effective operation designed to transform a total magnetic intensity (TMI) responses created by the asymmetrical causative body into the anomaly that this same body would produce if it were positioned at or close to the North pole and magnetized by induction only (Li, 2008).

### **3.5.3 Analytic Signal**

The analytic signal behaves like the reduction to the pole filter. It actually takes the magnitude of the square root of the vertical and horizontal components of the magnetic responses (Geosoft Inc., 1996). This processing enhancement can be helpful in mapping the edges of the permanently magnetized sources and for centering anomalies over their causative bodies in areas of low magnetic latitude but does not depend on the direction of magnetization (Ansari and Alamdar, 2009). Again, several papers have revealed that, it can be helpful in the depth estimation of magnetic bodies.

### **3.5.4 Vertical Derivative Filter**

The first vertical derivative filter does the removal of the long wavelength properties of the magnetic responses and most importantly enhances the quality of closely spaced and superposed responses (Keating, 1995). The application of the vertical derivative filter to a magnetic data is to improve the shallowest magnetic features and suppress the deeper anomalies in the data (Geosoft Inc., 1996). The vertical derivative emphasizes on the near surface geological features.

## **3.6 Principles of Radioactivity**

Radioactivity is simply the process in which, an unstable atom becomes stable through the process of decay of its nucleus (Kearey et al., 2002). Geologists and geophysicists measure the gamma rays emanating from the surface of the Earth. These radiations give a lot of information the soil and rock distribution within the Earth *i.e* (lithology).

### **3.6.1 Basic Radioactivity**

Isotopes are atoms of same element with equal number of protons but different neutron numbers. Isotopes have same chemical features, but different physical features. Unstable nuclei emit energetic ionizing radiations to become more stable.

These isotopes are called radioactive isotopes or radioisotopes. Nuclides with this feature are called radionuclide, and disintegration or nuclear decay is the breakdown of unstable nuclei (IAEA, 2003)

Each radioactive isotope has a distinctive chance associated with the radioactive disintegration of its nuclei. This is called as the isotope half-life and is the time taken for radioactive nuclei to decay to half its initial value. Hence, after one half-life, half the original radioactive isotopes remain, and after two half-lives, one quarter of the original radioactive isotopes remain, and so on (Minty, 1996). The law of radioactivity decay states that the reduction in the quantity of atoms of unstable nuclei with time is expressed as (IAEA, 2003)

$$N_t = N_0 e^{-\lambda t} \quad (3.8)$$

where  $N_t$  is the quantity of atoms after decay with time  $t$ (s),  $N_0$  is the initial quantity of atoms and  $\lambda$  = the decay constant of the unstable nuclei ( $s^{-1}$ ).

The half-life  $T_{1/2}$ (s) of an element is defined as the time taken for  $N_0$  to decrease by half.

Half-lives vary  $10^{-7}$ s for  $^{212}_{84}\text{Po}$  to about  $10^{13}$ Ma for  $^{204}_{82}\text{Pb}$  (Kearey et al., 2002).

$$T_{1/2} = \frac{0.693}{\lambda} \quad (3.9)$$

The  $\lambda$  multiplied by  $N$  gives the activity (Bq) of the unstable nuclei. Disintegration of unstable nucleus does not depend on additional physical factors (IAEA, 2003).

Minty (1996) indicated that radioactivity usually occurs as a sequence of the number of daughter products with a breakdown of the mother elements in order to have a stable isotope. At this period, the behaviors of all the radioisotopes of the decay series are the same. Hence, the extent of the quantity of any daughter nuclei can be helpful in estimating the quantity of any other radionuclei in the breakdown series. Emanations of gamma rays from the Earth

surface differ with many factors but most importantly depend on the amount of radionuclides in the top soil about 30 to 40 cm. The amount depends on the parent rock and the extent of weathering (Elawadi et al., 2004).

### 3.6.2 Disequilibrium

Minty (1996) indicated that the addition or removal of one or more radionuclide in a decay series completely or partly to the system is known as disequilibrium. Thorium in nature seldom takes place outside of equilibrium, and potassium is not affected with disequilibrium problems. Nevertheless, it is frequent in the disequilibrium of uranium decay series and can take place at numerous locations in the  $^{238}\text{U}$  decay chain,  $^{238}\text{U}$  can be carefully leached compare to  $^{238}\text{U}$ ,  $^{230}\text{Th}$  and  $^{226}\text{Ra}$  can be carefully taken out from the breakdown series and lastly  $^{222}\text{Ra}$  (radon gas) is movable and can flee into the atmosphere from soils and rocks (Elawadi et al., 2004 and IAEA, 2003).

Each member of the decay loses mass at the equal rate in equilibrium decay. In each case, the suitable constant of decay is multiplied by mass of the element. The constant of decays are hence inversely dependant on the equilibrium masses. If the required number of elements for equilibrium is exceeded or lessen, radioactivity will be faster or slower than the rate of equilibrium until equilibrium is again established.

Equilibrium can be interrupted if any gaseous or soluble intermediate products have half-lives extended enough to permit them to scatter prior to radioactivity. Approximations of the amount of uranium are then usually recorded as equivalent uranium (eU) because these approximations are calculated on the assumption of equilibrium circumstances. Thorium too is often recorded as equivalent thorium (eTh), even though the thorium decay chain is nearly constantly in equilibrium (Milsom, 2003).

### **3.6.3 Source-Detector Geometry**

Gregory and Horwood (1961) indicated that the observed spectra are greatly influenced by the thickness of the source detector. Moreover, the Compton range which depends on the scattering in the sources increases as the thickness of the source also increases. The peaks of the photons are hence reduced compared to the Compton background. In view of the fact that photons of low energy are simply damped than the photons of high energy, this effect is well associated with photons of lower energies. Any material between the source and the detector attenuates radiations coming from the Earth in the source. The nature of the observed spectrum is mainly influenced by the number of materials attenuating the radiations between the detector and source. For increasing damping, the photo-peaks are weakened compared to the range of energy. Measurement of spectra lines therefore depends on the amount and thickness of the source, the level of the detector above the Earth's surface, the size of the bedrock which is a non-radioactive and the response function of the detector (Elawadi et al., 2004; IAEA, 2003).

### **3.7 Measurement of Gamma Radiation**

Natural gamma radiations vary from cosmic emissions with energies above 3 MeV to X-rays. The various peaks match the exact radioactive events, the energy of individual photon occurring anywhere within a small range determined by the nuclear kinetic energies at the decay time and by errors made during the data acquisition (Milsom, 2003).

The modern gamma ray spectrometers usually record energies of range 0 to 3 mega electron volt (MeV) using the 256 or 512 channels of information.

Every channel hence reports all gamma radiations recorded by the detector which have energies in range of 11.7 keV, weak count rates are associated with each channel. With the

airborne gamma ray spectrometer, one or even zero counts in several channels of high energy are recorded for the duration of a second counting stage with sodium iodide (NaI) of 32 litres.

Figure 3.2 shows a typical spectrum from gamma ray energy distributions. The  $^{40}\text{K}$  decays with emission of gamma radiations of energy 1.46 MeV whereas uranium and thorium decays with emission of gamma radiations of energies of 1.76 MeV and 2.62 MeV respectively. Thorium portrays high peaks compared to all the three concentrations (IAEA, 2003).

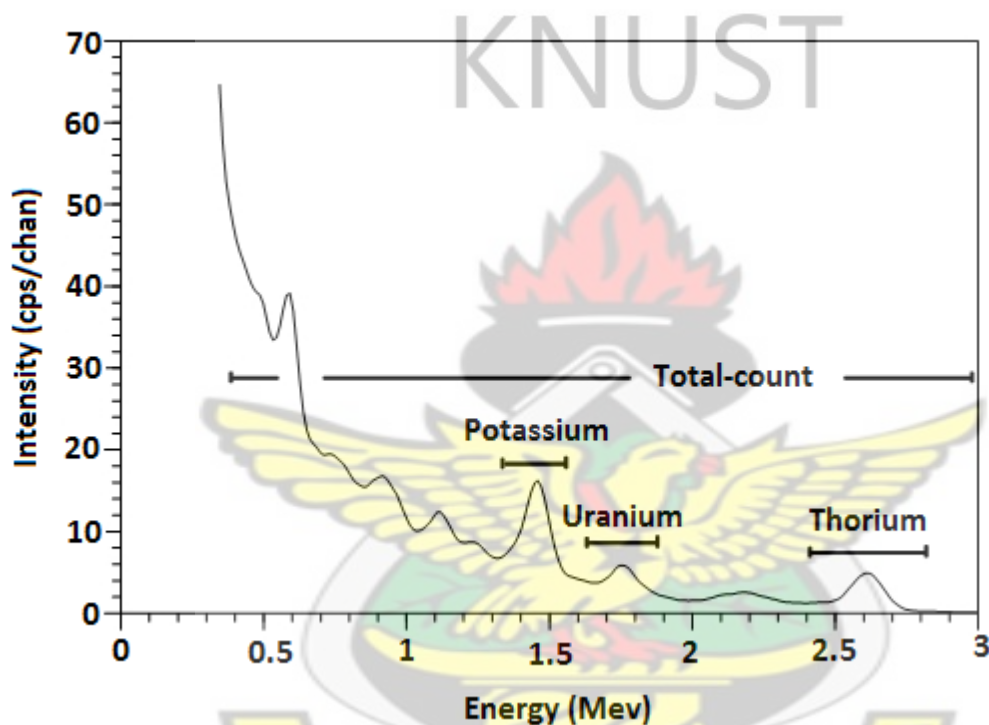


**Figure 3.2:** Typical spectrum of the gamma radiations showing the individual peaks (IAEA, 2003).

Granite contains sufficient amount of Potassium and Thorium and lesser portions of Uranium. The energy windows of uranium, thorium and potassium are conventionally used in the measurement of the gamma radiations. Telford et al. (1990) points it out that the totality of radioactivity produces the total-count window. Concentrations of radioactive elements in water, air and rocks with regards to nuclear geophysics and geology are expressed in

percentage (%) for potassium and parts per million for both uranium and thorium (ICRU, 1994)

### **3.8 Mapping Natural Sources of Radiation**

Naturally occurring radiation sources can be suitably classified into three groups according to their origin. The first group includes  $^{40}\text{K}$ ,  $^{238}\text{U}$ ,  $^{235}\text{U}$  and  $^{232}\text{Th}$ , which are believed to have been produced during the creation of the universe and have half-lives of the same order as the Earth's age (Minty, 1996).

The second group comprises radioactive isotopes that are daughter products from the decay of isotopes in the first group. These have half-lives varying from small fraction of one 1 s to 104 to 105 years.

The third group would include isotopes created by external causes such as the reactions of cosmic radiations with the Earth and its atmosphere. The concentration of cosmic radiation at surface of Earth is comparatively small such that all of them are absorbed in the atmosphere (Minty, 1996; Elawadi et al., 2004).

#### **3.8.1 Geochemistry of Radioelements**

##### **3.8.1.1 Potassium**

Potassium (K) is an alkali, lithophile and biophile metal. Potassium forms majority component in rock formation. Most of these rocks are the silicate minerals such as alkali feldspar, leucite, biotite, muscovite, phlogopite and some amphiboles.

Most igneous rocks have potassium being the main aggregate. The amount of potassium is used for the petrographic groupings. During magmatic differentiation, potassium is gradually concentrated thus more potassium is concentrated in felsic than mafic igneous rocks.

This is observed in the variations in K concentration of basalt, normally less than 1%, and granite, which is composed 2% to less than 6% (Elawadi et al., 2004, Fertl, 1983; Wedepohl, 1978).

Dickson and Scott (1997) indicated that during weathering process, the main potassium sources will be destroyed in the order biotite-K-feldspar-muscovite. When weathering is taking place, the freed potassium can be used for the formation of potassium enriched minerals like illite or may be taken up in small quantities by clays (montmorillonite) under better conditions.

The magmatic and metamorphic rocks series control almost all the potassium enriched minerals such as the feldspar mainly the feldspathoids leucite and nepheline, and the micas, biotite and muscovite.

### **3.8.1.2 Thorium**

Thorium (Th) is a part of the actinide group of elements. +4 is the main oxidation state of this element and thorium-232 ( $^{232}\text{Th}$ ) as the only natural occurring isotope. Thorium has a incredibly long half-life of  $1.4 \times 10^{10}$  years (Wedepohl, 1978). It is strongly lithophilic and is more abundant within the crust of the Earth. During the decay series of thorium, the parent thorium nuclide disintegrates with emission of gamma radiations of energy 2.62 MeV and  $^{208}\text{Tl}$  as the daughter nuclide. Granitic rocks records higher concentration of thorium than mafic igneous rocks. The concentration of thorium normally cannot move but due to environmental conditions there can be a small movement. Th fundamentally cannot dissolve in both surface and groundwaters so it is a helpful guide element in sediments of stream for finding deposits of uranium related with magmatic rocks (Chopin, 1988; Elawadi et al., 2004; Krishnaswami, 1999). Monazite and zircon are the main minerals enriched with thorium. They are immobile thus during weathering they are more stable and can be absorbed into

deposits of heavy sand minerals. Thorium released during weathering (*i.e* breakdown of rocks) possibly will be preserved in iron oxides, titanium oxides and with clays (Dickson and Scott, 1997).

### **3.8.1.3 Uranium**

Uranium (U) is an extremely heavy element and can be considered as the most the radioactive element in the world. Uranium produces the most abundant supply of concentrated energy. Uranium is contained in most soil of amount of 2 to 4 parts per million and is widespread in the crust of Earth such as tungsten, tin and molybdenum. In the crust of the Earth, most of the uranium is a combination mostly of two isotopes  $^{238}\text{U}$  and  $^{235}\text{U}$ .

Uraninite is widespread as tiny traces in the minerals forming up the rock in granites or as bulky grains in mineralized pegmatites and granites. In addition uraninite happens in hydrothermal layer and sedimentary rocks. Zircon, monazite, apatite, allanite and sphene (accessory minerals) which are related with igneous and metamorphic rocks are the most resistant to weathering (Langmuir and Hermans, 1980; IAEA, 2003). Uranium released during weathering possibly will be preserved in authigenic oxides of iron and minerals of under reducing environment forming deposits of uranium under conducive conditions (Dickson and Scott, 1997). Uranium itself does not emit gamma-rays during its decay but the most energetic gamma-rays emitted by its daughter isotopes come from  $^{214}\text{Bi}$  which occurs late in the decay series (Dickson and Scott, 1997).

### **3.8.2 Distribution of the Radioelements in Rocks and Soils**

For normal rocks and soils, 90% of the gamma rays measured by a spectrometer survey emanate from the uppermost 30 cm to 40 cm of the Earth. The content of potassium in rocks can have a range of 0 to 10% potassium but is usually 1 to 5% potassium with average of about 2% potassium. The content of Uranium and Thorium in rocks changes from near zero

to several hundreds of part per million (ppm). The amount of K, U and Th depends on rock type and the geological environment. In most areas beneath the Earth, the bedrock is covered with soil. Hence, the radiation from the soil is the most essential contributor to the terrestrial radiation. The amount of the radiation from minerals in the soil depends upon the content in the original parent rocks (IAEA, 1990). Moreover potassium is extremely unable to coexist during crystallization of magma. A rock of composition of 2.5% K, 3ppm U and 15 ppm Th could be a granite, felsic intrusive or shale (Dickson and Scott, 1997).

Available data for metamorphic rocks which include gneissic rocks resulting from granite and amphibolites resulting from dolerite suggest that metamorphism does not affect radioelement content. Sedimentary rocks generally have radioelement content reflecting the parent source rock. Hence, young sediments derived from granitic sources may be expected to have quite high radioelement content, but more mature sediments, composed primarily of quartz should have very low values when specific rock types such as pegmatite, aplites, quartz-feldsparporphyrites and mafic intrusives occur as narrow intrusions or in small areas, or are subject to faster weathering and erosion than the host country rock, it is difficult to find in-situ soils (Dickson and Scott, 1997).

Granite depicts a broad array of weathering behaviour, depending on its mineralogy and the weathering system, climate etc. Soils derived from granitoids generally lose around 20% of their radioelements contents during pedogenesis. Soils over radioelement-poor arenite, as over other poor radioelement-poor rocks; can show the effects of contamination by transported materials (Darnley, 1996).

Processes other than in-situ weathering can affect the radioelement content of soils. They include clay eluviation, colluvial and aeolian transport, and soil movement. All can affect the

concentration of radioelements in the thin 30 cm to 40 cm layer measured during aerial surveying (Wilford et al., 1997).

### **3.8.3 Direct Detection of Mineralization**

The radiometrics surveys are used extensively in many ways. This survey method was primarily used in mapping for the deposits of uranium but present day radiometric survey has diverse benefits such as delineation of lithologies. Applications of radiometric survey have been used in weak radioactive zones like sedimentary basins, volcano-sedimentary terrains, and heavily glaciated or tropical weathered areas (Elawadi et al., 2004).

Analyses of geochemical and microscopic of samples from rock or sediments are required to fully recognize the mineral phases that form the radioelements (Charbonneau, 1991).

Owing to the comparatively weak penetration of gamma radiations through rock and soil, the chance of detection of mineralizing of uranium is reliant on the Uranium content in the host rock, its surface dimensions, and the positions of the measured profiles (Elawadi et al., 2004).

Radiometric assay of samples in mineralized regions depicts that high percentage of potassium oxide ( $K_2O$ ) content in the rock and the strong differences in the potassium oxide concentration in the rock is possible owing to the large scale deformations in the rock (Bhattacharya et al., 2011).

Alteration, weathering, climatic conditions and hydrothermal processes can have effect on the concentration of the radioelements (Nicolet and Erdi-Krausz, 2003). Variations in the vegetation cover can also affect ground surveys. For example, the radioactivity of a soil covered by humus will be less than the radioactivity of the above soil. A mass equivalent to 0.08 m of water will reduce the exposure rate by about 50%. Because soil moisture has a

similar effect and because it varies as a function of time and rainfall, surveys carried out at different times of the year may not give the same estimate of the exposure rate. (IAEA, 1990)

Hydrothermal processes can result in variations to the radioelement content of the host rocks. Among the three radioelements, K is mostly affected by such processes, Th less often and U very infrequently. Potassium is often increased during alteration signature but weathering generally decreases the intensity of alteration signature (Dickson and Scott, 1997).

Potassium is generally added to the source rocks by mineralizing hydrothermal fluids. It may be hosted by K-feldspar or muscovite and potential outcropping or sub-cropping mineralization can be recognized by increase in K counts during radiometric surveying (Dickson and Scott, 1997). This could reflect the greater movement of U compared to Th during hydrothermal alteration processes and because Th is generally unaffected by alteration processes, the K/Th ratio can be a strong indicator of K alteration related with mineralisation than simply K. Thorium may be mobilized during mineralization processes for example, being partly depleted in regions of K-alteration or intense silicification, but concentrated in Th-rich materials such as laterite. The relationships between radioelement divisions and each of these types of deposit are varied and composite. A complete comprehension of the influences of silicification, K-alteration, process of weathering and local lithological differences is required to estimate the mineralization potential characterized with anomalies of radioelements.

## CHAPTER FOUR

### MATERIALS AND METHODS

#### 4.1 Project Site Description

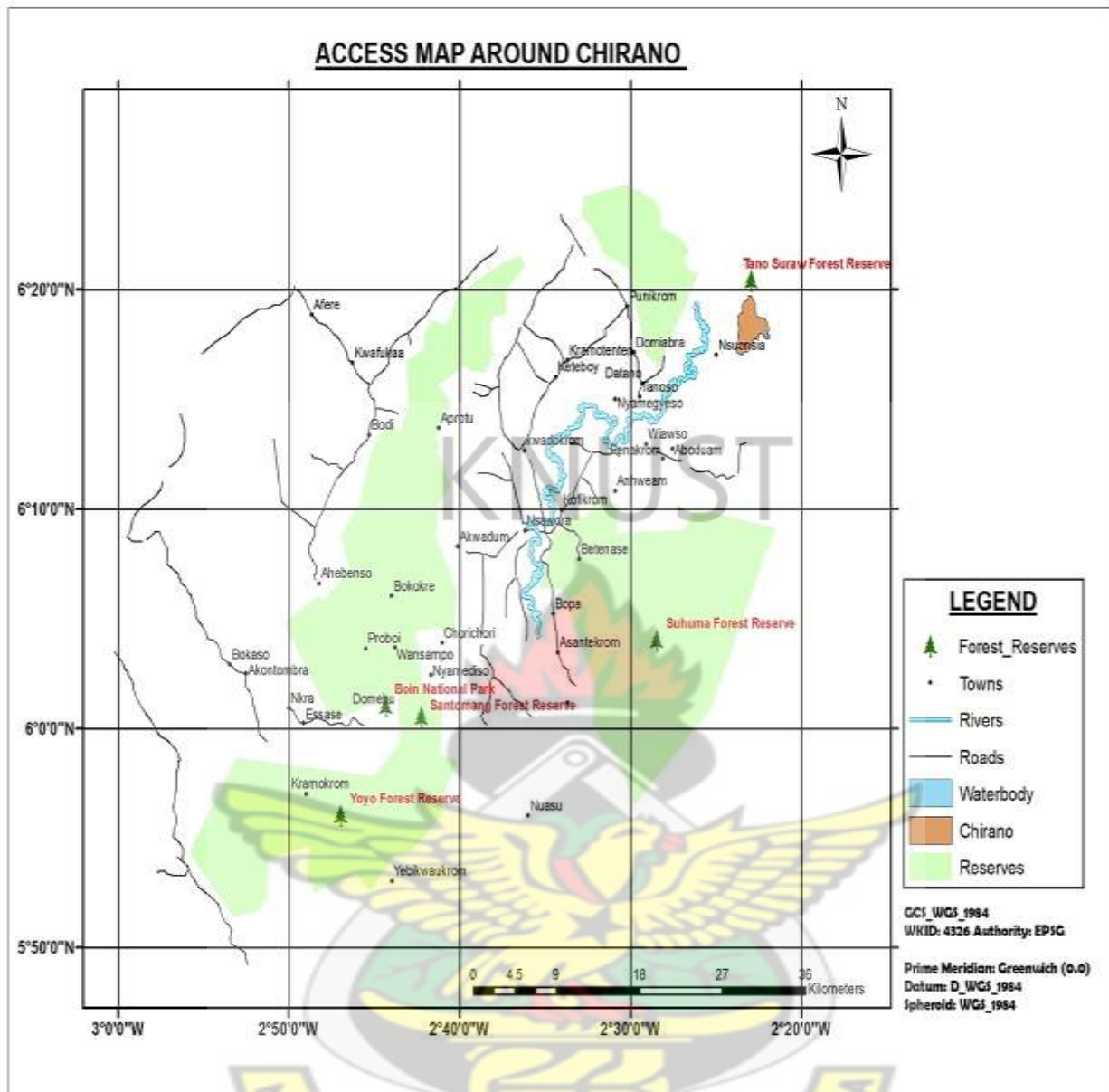
Chirano, the area under research falls along the western part of the metavolcanic rocks of Sefwi. It is located within the intensely faulted zones caused by the contact between the Sefwi metavolcanics and the adjacent Kumasi metasediments. It covers a strike length of about 20 km along this intensely faulted zone. The area is about 2500 km<sup>2</sup> in extent and occurs along the main Bibiani range which trends in the NNE direction. Chirano is dominated by very highlands of peaks height 600 m above the sea level and relief of almost 300 m (Griffis et al., 2002).

##### 4.1.1 Location and Accessibility

The area is situated about 90 km in a southwestern direction from Kumasi, the second largest city in Ghana and the northern boundary is only about 4 km south of the mines operated in Bibiani. A sealed road can be located that runs from the main Bibiani town through Anhwiaso, Bekwai and Ntretreso. Access to Chirano and some towns (Paboase, Akoti and Twebo) within the study area is possible by the untarred roads.

The rivers in the study area include Suraw and Chira which join the major Ankobra River. These flow roughly north south into the Ankobra and collect high amount of rainfall; thus they have normal flow of water (Griffis et al., 2002; Ghana Districts, 2014).

Its geographical projection coordinates referenced to the World Geographic System (WGS) 84 and longitude-latitude categories with units in degrees: (-2.8193<sup>0</sup>, 6.3044<sup>0</sup>) representing upper left corner, (-2.3733<sup>0</sup>, 6.3044<sup>0</sup>) as upper right corner, (-2.8173<sup>0</sup>, 5.8428<sup>0</sup>) and (-2.3733<sup>0</sup>, 5.8428<sup>0</sup>) representing lower left and lower right corners respectively.



OLE

**Figure 4.1:** Accessibility map of study area (Chirano)

#### 4.1.2 Physiography

The topography of Chirano is that of a gently rolling landscape locate above the thick sequences of the Birimian rocks series. Above the Tarkwaian series of rocks, the topography is rough and hilly rather than level and flat or gently rolling. The topography of the area is quite variable. To the northwestern, southwestern, and northeastern of the area are the prominent highlands, where elevations are about 550-600 m above sea level.

These hills are underlain by Birimian and Tarkwaian formation; the ridges have average elevations and relief of about 300 m above the surrounding valleys where we have the lowest lying areas (Southeast portion of the study area).

#### **4.1.3 Vegetation**

The vegetation of the study area mostly falls within the Equatorial Rain Forest Zone (Tano Suraw Forest Reserve). The natural vegetation is a moist-deciduous forest. Within Chirano area, Odum, Mahogany and Sapele are the main type of trees form the source of the successful Timber Industry of Ghana. On the other hand, most of the original forest has relapsed into secondary forest and grassland owing to arbitrary cutting down of trees, bush-fire and bad practices of farming which include shifting cultivation and bush fallowing (Griffis et al., 2002; Ghana Districts, 2014).

#### **4.1.4 Climatic Conditions and Occupation of Inhabitants**

The study area falls within the Sefwi-Bibiani-Ahiawso which is positioned in the equatorial climate with an average rainfall of about 2000 mm/yr annually. The pattern is bimodal, falling between March to August and September to October. November to January is the time where the dry season is experienced whereas the wet season is noticeable between June and October. The average temperature recorded all through the year is about 26°C. High relative humidity of about 75% during the afternoon and 95% during the night and early mornings are recorded within the study area. This means that the weather conditions in the area is suitable and appropriate for the cultivation of crops for exports like cocoa, pineapple and cashew

The Chirano area has about 70-80% of the population as farmers and it is a potential area for the cultivation of a variety of agricultural produce. Agriculture in the area is fundamentally rain fed and depends very much on the changes of the weather. Most of the local population

is engaged in small-scale farming but the district community has also depended on the mining activities in the area.

#### **4.2 Data Acquisition**

In the years between 1997 and 1998, the Finland geological survey (GKT) together with the Ghana geological survey and mineral commission of Ghana carried out geophysical surveys in the southern part of Ghana. This survey covered the Kumasi basin and the Sefwi gold belt.

Magnetic, electromagnetic and radiometric values were recorded from the area and these datasets have been used extensively in the delineating deposits of ore minerals.

With the acquisition of the magnetic data, the sensor of the magnetometer is attached on a fixed wing aircraft. During the flight, the aircraft travels through the air while the sensor records the magnetic field, attitude of the aircraft, Global Positioning System (GPS) position and altimeter data along the gridded pattern. A computer is used to store the raw magnetic susceptibility values and corrects for aircraft variations. The final data is microlevelled and these comprise diurnal variations correction, system parallax and the International Geomagnetic Reference Field (IGRF). The emission of gamma radiations comprises mainly potassium, uranium and thorium with energies of specific peaks during radioactivity. The mass spectrometer measures the spectrum of gamma radiations using NaI crystals that scintillate when it interact with gamma rays. These scintillations are changed into voltage which is equivalent to the gamma radiation energy using the Photomultipliers.

Applying highly developed processing methods, the raw gamma radiation spectrum is transformed to the respective ground concentrations of the three radioelements.

#### 4.2.1 Data Specifications

The Airborne geophysical datasets namely magnetic and radiometric were obtained from the Ghana Geological Survey Department (Accra) by the Physics Department (Kwame Nkrumah University of Science and Technology-Kumasi) on the 9th June, 2014.

This geophysical information was collected with the following aircraft equipment (Table 4.1) and survey parameters (Table 4.2).

**Table 4.1:** Airborne Geophysical Survey Equipment (Geological Survey of Ghana, 1998)

Survey Equipment	Aircraft	Magnetometer	Spectrometer
	(Fixed Wing)		
Equipment	Cessna	Scintrex	Exploranium GR 820-256 with 2048 in <sup>3</sup> NAI(TI) downward looking crystal and 256 in <sup>3</sup> upward looking crystal
Types	Titan 404 (C-FYAU)	Cesium SC-2	

**Table 4.2:** Airborne Geophysical Survey Parameters (Geological Survey of Ghana, 1998)

Survey Parameter	Parameter Specification
Period	1997-1998
Travel line Spacing	400 m
Travel line direction	NW-SE
Tie-line Spacing	5000 m
Tie-line direction	NE-SW
Nominal terrain clearance	70 m
Navigation	Global Positioning System (GPS)
Sampling time	0.1 s Magnetic, 0.1s Radiometric
Air Speed (Nominal)	250-290 km/hr (70-80 m/s)
Measurement Spacing	8m (magnetic), 80 m(Rad)

### 4.3 Data Processing

The major GIS software used to process and enhance the airborne geophysical data is the Geosoft (Oasis Montaj) and geophysical softwares that were used to enhance the data in a variety of formats is MapInfo 10.5 - Discover 11.1. The methodology applied involved the acquisition of two different Geophysical Airborne data sets (magnetic and radiometric), building of databases (projects), data processing and interpretation. Two databases were generated to process the acquired datasets; using Geosoft software for processing the radiometric and magnetic data. This part presents a summary of the airborne data processing methods. These methods include the orderly editing processes, the gridding method application and taking away of the Earth's magnetic background field.

Some corrections like removing diurnal differences of the magnetic field of the Earth, aircraft heading, instrument variation, lag error between aircraft and the sensor and inconsistencies between flight lines and tie lines were made by the Geological survey of Finland (GKT). The geophysical data set from the Chirano project area were co-registered to longitude-latitude coordinate system.

Using the Geosoft software, the unprocessed data from original tapes is extracted and positioned in x and y form which make up the pre-processing stage. The second phase consist of four procedures: a) gridding; b) calculating the residual magnetic field by subtracting IGRF from total magnetic data measured from the field c) micro-levelling the whole data set to get rid of any form of errors and d) integrating the different windows for each different type of data.

Using a series of linear and non-linear filtering routines, aerogeophysical datasets can be well improved for better interpretation.

A wide range of processing techniques can be specific to diagrammatically improve the effects of the selected geological host rocks using mathematical enhancement algorithms (Milligan and Gunn, 1997; Geosoft Inc., 1995). The discussions below show the effects of some of the applied mathematical enhancement algorithms.

#### **4.4 Aeromagnetic Data**

Even though the magnetic survey has been used extensively in mapping of mineral deposits for decades, modern advancement in acquiring magnetic data, processing and interpretations have amplified the significance of magnetic methods; predominantly the high resolution aeromagnetic survey (Clark, 1997).

The original data in the GDB (geodata base) format, after having been projected into Longitude and Latitude Coordinate System (using Geosoft software), the geographical coordinates of the study area (also in longitude and latitude) was superimposed to extract the database for this project. The minimum curvature technique was applied using the grid and image tool in gridding the extracted database for both the radiometric and magnetic data. The magmap tool offering a number of utilities was implemented to assist magnetic-anomaly grid (observed magnetic field less the Definitive International Geomagnetic Reference Field) to be calculated for the right time of year and altitude of the aircraft during survey and apply the following filters.

Magnetic variations in the magnetic field of Earth originate from the iron II oxide concentration in the localized rocks and the geological interpretation of these anomalies are made easier with the help of resulting images and maps (Liu and Mackey, 1998). Once a grid was produced and the necessary filters applied it was displayed as an image using the grid and image tool.

In order to facilitate interpretation, Analytic Signal Amplitude and Two-Dimensional Fast Fourier Transformation (2D-FFT) filters were used to improve the quality of the data. The 2D-FFT filters used included Reduction to the Pole, First Vertical and Horizontal Derivatives, Downward and Upward Derivative, and Analytic Signal.

#### **4.4.1 Reduction to the Pole (RTP)**

The reduction to pole (RTP) algorithm was applied to the total magnetic anomaly, TMI because the data was acquired from closer to the magnetic latitude. The azimuthal filter in the frequency domain was used to reduce the directional error created the alignment of the domains of the geomagnetic field (Phillips, 1997). The estimations of inclination and declination were prepared using the mean coordinates of the region, an inclination of  $-14.8^{\circ}$  and declination of  $-5.05^{\circ}$  to an average total field of 31955.84 nT.

#### **4.4.2 First Vertical and Horizontal Derivatives**

The Reduction to Pole (RTP) grid data was subjected to first vertical derivative (1VD) filter. This filter allows small and large amplitude responses to be more equally represented. The 1VD grid in gray-scale helped enhances linear features in the area (folds and fault). The RTP grid is also enhanced by the application of first horizontal gradient or derivative (1HD) which is significant when mapping linear geological structures like fault or dykes from the aeromagnetic data. The filter provides higher resolution and better accuracy at wider spacing. The horizontal derivative helped in identifying geologic boundaries of formations in the study area.

Higher derivative images with different filters such as 2VD produced interesting results but several distortions were noted to occur in the images due to the increase in the noise level introduced in the data by this process. These images were therefore not used in the

interpretation but were only used as a guide in the interpretation from the first derivative images.

#### **4.4.3 Analytic Signal Amplitude**

The analytic signal amplitude was estimated using the actual (residual) magnetic field. The analytic signals filter does not depend on the geomagnetism field direction (inclination and declination) of the host body. High analytical signal amplitudes are recorded around areas of large mineral deposits (Liu and Mackey, 1998).

#### **4.5 Airborne Radiometric Data**

Airborne radiometric data helped to map lithology of the area. Most often, a better relationship is recognized in the radiometric data around rocks that are weathered and unweathered. These data when correlated with that of electromagnetic, magnetic and geochemical are usually helpful in the explorations of mineral deposits (Gunn et al., 1997; Shives et al., 2000).

This is one of the most rapid techniques for soil chemistry surveying of the uranium, thorium and potassium. This part explains some enhancing techniques of the radiometric data which include ternary, Ratio, Potassium, Thorium and Uranium maps for the study area. The purpose of enhancing the data is to identify and interpret signatures related with the source rocks for potential mineralization.

##### **4.5.1 Total Count (TC), Potassium (K), Thorium (Th) and Uranium (U) Channels**

By using the grid and image tool in Geosoft software, the total count image was produced after micro-levelling the entire dataset to get rid of any apparent residual errors. These images were generated by using mini-curvature gridding since the data were collected in grid window. The images were then related with the geological units, patterns and trends.

The potassium image was developed to identify regions of strong potassium concentration. Thorium is usually considered as a stable element which does not move easily. However, several deposits of gold depict increases in potassium and thorium which suggest that thorium was moved during hydrothermal activities (Silva et al., 2003). Reduction in thorium and increase in potassium shows an signs of alteration for most deposits of ore (Ostrovskiy, 1975). It is for this and many more reasons that led to the developing of the Th image map. The uranium image especially ratio map of uranium and potassium (U/K) shows good definition in mapping the granitoid rocks which show low uranium but high potassium concentration.

#### **4.5.2 Composite Images and Ratio Maps**

The radioelement composite image presents a single display of the three radioelement concentrations. This map suggests to a great extent the lithological differences due to the variations in color. The uranium, thorium, and potassium maps emphasize regions where the specific radioelement has a total and pretty higher amount (Elawadi et al., 2004).

Uranium, potassium and thorium were represented with blue, red and green respectively in generating the ternary map. In order to minimize the poor signal-to-noise ratio especially in the uranium concentration the blue color was used. The maps discussed in the chapter five were generated with the relative intensities of color to represent slight differences caused the rock types. To enhance the contrast of the histogram of potassium, thorium and uranium a histogram was used to present the finest color differences prior to generating the ternary map.

Nevertheless, for this research, the ternary image generated demonstrated a better outcome.

In order to get rid of lithological differences and variations caused due to soil moisture, non-planar nature of the host rock and errors related with altitude correction, ratio images were as well produced. According to Silva et al. (2003), lithological variations have a tendency to be

removed because radioelement amounts normally change as lithology change. For example U/Th and U/K ratios were created for locating the areas where relative amount of uranium are strong.

#### **4.6 Interpretation of Airborne Geophysical Data**

The different lithological units and associated geological structures were deduced from the aeromagnetic and airborne radiometric datasets of the Chirano area by considering the signatures that are associated with these features. Usually, lithologic units of sedimentary, metamorphism, igneous and geological processes such as deformational tectonic geological structures (fault, folds and other lineaments) produces distortion on a uniform magnetic and radiometric signal. These deformations thus assist in the interpretation of geological structures and various lithological units in the study area.

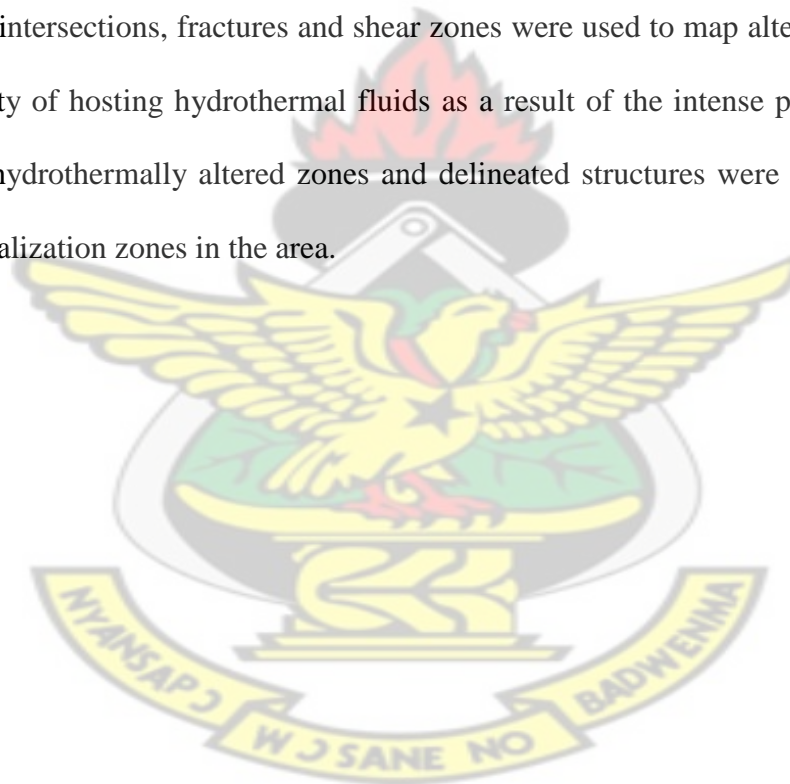
The major geological unit boundaries and structures outlined along with the magnetic signatures and their boundaries coinciding with regions of increasing contrast in intensities of the geophysical data. The major litho-stratigraphic unit of the area and the sequence of geological events (intrusion, deformation) were used to establish the tectonic framework to aid geology and structure mapping.

High magnetic anomalies associated with low K concentrations were used to map meta-volcanics. High K concentrations associated with moderate magnetic anomalies were used to map the weathered granitoids. Meta-sedimentary rocks typically have a layered magnetic response, largely composed of linear magnetic anomalies.

Planar fracture or discontinuity in geophysical signatures associated with the various lithological units, across which there has been major displacement along regions of weakness as a result of tectonic movement and undulating lineaments resulting from permanent deformation were used to delineate faults and folds respectively. Local separation or

discontinuity plane in magnetic signatures about which there are no displacement were used to delineate fractures. Discontinuities that mark distinct terranes which involve rock deformation at the edges of lithological tectonic units and corresponding to anomalous low Th/K ratio were used to mark shear zones.

Hydrothermally altered zones are often associated with elevated K. The reason is that K becomes more receptive in shear zone due to the breakdown of feldspars, biotite and muscovite in clay minerals. High structural connectivity and areas reflected by low magnetic anomalies were of much importance. In regions where the two coincide and are also marked by faults, fault intersections, fractures and shear zones were used to map alteration zones due to the possibility of hosting hydrothermal fluids as a result of the intense permeability. The integration of hydrothermally altered zones and delineated structures were used to generate potential mineralization zones in the area.



## CHAPTER FIVE

### RESULTS AND DISCUSSIONS

Aeromagnetic and airborne radiometric datasets were used to explain the geology, structure and alteration zones in the study area. High resolution maps were created from the airborne magnetic and radiometric datasets that depict main lithology and structural features present in the Chirano area. The reasons for interpreting these maps are to identify visually:

- the individual lithology and
- delineate geological structures

To delineate potential mineral deposits areas with high patterns of the radiometric elements which coincides low magnetic anomalies are suspected. This may occur from alterations or possible invasion of hydrothermal fluids which are capable of transporting economical metals.

#### 5.1 Interpretation of Magnetic Data

Magnetic variations in the geomagnetic originate from the iron II oxide concentration in the localized rocks and the geological interpretation of these anomalies are made (Silva et al., 2003). The main aim of using the magnetic data is to outline the geology and geological structures. Geological structures normally serve as means through which hydrothermal fluids are deposited and are important element in mineral exploration (Amenyoh et al., 2009). Linear features in the granitoid, metamorphosed belt and basin rocks are observed as high magnetic anomalies. The concentration of magnetic minerals or their excessive destruction by alteration especially along tectonic structures allows the detection of geological structures (Plumlee et al., 1992).

### 5.1.1 Total Magnetic Intensity (TMI) Image

Fig. 5.1 is a total magnetic intensity map of the chirano area. This map was gridded with minimum curvature method and displayed with pseudo colors. This map shows different magnetic anomalies corresponding to different lithologies and geological structures in the study area. The amplitude of a magnetic anomaly depends on magnetization which subsequently corresponds to the magnetic susceptibility of the rocks at specific geographical locations.

The rocks formations at low magnetic latitude (Close to the Earth's equator) areas are magnetized in the same direction as the magnetic field of the Earth therefore a good number of the high magnetic susceptible regions show low magnetic values while less magnetic susceptible areas also show high magnetic values. This does not correlate to the expected magnetic anomalies (signatures) of the belt type granitoid (B1 and B2) metasediments (MS) and metavolcanics (MV) in the Chirano area. Hence, mafic formations with rich content in iron are producing weak magnetic anomalies whereas strong anomalies are produced by felsic formations which have low iron content.

Observed to the eastern end of the concession is another belt type granitoid B2 which has intruded the metavolcanics recording a very high magnetic susceptibility values.

When the data is transformed to correct the directional noise, the contact between the Sefwi metavolcanics and Kumasi metasediments and that of the fold caused by the intruding the belt types B1 and B2 showed demagnetization of the strong magnetite metavolcanics into less magnetic minerals such as hematite. This gave way for the inflow of hydrothermal fluids which is responsible for the demagnetisation through the faults and the serve fractures caused by the contact and the intrusion. These areas of quiet magnetization are likely to host the gold mineralisation (Griffis et al., 2002). Some lithologic contacts, faults and fractures are shown

as magnetic low although not continuous in some regions. The folding of B1, MV and MS at the central part of the area is as a result of the intrusion of the Belt-type granitoid.

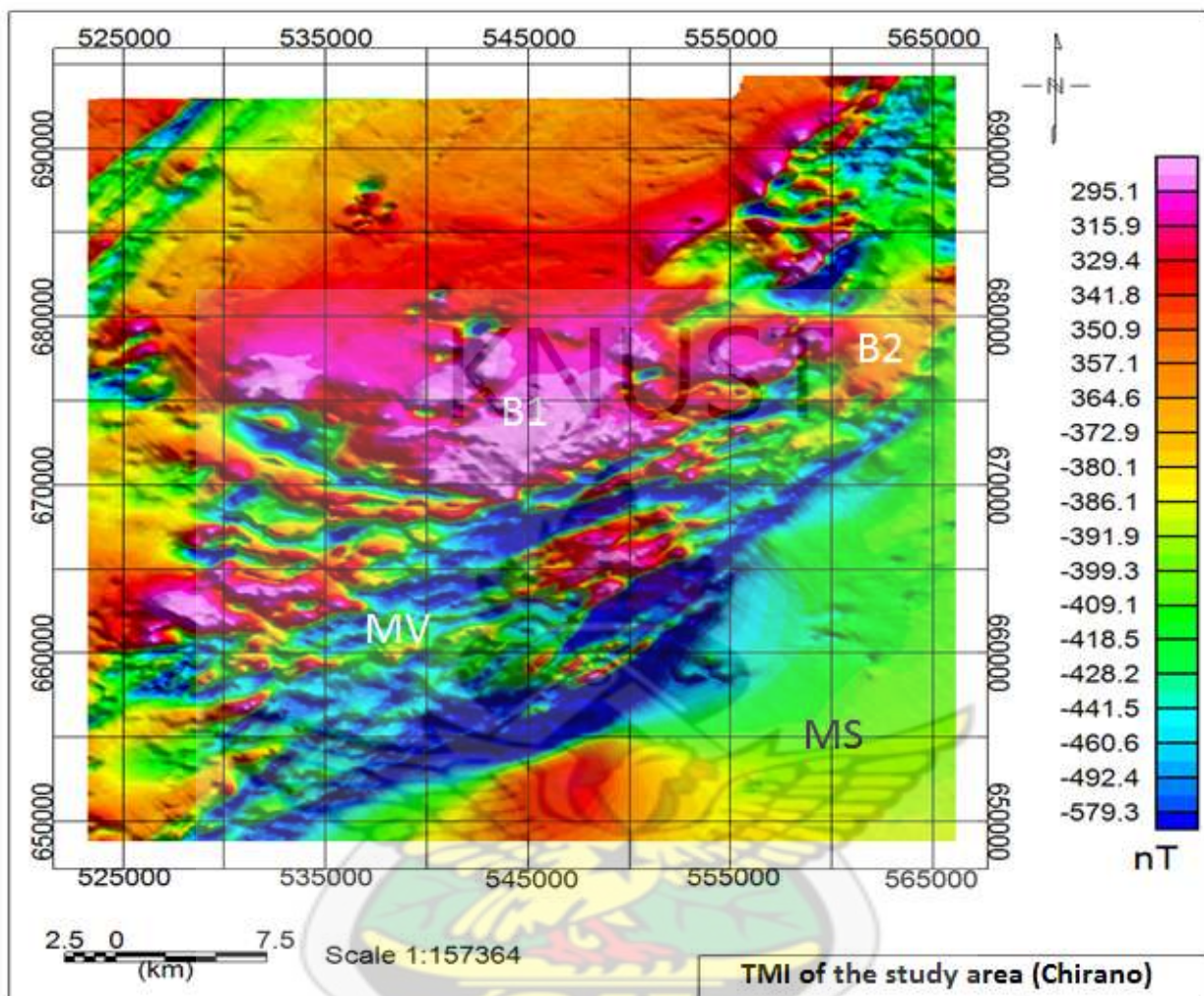


**Figure 5.1:** TMI Map of the Study Area (Chirano Area).

### 5.1.2 Reduction to the Pole (RTP) Map

The reduction to pole magnetic anomaly image (Fig. 5.2) depicts both low and high frequencies coming from the magnetized rocks in the region. The strong anomalies with high frequency shows the rich content of iron oxides within metavolcanics. Asymmetric anomalies (caused by the non-vertical inducing field) are difficult to relate to the source bodies or geometry causing the anomalies in magnetic survey (Murphy, 2007). To place the anomalies from the residual magnetic field directly over the magnetic field resulting from causative rocks that bring about these anomalies, the TMI grid was transformed into

reduction to the pole (RTP) grid using the 2D-FFT filter in Geosoft software to make easy the interpretation of the magnetic data set. This map of RTP sharpens the contacts between the magnetic high and low patterns and also emphasized on anomalously magnetic susceptible zones possibly coming from deeper sources. The RTP map clearly illustrates B3(belt type granitoid) which was not very evident in the TMI map. The foldings of the metavolcanics MV by the intruding belt type granitoid (B1) and metasediment (MS) are clearly defined.

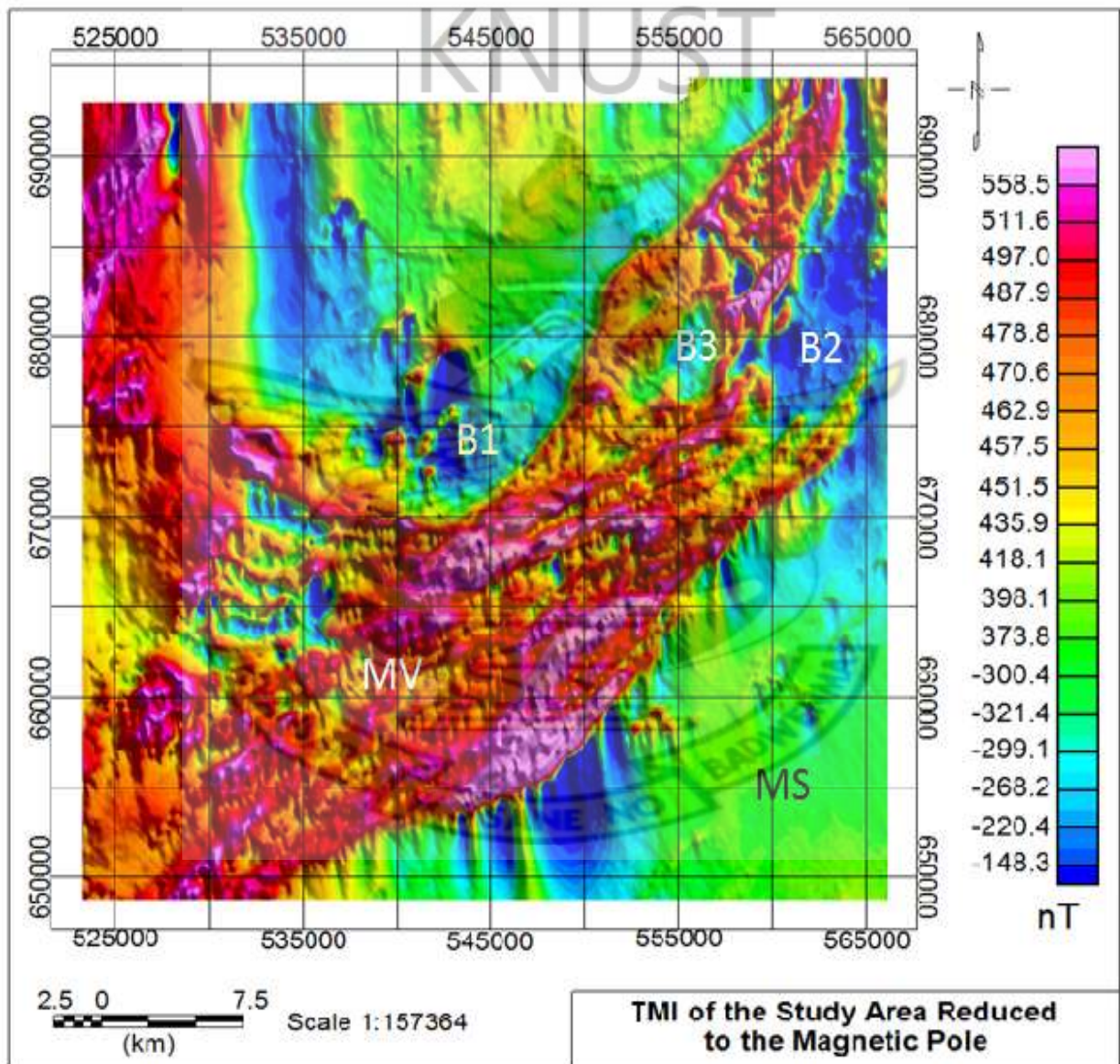


**Figure 5.2:** TMI reduced to the magnetic pole with  $I = -14.80$ ,  $D = -5.1^\circ$

The metasediments recorded low magnetic susceptibilities mainly due to the mineral content of the rocks beneath generally muscovite and biotite. The belt type granitoid (B1) also revealed very weak concentrations of magnetic minerals because its intrusion destroyed the magnetization around.

### **5.1.3 Analytic Signal Grid**

A significant feature of the analytical signal is that it does not depend on the magnetization field of the source rock. The mineral deposits with high concentrations always show high analytical signal amplitudes. This shows that analytical signal amplitude depends on the magnetizing amplitude of the causative body (Nabighian, 1972; Roest and Pilkington, 1993). Figure 5.3 was generated from the total magnetic intensity (TMI) by applying the analytic signal filter. With the application of this filter, the main NE-SW fold was clearly mapped and recorded low magnetic susceptibilities values, an indication of demagnetization.

This algorithm shows the differences immediately obvious along the edges of the metavolcanics MV in the southwestern and the middle sections of the concession compared to the TMI and RTP maps in fig.5.1 and 5.2. The analytical signal amplitude was very helpful in mapping the edges of the individual lithologies (Fig. 5.8).

This filter just like the reduction to the pole also delineated the metavolcanics MV and MV1 to record high magnetic anomalies whereas the metasediments, MS and the belt type granitoids, B1, B2 recorded the low magnetic anomaly in Fig. 5.3 (Ansari and Alamdar, 2009) when applied to magnetic data acquired from regions close to the equator.

The weak magnetic susceptibility values of the felsic intrusive formations B4 and B5 which is similar to that of B1, B2 and B3 are delineated better in the figure 5.3 than in the reduction to pole and TMI images. The contact between the metavolcanic formation and metasediments

brings about the Bibiani shear zones (S1-S1) which the chirano shear zone forms part. It is responsible for the primary function in the localization of mineralization of the gold deposits.

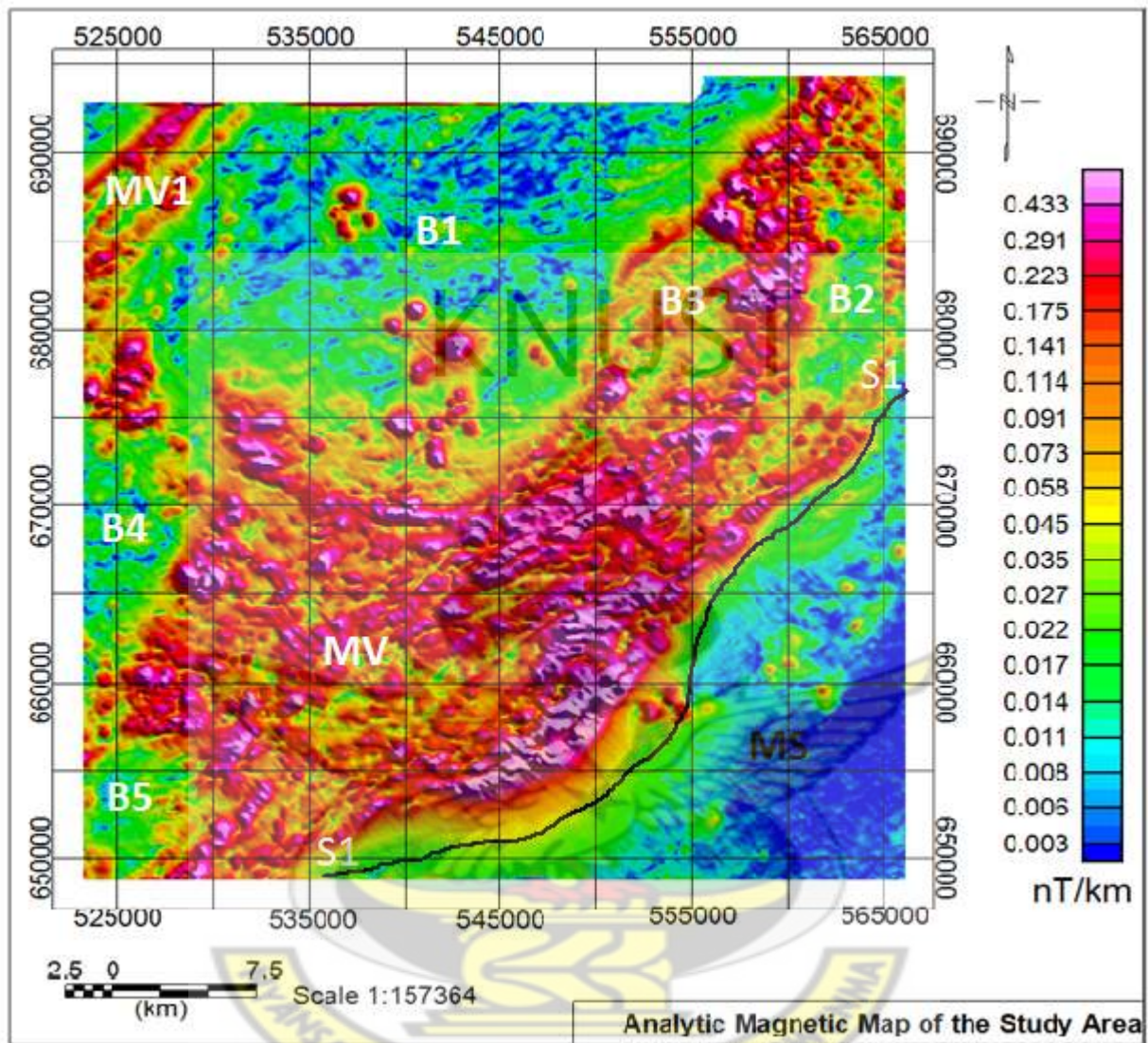


**Figure 5.3:** Analytic Signal magnetic map

#### 5.1.4 Digitized Elevation Map (DEM)

The Fig. 5.4 is a digitized elevation map that reveals the highlands and lowlands in the Chirano area. To the western, north-eastern and southern parts are the highlands (H1, H2 and H3) respectively. These regions are separated by lowlands. Fair lowlands, L2 of average peak 154 m is sandwiched between H1 and H2 just like the lowlands, L1 located at the southwestern regions are expected to amass the remains of weathered formations of H3. The

highlands H2 and H3 correspond to the high magnetic anomalies of the mafic metavolcanics, MV in the figure 4.2. The belt type granitoid, B1 is also associated the lowlands, L2 which produced low magnetic anomalies due to low content of magnetite.

The Kumasi metasediment basin MS located at the south-east of the area as L3 are seen as lowlands corresponding to the weak to moderate signatures of the magnetic data due to small content of iron forming minerals and expected to show like signatures when the reduction to the pole filter is applied. It is probable to amass weathered remains from H2 as well as H3.

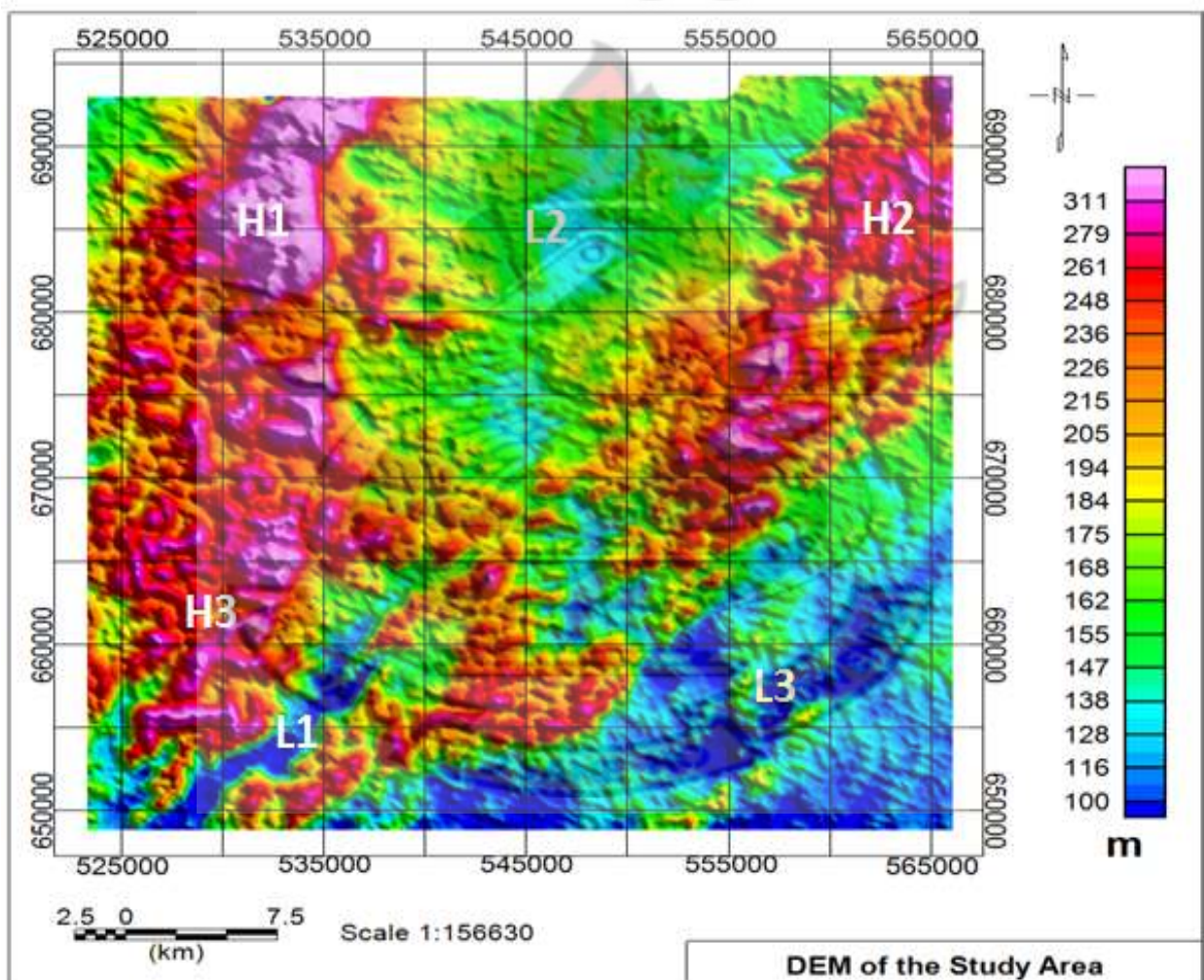


**Figure 5.4:** Digitized elevation map of the study area.

### 5.1.5 First Vertical Derivative (1VD) Map

The Fig 5.5 is a grayscale of the first vertical derivative continued upward to 100 m displaying near surface source magnetic features that are associated with geological structures. The 1VD and Upward Continuation operators have helped attenuate broad, more regional anomalies and enhanced local, more delicate magnetic responses because of their sensitive to shallow magnetic source bodies and contacts.

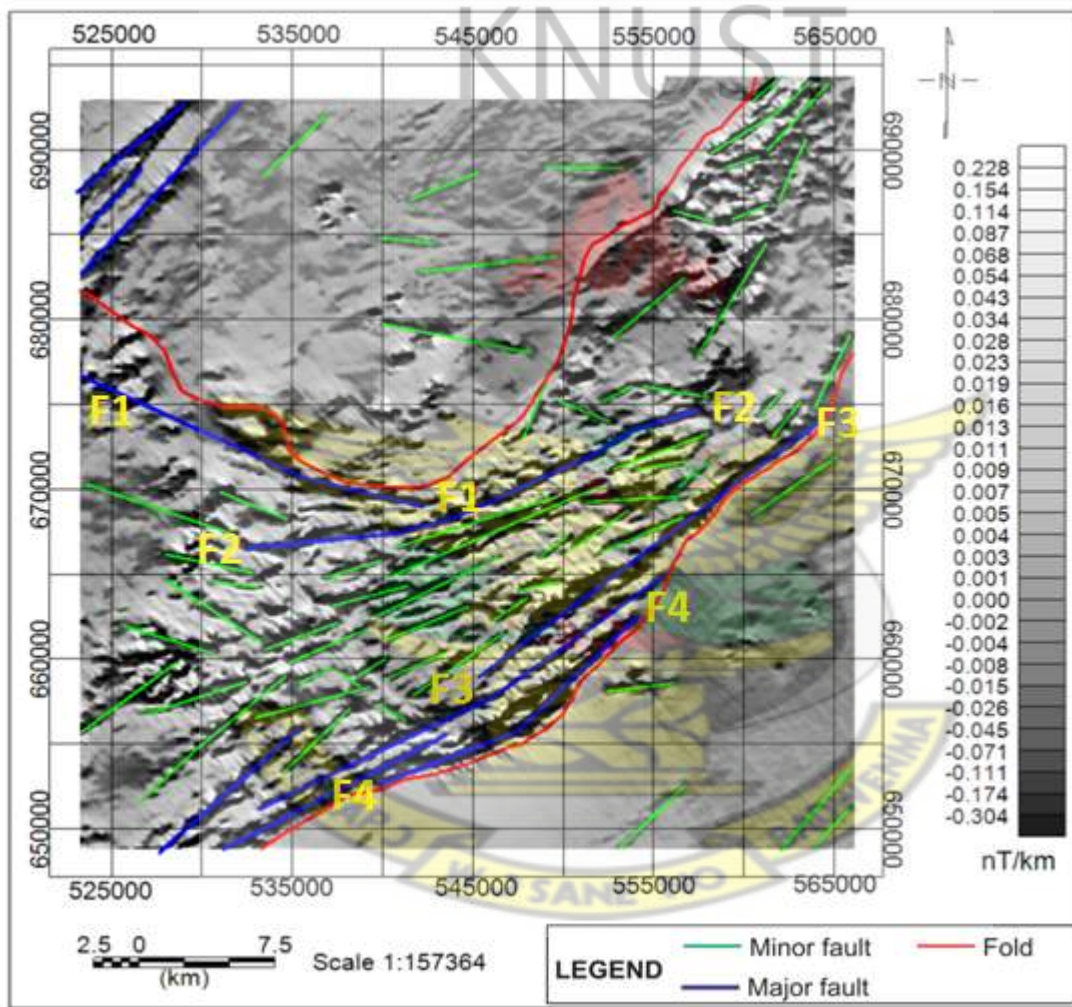


**Figure 5.5:** First order vertical derivative map showing magnetic structures

Keating, (1995) indicated that application of the first vertical derivative filter was used to remove the long waveforms of the field produced the magnetic causative body. This was very significant in improving the closely spaced resolution and superposed anomalies.

Assessment of the 1<sup>st</sup> vertical derivative image continued to 100 m (Fig 5.6), with the total field map (Fig. 5.1), depicts a clear enhances observed of structural features such faults F1-F1, F2-F2, F3-F3 and F4-F4 (green and blue lines), folds and fractures marked in the red lines, particularly in the southern and middle regions of the study area. The elongated folded meta-volcanic unit MV seen in the TMI and RTP maps is rather exposed in the 1VD continued to 100 m map as a collection of faulted structures trending in the NE-SW direction with the boundary well defined. The granitoid intrusions B1, B2, B3, B4 and B5 also have their boundaries well enhanced by the low magnetic anomaly forming an oval shape.

#### **5.1.6 Tilted Magnetic Filtered (TDR) Map**

The magnetic map Fig. 5.7 was used to infer the delicate geological outlines of the different structures improved by the previous filters. The structures seen in the analytic map (Fig. 5.3) as high magnetic anomalies are now identified in the magnetic TDR map (Fig. 5.6) as low magnetic anomalies cutting across the collection of the structures related to metavolcanics, MV, MV1. The structures noted in fig. 5.5 (faults and folds) with the magnetite and pyrrhotite contents were destroyed by magnetization and carbonate alterations (Airo and Karell, 2001), hence, registering a low magnetic signature.

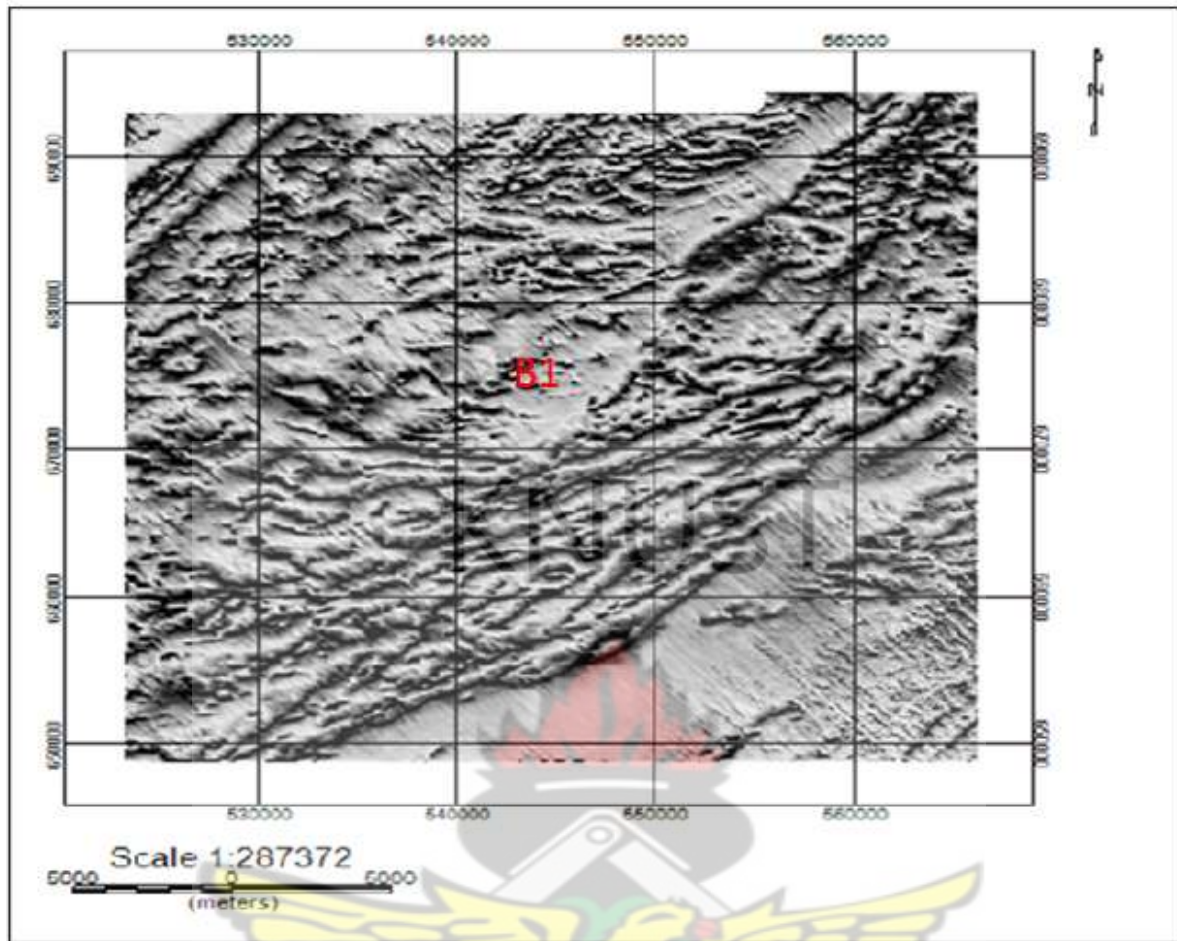


**Figure 5.6:** A Magnetic TDR map in grayscale.

### 5.1.7 Delineated Geological Structures

Two main exercises are entailed in the interpretation of the aeromagnetic data. To start with is the behavior of the magnetic data and the physical features of delineated anomalies that are to be discovered. Again, the geological importance of the indications of the magnetic data has to be deduced. When the RTP map was superimposed on the geological map of the area, it gave a rough idea about the time-sequence of formation of the lithologies and some geological formations within the study area.

In the attempt to identify the structures and geology of the area, the first step involved identifying various recognizable patterns directly from the TMI and mathematically enhanced maps of the residual data and connecting them to likely physical sources pertinent to the

division of the specified property of the causative body. Secondly the geophysical interpretation will be appropriately related to the geological settings to obtain the utmost gain from the aerogeophysical survey. The airborne magnetic maps of the Chirano area reveal high magnetic resolution and good contrast between geological structures and their host lithologies providing information useful for structural delineation. Rock deformations such as fracturing, faulting and shearing are not uniformly distributed in their host rocks. Often these structures are associated with different uncharacteristic magnetic signatures of the host rocks. Aeromagnetic data record these magnetic signatures which are used to identify these structures and their sequence of occurrence (Amenyoh et al., 2009).

The TMI map (Fig. 5.1) regardless of the degree of magnetization, shows the apparent system of the structures dominating in the area. Folding of the meta-volcanic rock units MV caused by the contact of the metasediments formation (MS) between them, trending in the NE-SW direction were clearly seen. Again another folding caused by the intrusion of the belt type granitoid (B1) was also identified around the central part of the map. This is a possible volcanic crater that might be associated with the meta-volcanic belt or a disseminated sulphide deposits. Fig. 5.10 reveals enhanced structural features that include shear zones, faults, shear and fault intersections and fracture systems as magnetic anomalies that mainly trend NE-SW.

The main Bibiani Shear Zone of which the Chirano Shear zone form part which is caused by the contact between the metavolcanics MV and metasediments MS shows a widespread faulting which includes F1-F1, F2-F2, F3-F3, F4-F4 and a very prominent splay faults (Fig. 5.5 and Fig. 5.8) (Griffis et al., 2002). The contact zone is noticeably a main fracture system of regional level (Griffis et al., 2002) and is primarily responsible for the localization for the mineralization of gold. There is an old reactivation structure, which seems to be led by the

several intrusions of granitoid including B1, B2, B3, B4 and B5 in figures 5.3 and 5.5 which are found along the contact zone.

The deformations of structures along S1- S1 are of a later deformational event appearing in the NE-SW direction which is characterized with low magnetic anomalies. Open folding is evident within the basin metasediments whereas the folding of the metavolcanic formation to the central part due to the granitoid intrusion, B1 develops many more open structures. The transitional zone between the basin and belt units displays extensive faulting with a complicated and prolonged history of deformation. Intensively faulted and fractured zones associated with folded magnetic signatures are described as shear zone. The regional NW-SE directed compressions which occurred within the area produced the strong angle reverse structures such as the NE trending shears in figure 5.5 (Cozens, 1989). The mineralization of gold is strongly characterized with the series of quartz stockwork mostly sourced in granitoids like B1 as indicated in the TDR image in figure 5.7 (Griffis, 1998). The intrusive belt type granitoid B1 created severe fractures which made it possible for hydrothermal liquids to settle along these open fractures.

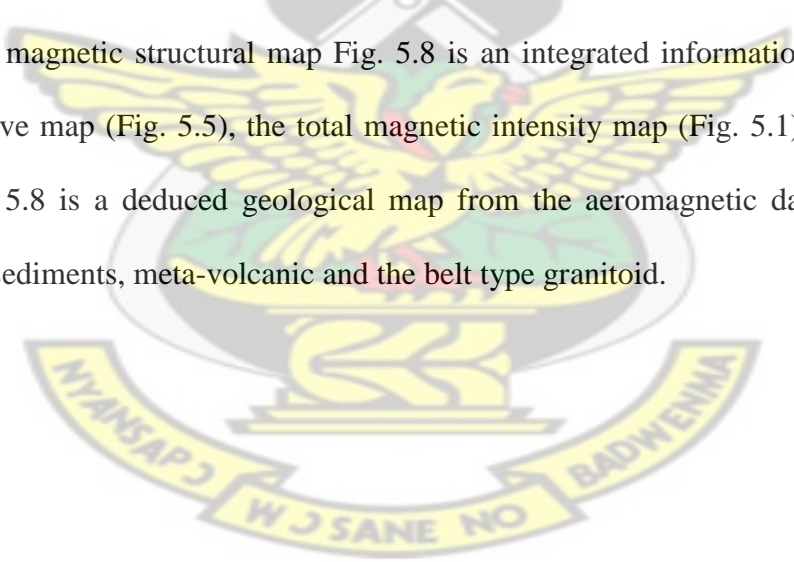
Chirano host numerous intersecting faults found almost in the NNW to N, NE and E-W directions. The intense folds along the central and southern edges of the metavolcanics MV were caused by the intrusive belt type granitoids B1, B2 and B3. The strength of the invasion is accountable for greater part of the faults and shearing happening along the edge of the Kumasi metasediments basin.

Faults that evolved through linkage are commonly associated with sets of splays that break off the main faults. Each splay accommodates a portion of the deformation transferred from the main faults and has its own termination point. Structures are interpreted from the aeromagnetic data where they terminate as a series breaks in smooth magnetic signature serve

as marker units within the stratigraphy (Murphy, 2007). The structural features throughout southwestern Ghana are believed to have resulted from one major, progressive NW-SE deformational event (Eisenlohr and Hirdes, 1992) which is thus responsible for the folding of the discontinuous structures of MV and MV1.

After the application of several filters like analytical signal, 1<sup>st</sup> vertical derivative, magnetic TDR to the magnetic data, numerous faults and some folds were clearly delineated (Fig 5.8). Severe faulting and shearing within the Sefwi metavolcanics were caused by the intruding the belt type granitoids. These shears and faults paved the way for the hydrothermal liquids from high pressurized zones to settle along the shears and faults which destroyed the magnetization of these regions because of the high temperatures of the liquids. Therefore it can be inferred that magnetic intensities related faults are mostly weak.

The interpreted magnetic structural map Fig. 5.8 is an integrated information from the first vertical derivative map (Fig. 5.5), the total magnetic intensity map (Fig. 5.1) and TDR map (Fig. 5.7). Fig. 5.8 is a deduced geological map from the aeromagnetic data showing the Birimian meta-sediments, meta-volcanic and the belt type granitoid.



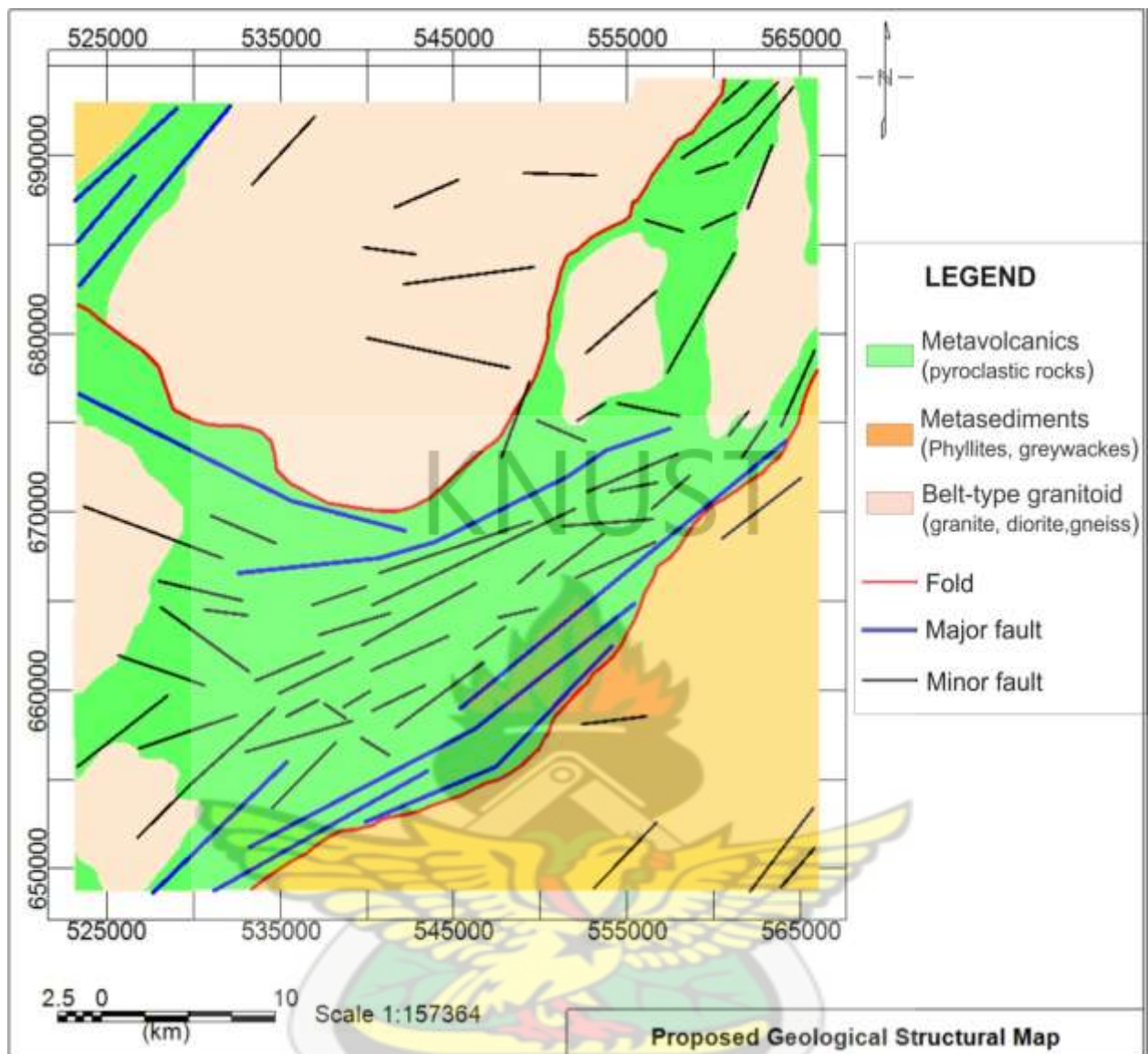


**Figure 5.7:** Proposed geology map from aeromagnetic data.

## 5.2 Interpretation of Radiometric Data

The differences in the mineral content of surface geology can be better explained using the radiometric survey data which is also useful in mapping lateral lithologies. Airborne radiometric surveys determine concentration of gamma radiations resulting from the mineral forming rocks (Telford et al., 1990). These gamma radiations comprise thorium (Th), potassium (K) and uranium (U) which are present in small amount in the soil and naturally breakdown to emit the gamma radiations. The gamma ray spectrometer is used to measure the gamma ray emissions; also the individual energy levels of the associated radionuclides

are established. This information about the energies of the radionuclides was helpful in the mapping of the lithologies by determining if a spatial correlation exists between the radiometric data and lithological rocks.

### 5.2.1 Potassium (K), Thorium (Th) and Uranium (U) Channels

The radiometric survey data produced the various potassium (K), uranium (U) and thorium (Th) anomalies. The Kumasi metasediments produced high anomalies of potassium at the south eastern regions of the study area in figure 5.9.

Radiations of potassium basically emanates from potassium feldspar, predominantly micas include muscovite and biotite (Boadi et al., 2013) which is widespread in the felsic breccia of the metasediments, MS and are weak in mafic metavolcanic series (Manu, 1993) thus the weak K anomaly in the metavolcanics MV.

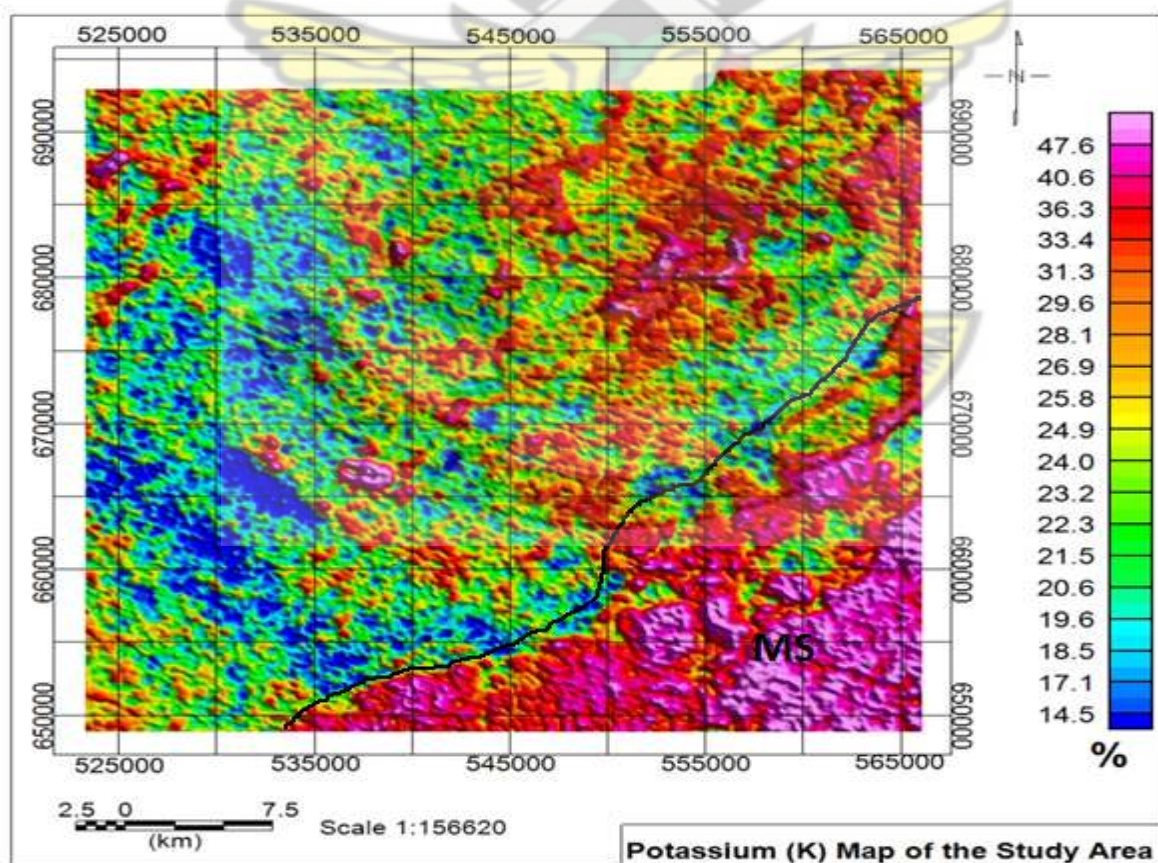


**Figure 5.9:** Potassium (K) Concentration Map of the Radiometric Data

Comparing Fig. 5.9 to the TMI map (Fig. 5.1) the hosting K concentrations evenly distributed in the SW direction represent the coarse-grained metasediment formations MS. The metavolcanics MV has a fairly low K concentration except around the NE directions which noted high K concentration.

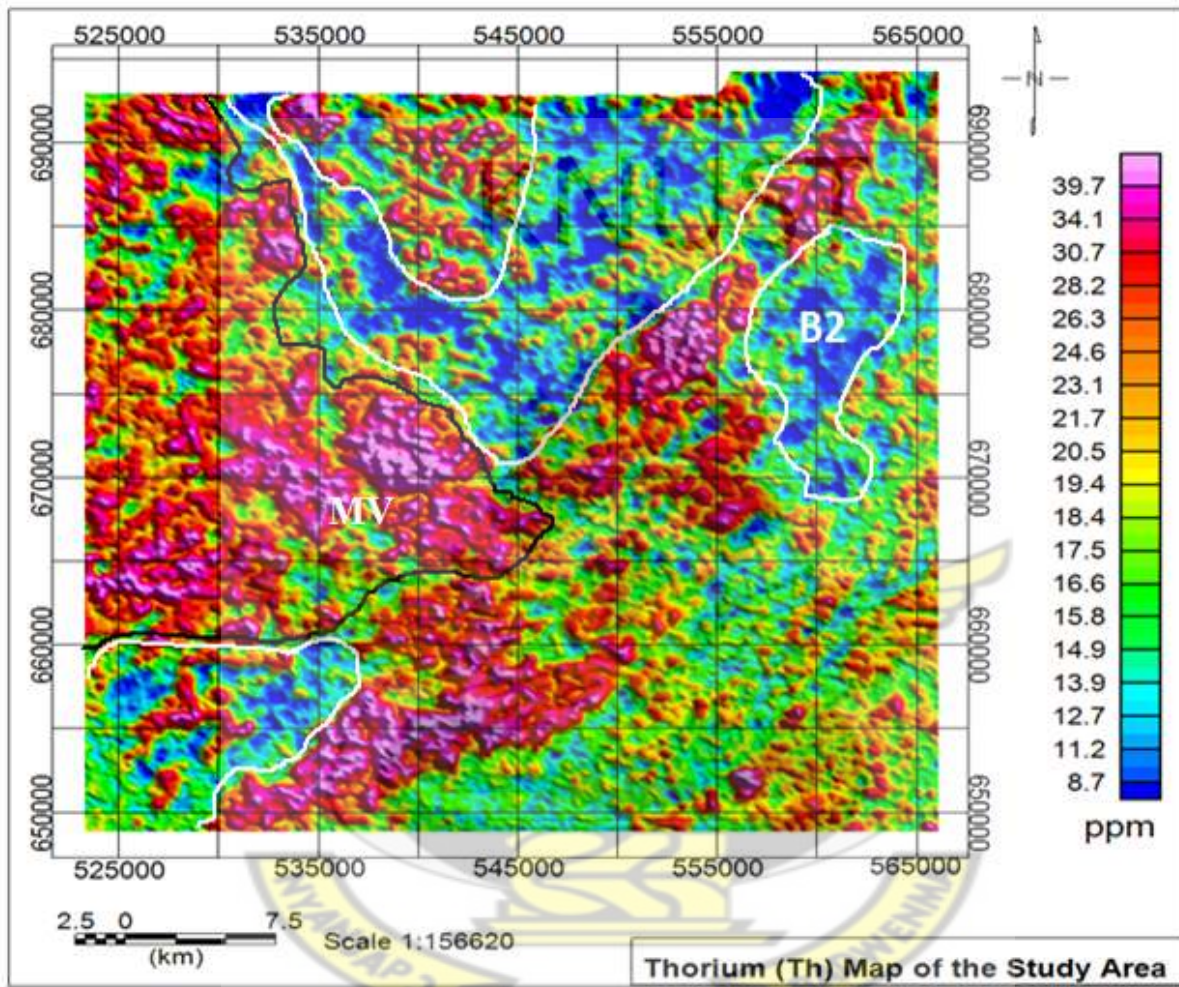


**Figure 5.10:** Thorium (Th) Concentration Map of the Radiometric Data

Anomalies in the thorium data in Fig. 5.10 helped map the boundaries of the metavolcanics and the meta-sediments. The western and southwestern regions of Chirano produced the highest thorium concentrations and are related partly with metavolcanics and the granitoids (B3 and B4).

The metasediments also produced low intensities of immobile and mobile Thorium (Silva et al., 2003) (Fig. 5.10) and U (Fig. 5.11) even though some high trace of these radionuclides can be marked within the formation.

The Belt type granitoid B2 registered relatively low Th concentration hence the areas with high thorium content suggest Thorium was moved during hydrothermal activity. The high elevation features H1 in the DEM map (Fig. 5.4) registered high Th concentration in the NW direction of Fig 5.4.

The south-west, north-west and north-east are associated with strong Th anomaly (Fig. 5.10) and U anomaly (Fig. 5.11) with the southeast and northern regions producing low thorium and uranium contents. The metavolcanics, MV depicts higher thorium anomaly (Fig. 5.10) such that its edges with metasediments, MS and the belt-type granitoids (B1, B2 and B5) are defined. Dissimilar to the potassium and the thorium images, the uranium image was not able to evidently indicate distinct edges between the MS and MV. To some extent low potassium and thorium intensities are recorded at the areas which match up to the belt-type granitoids B1, B2, B3 and B4. Thorium in general is considered very immobile (Silva et al., 2003) therefore the regions with low thorium concentration suggest thorium was moved during the invasion of the hydrothermal liquids. The high elevation feature H1 in the DEM map (Fig. 5.4) registered high Th concentration in the NW part. The region marked by the black polygon registering high Th concentration is as a result of highly weathered colluvial deposits from the high elevated geological units in the DEM map.

The uranium map depicts good characterization in delineating the B1, B5 and MS rock series which have low elevations in the DEM map (Fig. 5.4). The noise caused by the disparities in atmospheric radon contents at time of surveying depicts anomalies of short wavelength

causing an important streaking in the map. Despite the microleveling of the data, uranium maps displays such character (Minty, 1996)

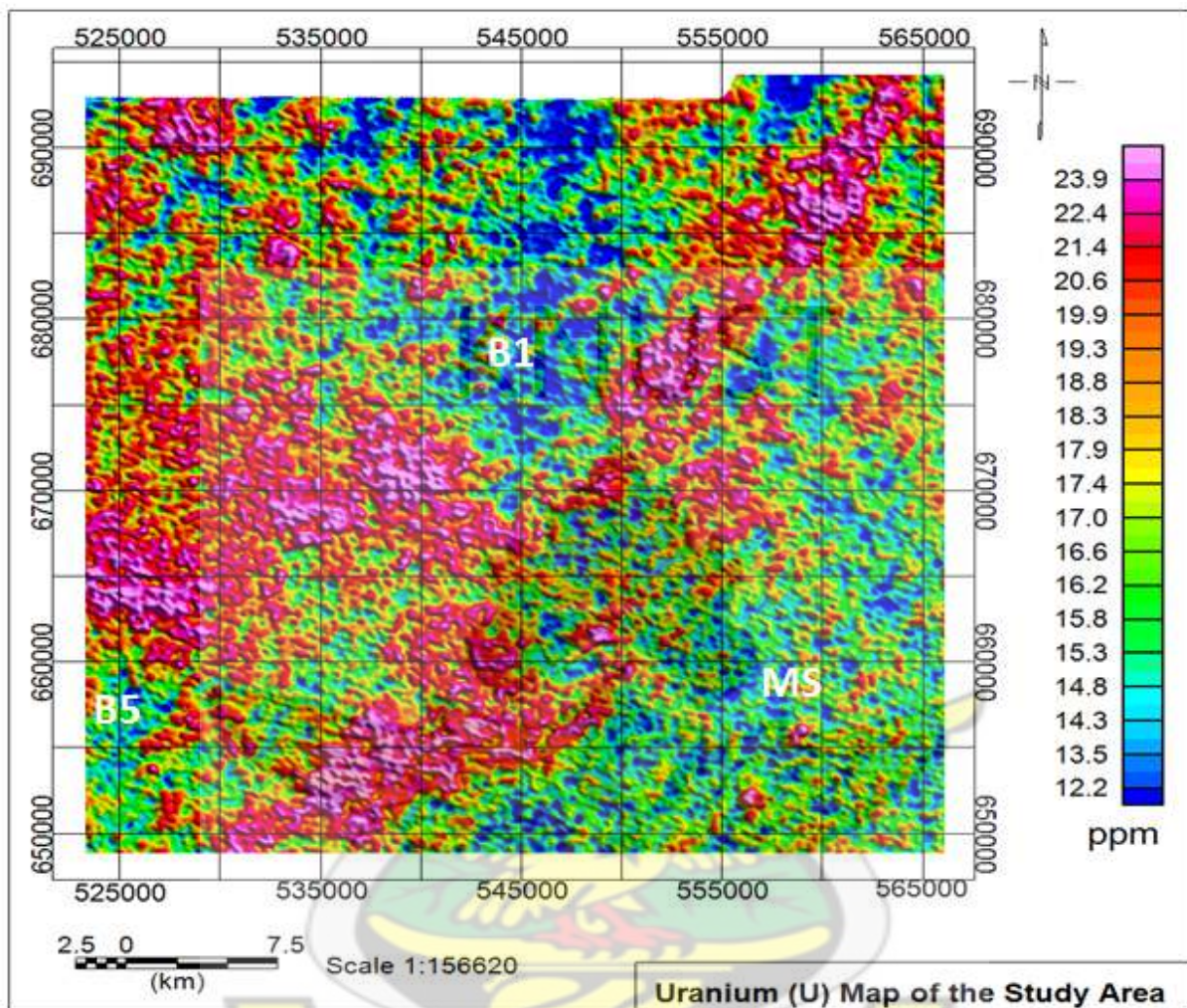


**Figure 5.11:** Uranium (U) Concentration Map of the Radiometric Data

### 5.2.2 Ratio Maps of K/U, K/Th and Th/U

Histogram stretching and band rationing of the channels were used to maximize contrast and highlight subtle features in the data. The Th channel and ratio channels (Th/K and Th/U) were used to assess the degree to which the source materials of regolith are weathered or leached since K response is associated with easily weathered minerals, whereas thorium and uranium are usually related with residual clay, oxides and accessory minerals (Wilford et al., 1997).

Fig. 5.12 represents K/Th (reverse Th/K) concentrations which map some lithologic contrast and enhanced alteration signatures. The increase in K content and decrease in K/Th ratio observed for the mafic meta-volcanic rocks (MV) is indicative of hydrothermal alterations. This is because mafic volcanic rocks generally lack K-bearing minerals and K enrichments are not accompanied by Th during hydrothermal alteration processes (Dickson and Scott, 1997). The K/Th ratio image of (Fig. 5.12) shows that, high content of the potassium in the red color implies weak content of thorium and vice versa. Reduction in the thorium with increase in potassium (Ostrovskiy, 1975) occurring at the shear contact zone between metavolcanics and metasediments in the NE direction has accumulated various deposits of ore. On the other hand, a number of mineralization of gold districts demonstrate a rise in potassium and thorium like the intrusion of the belt type granitoid in the NE within the metavolcanics implies that thorium was mobilized during the hydrothermal activities.

This information led to the detection of hydrothermal alteration zones within the area (Fig. 5.12). Generally, only K and other metal constituents are added to the host rock by hydrothermal solutions, and it is easily observed in mafic units or along lithologic contacts where the hydrothermal alteration is intensive.

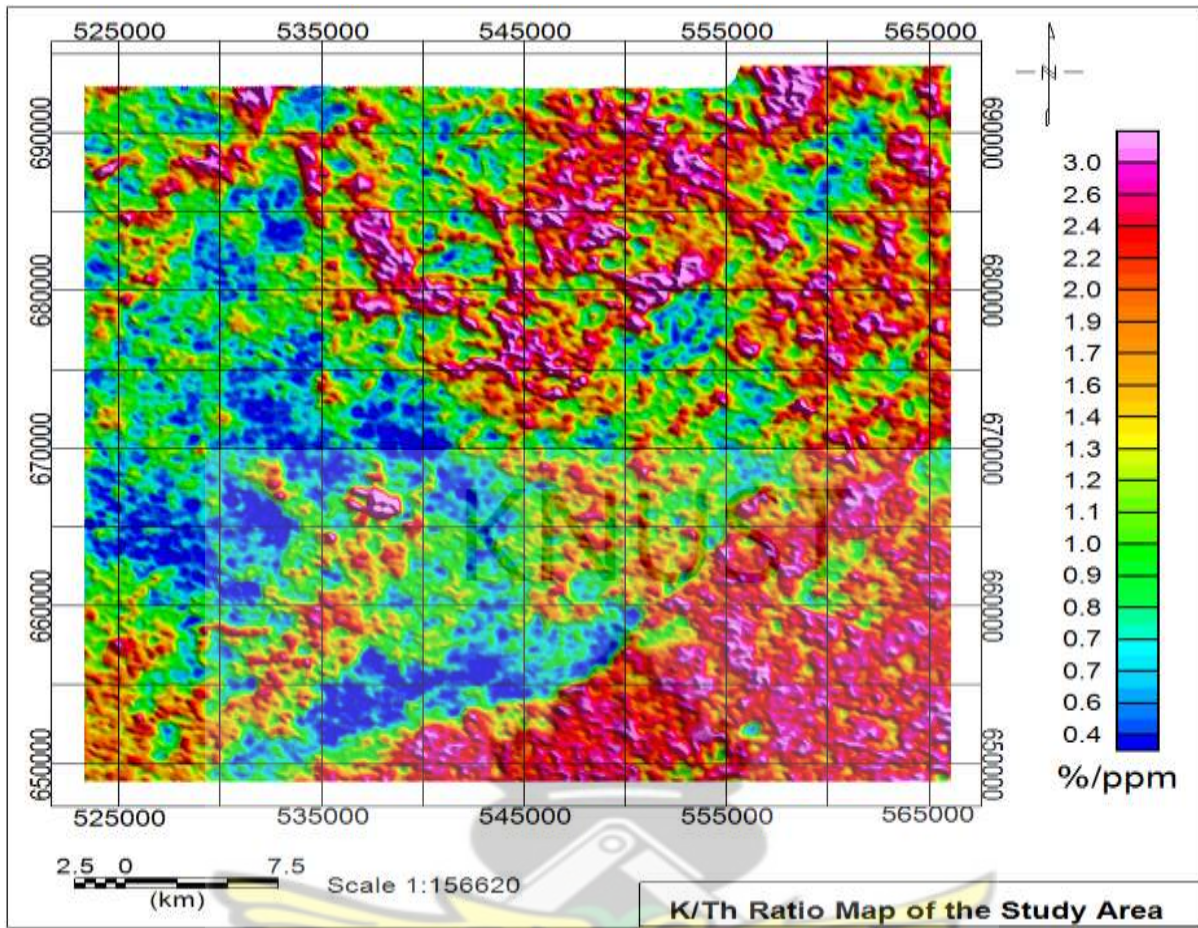


**Figure 5.12:** A ratio map of thorium and potassium (K/Th)

The U/K (reverse of K/U) ratio was used to determine areas where contents of U are relatively strong. A number of the U intensities are associated with zones of mineralization of gold delineated in contact with and within the metavolcanics. The Metavolcanic lithologic units and the belt type granitoid at the NE and central parts of Fig. 5.13 recorded high U concentration (but low K) and the metasediments showed high K concentration (low U).

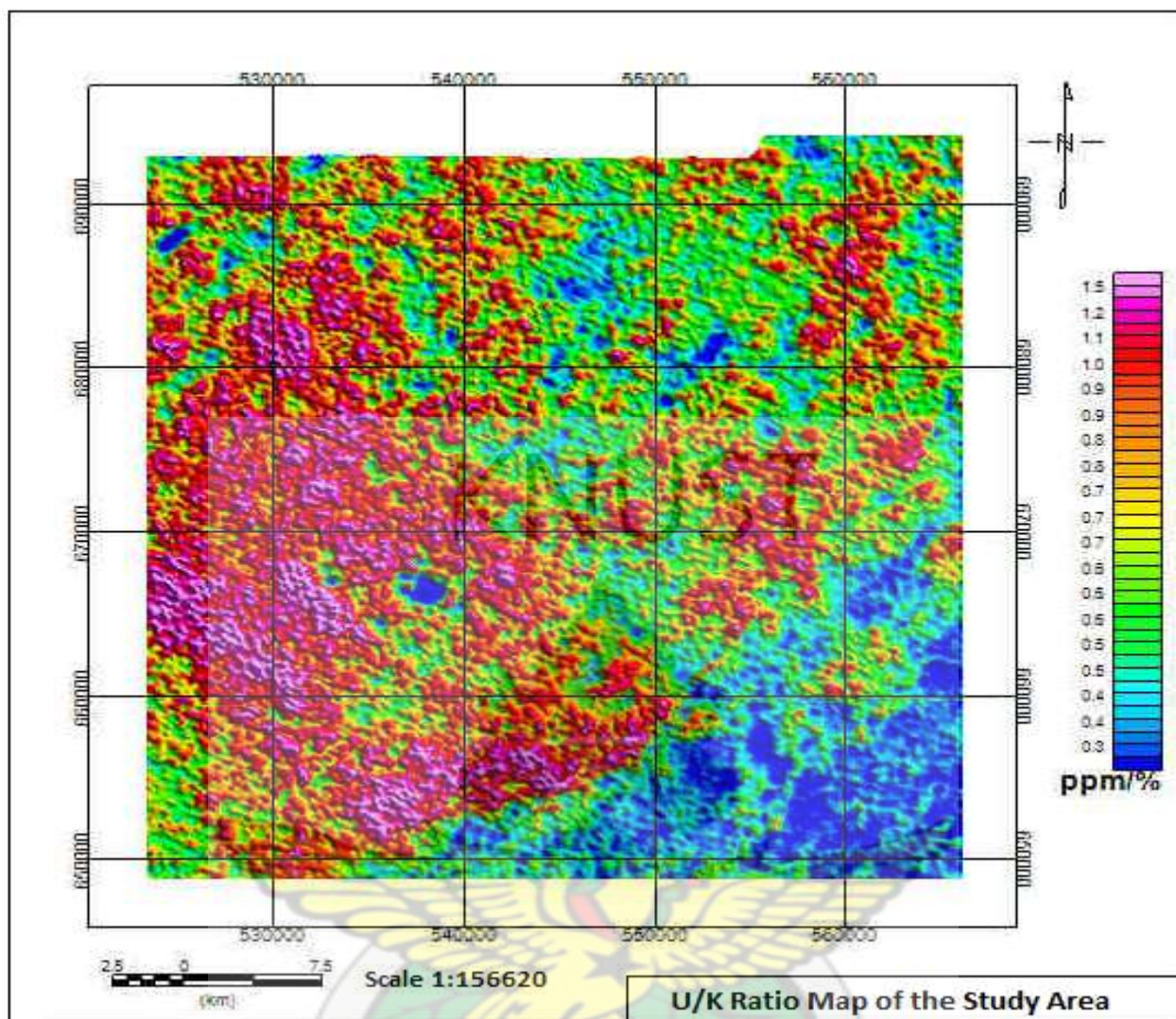


**Figure 5.13:** A ratio map of uranium and potassium (U/K)

High K/Th (Fig. 5.12) and low U/K (Fig. 5.13) over potassic formations within the concession are likely to be characterized with slightly weathered and highly leached soils respectively. The ratio images of Th/U (Fig. 5.14) shows that two-thirds (2/3) of the area is dominated by high Th concentration which correspond to high elevations in the DEM map (Fig. 5.5). The Th/U map highlights Th alteration zone, reflecting coincidentally increased Th and lowered U or K. The Kumasi basin (metasediments) formations are seen to record high Th concentration and low U concentration in Fig 5.14

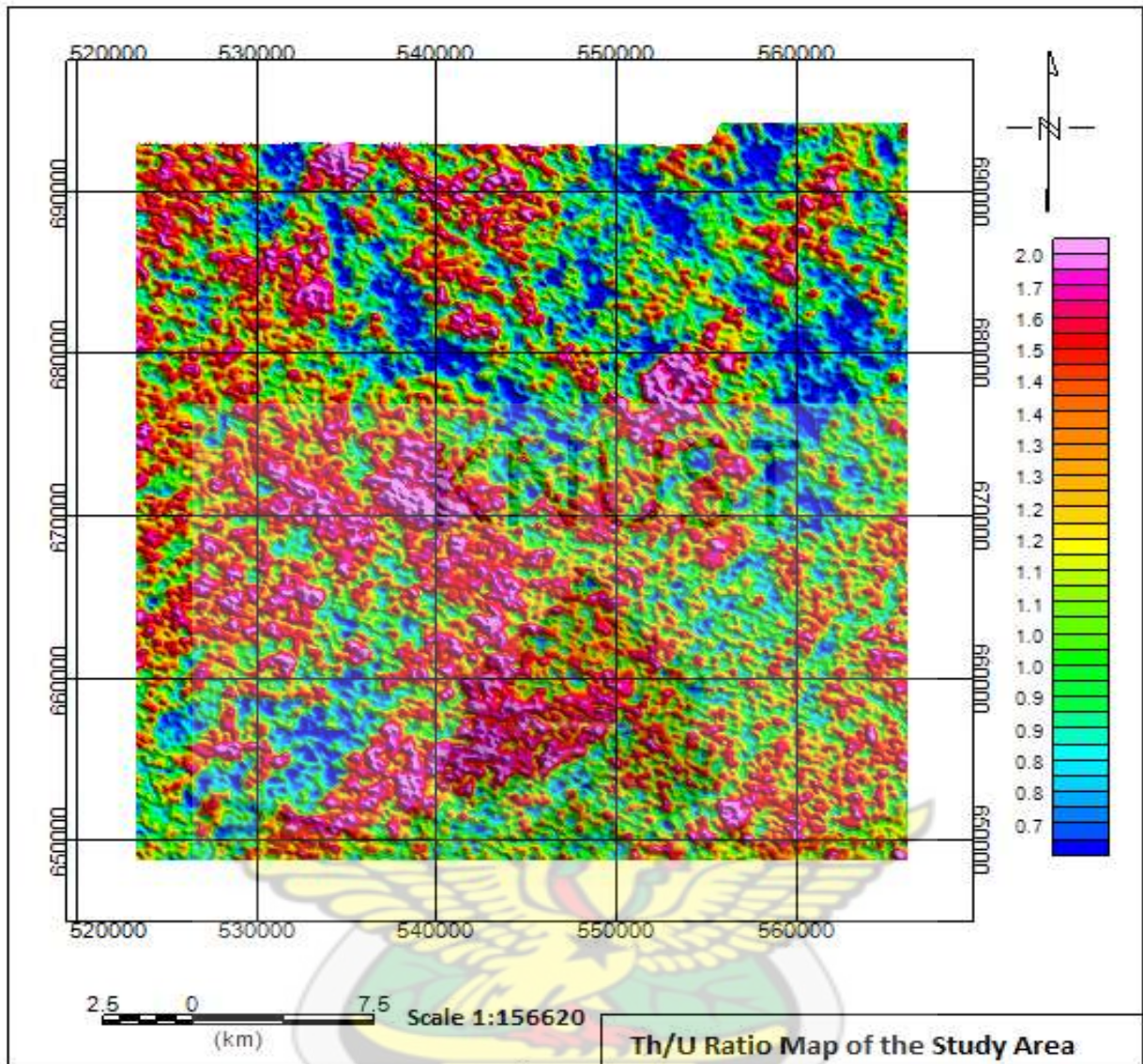


**Figure 5.14:** A ratio map of thorium and uranium (Th/U)

### 5.2.3 Composite Images (Ternary map)

The Ternary image Fig. 5.15 consist of colors produced from the individual concentrations of the gamma radiations and corresponds to slight differences in the relative amounts of the three components. The mafic and ultramafic, as well as magnetite-rich formations (MV) are in Cyan, the granitoids rocks and meta-sediments with strong K has a magenta color with some traces of U. Potassium, uranium and thorium was represented by the red, blue and green respectively. The ternary map shows high spatial relationship with identified geological formation. This high relationship depends on the actuality that the Kumasi metasediment

basins are composed of the high potash content (have high potassium content) formation which appear in the shape of muscovite, biotite, granite and granodiorite, porphyroblastic biotite gneiss, aplite and pegmatite.

The mafic, ultramafic, the probable Paleoproterozoic magnetite-rich formation and some identified granitoids show darker than the neighboring formations, indicating weak contents in potassium, uranium and thorium. The white areas in the composite map are indication of strong content of K, Th and U whereas the yellow indicates areas of strong potassium and thorium but weak uranium contents. The magenta shows areas of strong potassium and uranium but weak thorium contents whereas the yellow indicates areas of strong potassium and thorium but weak uranium contents.

Also the blue-dark blue regions in the ternary map are related with the belt-type granitoids (B2, B3, B4, B5 and the western part of B1). The potassium, thorium and uranium images depict that the granitoids produced low intensities of potassium and thorium (Fig. 5.9 and Fig. 5.10 in that order) but high uranium intensity (Fig. 5. 11). The high uranium anomaly related to the belt granitoids B2, B3, B4 and B5 suggest these granitoids are young than B1 even though these granitoids had similar weak magnetic intensity. Excessive weathering has perhaps used up majority of the uranium content of belt type granitoid, B1 within the middle and eastern regions with only small marks at the western region. These dark/black areas which happen within faulted regions and in some areas at the contact zones of the rock formation can be credited to the weak content of the potassium, thorium and uranium.

It was identified by Hoover and Pierce (1990) that airborne gamma-ray surveying marks of deposits of gold were changeable with potassium being the most dependable guide. Regions with the gold within quartz veins, hydrothermal alteration of causative body can provide noticeable way out. This notice seems valid in the study area, where K is related with most of

the favourable host rocks along the bibiani shear zone. Even though there is no unique radiometric pathway for deposits of gold, research conducted by Hoover and Pierce (1990) depict that transforms in the all three radioisotopes can happen and could be identified in airborne radiometric prospecting.

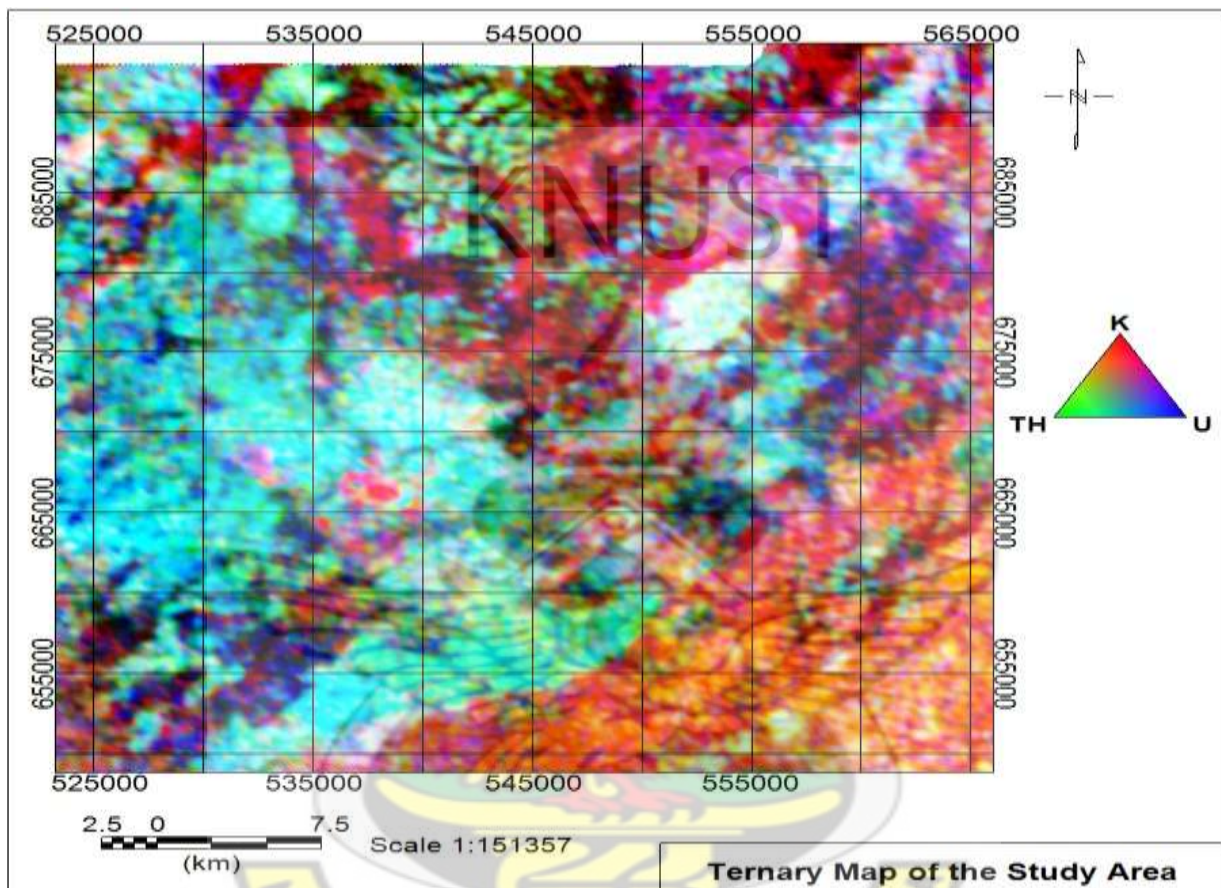


**Figure 5.15:** Composite (Ternary) Image of the Chirano Area.

#### 5.2.4 The Composite Lithological Map from the Radiometric Datasets

Uranium (U), thorium (Th) and Potassium (K) are the three commonest, naturally happening radionuclides in the Earth. K is a main element of a good number of rocks and is a general deformation element in different kinds of reserve of mineral. U and Th occur in smaller concentrations, as mobile and relatively immobile metals, in that order (Dickson and Scott, 1997). As the concentrations of these various radionuclides vary between various types of rock, the data is recorded by using a gamma-ray spectrometer which aids in mapping the

rocks. Low potassium anomalies are coincident within two regions of interest within the study area situated within or along the strongly altered regions in the NE-SW caused by contact between metavolcanics and metasediments and zones of severe faulting caused by the intrusion of the belt type within the metavolcanics. Hydrothermal zones, small fault splays, veins and foliation host the mineralisation of gold within Chirano (Kenworthy et al., 2009). The contact zone SW MV-MS depicted low potassium (Fig. 5.9), high thorium and uranium (Fig. 5.10 and Fig. 5.11 respectively). The weak K anomaly could indicate potassic alteration associated with an increased fluid entry that migrates through the low pressured and highly faulted zones within this region.

The most significant radiometric response in all potassium, uranium and thorium maps (Fig.5.9, Fig 5.10 and Fig. 5.11) recording moderate concentration of K, U and Th respectively is associated with the belt type granitoid (B1) within the region. This high relationship depends on the actuality that the belt intrusives also include more mafic (diorite) phases and some complexes have more felsic phases (close to the true granites) but these are not usually very extensive. The Belt type occurs mainly within the confines of the volcanic belts; they are also generally of an intermediate composition although more mafic and felsic phases are not uncommon. They tend to be more Na-rich and in the literature are often referred to as plagiogranites. Hornblende is usually the dominant mafic mineral and, in many cases, the intrusives lack strong foliation. They occur in quite small plutons to very large batholiths, although not as extensive as the major 'Cape Coast' complexes. They are frequently described as discordant intrusives (Griffis et al., 2002).

The metasediments formation was identified by the significant K signature at the south-east of Fig. 5.9 but possess low magnetic anomaly. The meta-volcanic rocks (MV1) have high magnetic anomalies, but possess high K and U concentrations around the north eastern direction. Again the metavolcanics tends to have low potassium towards the NW and SW.

The contact between the metavolcanic formations and the metasediment formations showed a mobilization of immobile Th concentration also indicated hydrothermally altered zones.

Silva et al. (2003) made some remarks, indicating that radiometric information is an outstanding method which helped in delineating and tracing of various lithologies in areas of outcrop. The mafic, ultramafic and Paleoproterozoic rocks are unique in potassium, ternary map (composite map of K, Th and U) and RBG maps, because of their low radiometric marks (Fig. 5.15). The granites and dacitic rocks have a strong concentration of the three radioelements, occurring as white in the composite map (Fig. 5.15).

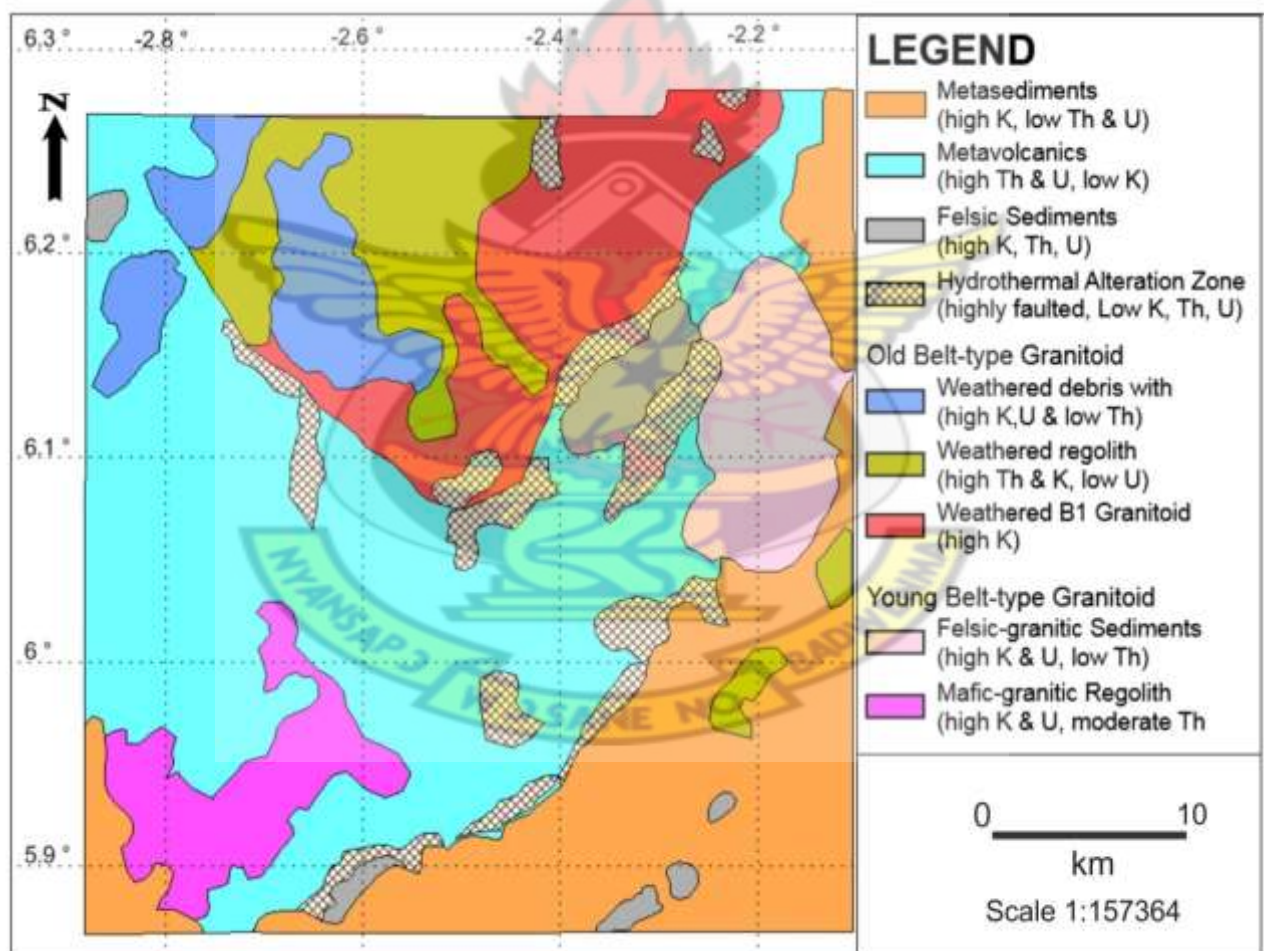


**Figure 5.16:** Proposed geology map from airborne radiometric data.

The gamma-ray spectrometric signatures indicated in the ternary image can be classified as follows: Red (K): regions associated with exposed granitic bedrock. Green (Th): various

ferruginous materials at the surface. Blue (U): calcrete, calcareous sediments and soils. Black to brown: (Low in K, Th and U): dry in situ soil and exposed bedrock. These areas correspond to greenstones and some sand plains. White to yellowish (High K, Th, and U): geomorphic active areas with exposed weathered granite and sediments derived from granite.

### **5.3 Relating Geophysical Datasets to Geology**

Geochemical characteristics related with gold exploration in the study area have resulted in elevated amounts uranium and thorium. Despite that the amounts of these radio nuclides are widespread; the levels have been seen to be dependent on the geological settings of the area. The individual energy levels in soil are associated to the soil types.

#### **5.3.1 Integrated Aeromagnetic and Airborne Radiometric Geological and structural map**

The proposed geological and structural map generated from the magnetic and the radiometric maps of the area were incorporated together to create the new geological map of the Chirano (Fig. 5.17). Regions of severe hydrothermal alterations which are potential gold mineralization zones were delineated as X1 and X2 in figure 5.17. This geological and structural map produced is more detailed than the existing geological map of Chirano showed in figure 2.2. The existing geological map failed to map the belt type granitoids B2, B3, B4 and B5 intrusions. Also the metavolcanics (MV1) were not well mapped in the NW in the existing geological map.

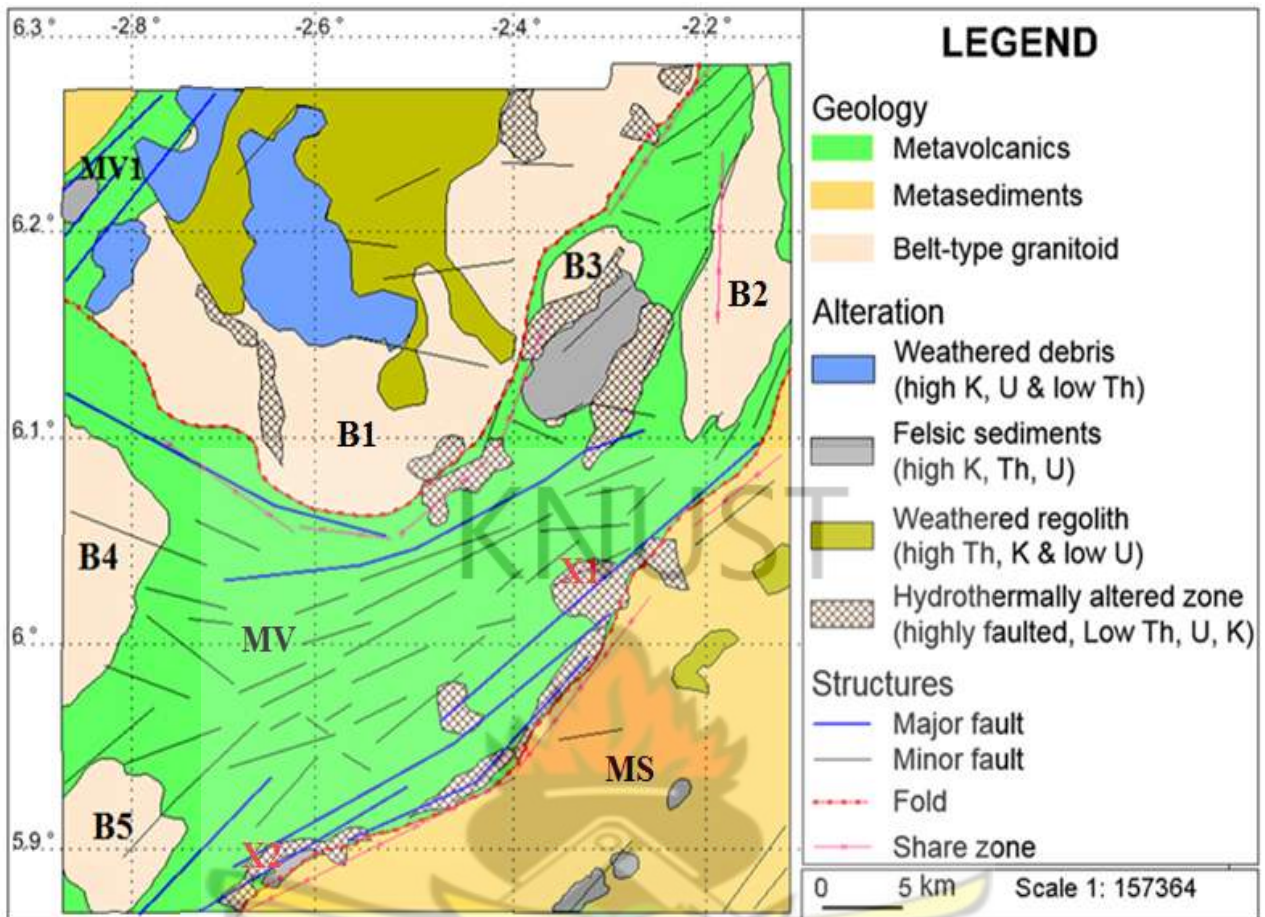


**Figure 5.17:** Proposed geological and structural map from the aeromagnetic and airborne radiometric data of the study area.

The integrated use of the well processed airborne radiometric and magnetic geophysical datasets productively delineated the geology, geological structures and hydrothermal alteration patterns of the study area. The enhanced knowledge on the geology, geological events and rock alterations that have affected the local geological rock units made the prediction of possible locations for economic mineral deposits in the Chirano area easier.

### 5.3.2 Alteration

Amenyoh et al. (2009) indicated rock alteration could be due to structural deformation, or chemical reaction and mineralization of gold in the Birimian is related with an event that promotes rock alteration (Leube et al., 1990; Milesi et al., 1992). The geological and structural map in the figure 5.17 showed the intensely hydrothermally altered regions

particularly along the contact zone between the metavolcanics alternating the metasediments in the study area. Hydrothermal solutions are capable of dissolving and transporting wide range of metals and salts and consequently play important role in ore deposition processes (Boamah, 1993; Manu, 1993). Griffis et al. (2002) recognized that the gold mineralization in the Chirano area is strongly related with quartz stockwork series principally sourced in granitoids.

Alterations from the contact of the metavolcanic and metasediment and some intrusion of the belt type granitoids have changed or destroyed the chemical composition of the good number types of rock within the research area and the effects is evidently seen in both datasets (magnetic and radiometric), but particularly in the radiometric data set.

The decrease in K content and increase in Th (Fig.5.9 and Fig. 5.12 respectively) indicated as MV, MV1 observed for the metavolcanic rock is indicative of hydrothermal alterations. According to Griffis et al. (2002), mafic volcanic rocks generally lack K-bearing minerals and K enrichments are not accompanied by Th during hydrothermal alteration processes.

In the magnetic data such as the TMI and Analytic maps, the contacts between the meta-volcanic rock (MV) and the meta-sedimentary rock (MS) are bounded by shear zones, faults, fractures and low magnetic anomalies (Fig. 5.1 and Fig. 5.3). This is due to the hydrothermal activities that accompanied the rock deformations and metamorphism especially within brittle shear zones (Griffis et al., 2002). The extent of hydrothermal liquids throughout the faults and fractures as indicated are caused by rock alteration which brings about a quiet magnetization zones.

Thus the regions that are hydrothermally altered are possible targets that control gold mineralization in Chirano. Notably these regions loll inside or nearby to major faults like F3-F3 and F4-F4.

### 5.3.3 Possible Zones of Mineralization

Boadi et al. (2013) revealed the three episodes of deformation D1-NE, D2-NNW and D3-NNE which are observed in the Birimian formations considering the tectonics history. The early deformational event D1 produced sets of NE-SW striking local and regional faults and fractures. D2 deformational event produced mainly NNW-SSE and NW-SE faults and fractures some of which intersected the earlier D1 structures.

In looking out for zones with likely mineralization of gold in Chirano, the geological and structural map was well thought-out. The hydrothermal zones which recorded weak magnetite concentration and high concentration of potassium that loll inside or nearby to major faults that include F3-F3 and F4-F4 trending in the NE-SW direction are recognized as good regions for mineralization of gold.

These zones were identified particularly in the Fig 5.16 (Proposed interpreted geology from airborne radiometric data). At the positions labeled X1 and X2 of the geological and structural map (figure 5.17) along the contact zone between the metavolcanics and metasediments, it is observed that the faults F3 and F4 in the strongly altered zone with inflow of the hydrothermal liquids within the metavolcanics. This is an excellent signal of a region that controls the gold mineralization in Chirano.

## CHAPTER SIX

### SUMMARY AND CONCLUSIONS

#### 6.1 Summary

The airborne radiometric and magnetic survey data were helpful in delineating the geologic units, formations that host mineralization and likely hydrothermal alteration zones of the study area. The magnetic map improving filters like the reduction to the pole (RTP), analytic signal, first vertical derivative (1VD) and tilted magnetic (TDR) were applied to the magnetic data helped in the delineation the geological formations (faults, folds, fractures, shear zones) and geological boundaries.

The radiometric data gave the radioelement composition of uranium (U), potassium (K) and thorium (Th) that were used importantly in mapping the lithology of the area such as the belt type granitoid, mafic metavolcanics, basin metasediment formations. To get rid of the lithological variations caused by differences in the water content in soil, non-planar source geometry and errors related with altitude correction ratio maps such as Th/K, U/K and Th/U were generated. U/Th and U/K ratios helped to delineate areas where relative concentrations of uranium are high.

#### 6.2 Conclusions

The aeromagnetic and airborne radiometric datasets were successfully employed to delineate the rock types and geological units of the study area (Chirano). The Birimian metavolcanic, metasediments and the several belt type granitoids which intruded the metavolcanics were clearly mapped. From the NE through the central and the SW parts of Chirano are dominated with metavolcanics. The southeastern parts are mapped to be mainly associated with metasediments with pockets of weathered regolith and felsic sediment. The Northern Chirano

mostly characterized with belt type granitoids with weathered regolith and remains with strong potassium, uranium and weak thorium.

The examination of the geophysical datasets in the study area provides fresh information into structural construction. This reveals enhanced structural features that include shear zone, faults, shear and fault intersections and fracture systems as magnetic anomalies that mainly trend NE-SW.

Also, the datasets were helpful in the identification of hydrothermal zones in the study area. These hydrothermal zones were evidently mapped. The contact between the metavolcanic and the metasediment characterized with severe faults. This information inferred from the aeromagnetic maps show the detailed assessment of the contact zone having very low or 'quiet' magnetic anomaly trending NE-SW direction. This may be attributed to the hydrothermal activity where hydrothermal fluids move to low pressured regions where these faults occur and the generated heat destroys the magnetization within the causative rocks hence low magnetic intensities are related with the delineated faults.

The airborne radiometrics showed a mobilization of the immobile Th concentration and this also indicated hydrothermally altered zones. The rise in potassium content and decrease in Th/K relation observed from radiometric interpretation are very pinpointing of hydrothermal activities within Chirano.

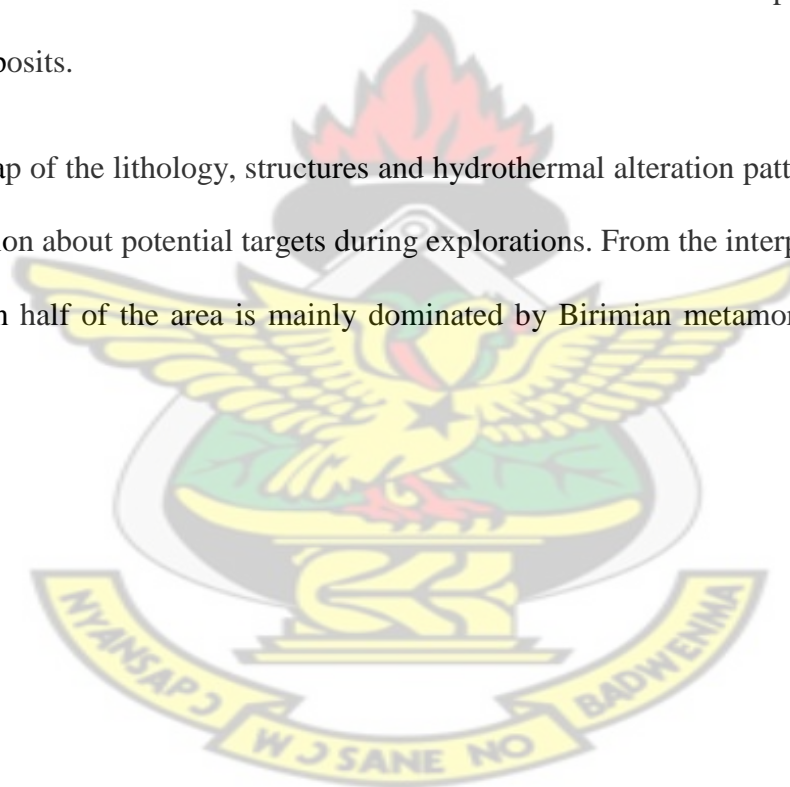
Lastly, known mineral deposits were identified. The mineralization of gold is strongly characterized with quartz stockwork rocks sourced predominately in granitoids. The gold can be found within the veins and in the adjacent, highly deformed host rock; the high-grade regions are more often than not accompanied by about up to 5% of pyrite. The deformation seems to comprise principally of silica, albite, sericite and iron-rich carbonate, along with fine-grained hematite and magnetite. The gold happens in very fine grains, strongly

characterized with pyrite and seems to have been introduced along with carbonate and sulphur, which post-date the previous deformation (silica, sericite, iron oxides) (Griffis et al., 2002).

Primary and secondary structures, which are critically important in controlling gold mineralization throughout the extensive metasedimentary and metavolcanic units, were observed directly in magnetic and radiometric pattern.

The delineated geological structure, rocks and further hydrothermally deformed zones from the geophysical datasets which have shown the Chirano district is potential host of commercial deposits.

A collective map of the lithology, structures and hydrothermal alteration pattern has provided better information about potential targets during explorations. From the interpreted geological map, more than half of the area is mainly dominated by Birimian metamorphosed belt and basin.



## CHAPTER SEVEN

### OUTLOOK AND RECOMMENDATIONS

The chirano area host complex geological structures which are mainly folded and faulted as the contact between the metasediment and metavolcanic and the intrusion of the belt type granitoid. High structural connectivity regions and areas of concentrated alterations reproduced as low magnetic anomaly and high K concentration should be considered in further exploration particularly, where the two alteration types concur and also marked by faults, fault intersections, fractures and shear zones

The hydrothermal alteration zone that marked the contact between the belt metavolcanic and the metasediment can also be regarded as probable target. The analysis of airborne data is a tremendous way of mapping lithology, structure and, to some extent, the alteration zones. On the other hand, structural features and alteration informations could only be seen more into by field trip to perform a ground survey.

Additional studies to improve this interpretation are hence required and recommended. These may include field survey of geology and geological structures, radiometric and magnetic anomalies, soil geochemical sampling and alteration mapping as well as the application of any cost effective exploration technique to delineate mineralization.

The Birimian metasediments and metavolcanics in the chirano area host major NE-SW and few NNW geological structures which are extension of the regional gold bearing structures in the Sefwi belt. These NE-SW and NNW regional geological structures display evidence of extension beyond this project area. This means that the structures have not ended suddenly at the borders of the research area. Kesse in 1985 revealed that the majority of mineralization occurrences are hosted in Birimian metasediments and metavolcanic. For this reason, more

geophysical works should be carried out in order to confirm if the continuations of these geological structures may have prospective targets of gold mineralization.

Many of the parts in the study area with concentrated shearing especially along the contact of the metasediment and metavolcanic which hosts the inflow of epithermal deposits are often associated with elevated K. These parts are especially appropriate for more geophysical surveys such ground electromagnetic; induced polarization and drilling in order to confirm the presence of gold or mineralization of any metal ore.

Geochemical prospecting would be needed to distinguish the host rock within the extremely deformed and altered regions within the study area.



## REFERENCES

- Afloe A. B. 2014. Geochemistry and Alteration Mapping Of The Paboase Deposit At Chirano Gold Mines, Ghana. University of Ghana. <http://ugspace.ug.edu.gh>
- Airo M. L. (2007). Application of Aerogeophysical Data for gold exploration: Implications for the central Lapland greenstone belt.
- Airo, M. L. and Karell, F. (2001). Interpretation of airborne magnetic and gamma-ray spectrometric data related to Mammaslhti Cu-Zn-Au deposit in eastern Finland. Special Paper 31, pp. 97–103
- Allen, D. G. (2011). The Fahiakoba gold project Ghana, West Africa. Technical report, Asante Gold Corporation.
- Allibone, A., Teasdale, J., Cameron, G., Etheridge, M., Uttley, P., Soboh, A., Appiah-Kubi, J., Adanu, A., Arthur, R., Mamphey, J. (2002). Timing and structural controls on gold mineralization at the bogoso gold mine, ghana, west africa. *Economic Geology*, 97(5):pp. 949–969.
- Allis, R.G. 1990. Geophysical anomalies over epithermal systems. *Journal of Geochemical Exploration* pp. 36:339-374.
- Amenyoh, T., Wemegah, D. D., Menyeh, A., and Danuor, S. K. (2009). The use of landsat and aeromagnetic data in the interpretation of geological structures in the Nangodi Belt, University of Cape Coast.
- Anderson H. and Nash C. 1997. Integrated lithostructural mapping of the Rössing area, Namibia using high resolution aeromagnetic, radiometric, Landsat data and aerial photographs
- Ansari, A. H. and Alamdar, K. (2009). Reduction to the pole of magnetic anomalies using analytic signal. *World Applied Sciences Journal*, 7(4):pp. 405–409.

- Appel P.W. U., Christian M. Glahder, Saidi Mnali, Sospeter Muhongo, Faustin Petro, Thorkild M. Rasmussen, Henrik Stendal, E. Brian Temu, Leif Thorning & Tapani Tukiainen, (2000). An integrated approach to mineral exploration and environmental assessment in southern and eastern Africa - a pilot study in Tanzania
- Appiah, H. (1991). Geology and mine exploration trends of Prestea Goldfields, Ghana. *Journal of African Earth Sciences (and the Middle East)*, 13(2): pp. 235–241.
- Aryee N.A.B, 2000. Ghana's mining sector: its contribution to the national economy. Minerals Commission, Accra, Ghana
- Beard, L. P. and Goitom, B. (2000). Some problems in interpreting low latitude magnetic surveys. 6th EAGE/EEGS Meeting.
- Bhattacharya D., Joshi G.B and Sharma Rakesh 2011. Uranium Mineralisation Associated with Felsic Volcanism at Mohar, Shivpuri District, Madhya Pradesh. *Journal Geological Society of India*, 78, pp 55-62
- Boadi, B., Wemegah, D. D., and Preko, K. (2013). Geological and Structural Interpretation of the Konongo Area of the Ashanti Gold Belt of Ghana from Aeromagnetic and Radiometric data. *International Research Journal of Geology and Mining (IRJGM)* (2276-6618), 3(3), pp. 124-135.
- Boamah, D. (1993). Application of soil geochemistry to gold exploration in the Birimian rocks of Ghana. pp 1–6. Case study from Demoni/Dankyira area (Unpublished).
- Charbonneau, B. (1991). Geochemical evolution and radioactive mineralogy of the Fort Smith radioactive belt, Northwest Territories, Canada. In *Primary Radioactive Minerals (The textural patterns of radioactive mineral paragenetic associations)*, pp. 21–48. Theophrastus Publications.
- Chopin, G. R. (1988). Humics and radionuclide migration. *Radiochimica Acta*, 44/45: pp. 23–28.

- Clark, D. A. (1997). Magnetic properties of rocks and minerals. *AGSO Journal of Australian Geology and Geophysics*, 17(2).
- Clark, D. A. and Emerson, D. W. (1991). Notes on rock magnetic characteristics in applied Geophysical studies. *Exploration Geophysics*, pp. 22:547–555.
- Cooley, J. W. and Tukey, J. W. (1965). An algorithm for the machine calculation of complex Fourier series. *Math. Comput.*, 19(90): pp 297–301.
- Cozens, B. (1989). The geology and structure of the Konongo gold mine, Ghana, and its implications in exploration. In Le Maitre R. W. (ed.) *Pathways in geology- essays in honour of Edwin Sharbon Hills*, pp. 439–456. Blackwell, Melbourne.
- Cudjoe J. E. 1961. A Programme for Geophysical Exploration in Ghana.
- Dalan, R.A. 2006. A geophysical approach to buried site detection using down-hole susceptibility and soil magnetic techniques. *Archaeological Prospection* 13, pp. 182–206
- Darnley, A. G. (1996). Uranium exploration data and global geochemical baselines: The need for coordinated action. In *Uranium Exploration Data and Techniques Applied to the Preparation of Radioelement Maps*. IAEA-TECDOC-980.
- Darnley, A. G., and Ford, K. L., 1989, Regional airborne gamma-ray survey: A review; in “Proceedings of Exploration 87: Third Decennial International Conference on Geophysical and Geochemical Exploration for Minerals and Ground Water”, Geological. Survey. of Canada, Special, pp. 960 .
- Dearing J.A, 1994. Environmental magnetic susceptibility, using the Bartington MS2 system.
- Dickson, B. L. and Scott, K. M. (1997). Interpretation of aerial gamma ray surveys-adding the geochemical factors. *AGSO Journal of Australian Geology and Geophysics*, 17(2): pp.187–200.

- Dzigbodi-Adjimah, K and Bansah, S (1995) Current Developments in Placer Gold Exploration in Ghana: Time and Financial Considerations. *Exploration and Mining Geology* 4(3): pp. 297–306.
- Eisenlohr, B. N. and Hirdes, W. (1992). The structural development of early Proterozoic Birimian and Tarkwaian rocks in southwest Ghana, West Africa. *Journal of African Earth Science*, 14(3):pp. 313–325.
- Elawadi E, Ammar A, and Elsirafy A 2004, Mapping surface geology using airborne gamma-ray spectrometric survey data - A case study. *Proceedings of SEGJ international symposium*. Nuclear Materials Authority of Egypt, Airborne Exploration Dept.
- Etheridge, M., Rutland, R., and Wyborn, L. (1987). Orogenesis and tectonic process in the early to middle proterozoic of northern australia. *Proterozoic lithospheric evolution*, 17: pp. 131–147.
- Evans, M. E. (1993). An archaeointensity investigation of a Kiln at Pompeii. *Journal of Geomagnetism and Geoelectricity*., 43: pp. 357–361.
- Fertl, W. H. (1983). Gamma-ray spectral logging: a new evaluation frontier. *World Oil*, pp. 79–91.
- Geosoft Inc., 1996: OASIS montaj Version 4.0 User Guide, Geosoft Incorporated, Toronto.
- Geosoft Inc., 1995: OASIS Airborne Radiometric Processing System Version 1.0 User's Guide, Geosoft Incorporated, Toronto.
- Graeme D. 2014, Chemical contrast and high grade gold mineralization, Chirano Mine, Ghana Kinross Gold Corporation, Reno, USA
- Grant, F. S. (1985). Aeromagnetic, geology of an ore environment, Magnetite in igneous, sedimentary and metamorphic rocks. *An overvie of Geoexploration*. 23: pp. 303–33.
- Grant, F.S. and Martin, L., 1966, *Interpretation theory in applied Geophysics*, McGraw-Hill Book Co., New York.

- Gregory, A. F. and Horwood, J. L. (1961). A laboratory study of gamma-ray spectra at the surface of rocks. Department of Energy, Mines and Resources, Ottawa. Mines Branch Research Report R85.
- Griffis, R. J. (1998). Explanatory Notes - Geological interpretation of geophysical data from Southwestern Ghana. Minerals Commission, Accra, pp. 51.
- Griffis, R. J., Barning, K., Agezo, F. L., and Akosah, F. K. (2002). Gold deposits of Ghana. Minerals Commission Report, pp. 7–12, 19–37, 163–169.
- Gunn, P. J., Minty, B. R. S., and Milligan, P. (1997). The airborne gamma-ray spectrometric response over arid Australian terranes. *Exploration*, 97: pp. 733–740.
- Hall, J. M. and Fisher, B. E. (1987). The Characteristics and significance of secondary magnetite in a profile through the dike component of the Troodos, Cyprus, ophiolite. *Canadian Journal of Earth Science*, Vol. 24: pp. 2141–2159.
- Hammond, N.Q and Tabata, H, 1997. Characteristics of ore minerals associated with gold at the Prestea mine, Ghana. pp. 3
- Harris M.C, Cassidy J, Locke C.A., Mauk J.L., Stevens M. and Vidanovich P. 2003 Geophysical characteristics of the Karangahake epithermal deposit, Hauraki Goldfield, New Zealand in impact structures: a review. *Impact tectonics*, Geology Department, University of Auckland, Private Bag 92019 Symonds Street, Auckland, New Zealand, email mc.harris@auckland.ac.nz pp. 479–552
- Harrison R. J., Dunin-Borkowski R. E., Kasama T., Simpson E. T., and Feinberg J. M (2007). Properties of rocks and minerals. Magnetic properties of rocks and mineral. University of Cambridge, Cambridge, UK

- Hirdes, W. and Nunoo, B. (1994). The Proterozoic paleoplacers at the Tarkwa gold mine, SW - Ghana - sedimentology, mineralogy, and precise age dating of the main reef and west reef, and bearing of the investigations on source area aspects. In Oberthür, T. (ed.), *Metallogenesis of Selected Gold Deposits in Africa*, pp. 247–298. *Geologische Jahrbuch, Reihe D, Heft 100*, Hannover.
- Hirdes, W., and Leube, A. 1989. On gold mineralisation of the Proterozoic Birimian Supergroup in Ghana/West Africa. Ghanaian-German Mineral Prospecting Project, Technical Cooperation Project No. 80, 2046.6, pp. 179.
- Hoover, D. B. and Pierce, H. A. (1990). Annotated bibliography of gamma-ray methods applied to gold exploration. U.S. Geological Survey Open-file Report pp. 90-203.
- [Http://www.ghanadistricts.com/districts/?news&r=5&\\_=135](http://www.ghanadistricts.com/districts/?news&r=5&_=135) (25/05/2014)
- IAEA (International Atomic Energy Agency) 1990, *The use of gamma rays data to define the natural radiation Environment*, Vienna.
- IAEA (International Atomic Energy Agency) 2003 *Guidelines for radioelement mapping using gamma ray spectrometry data*, Vienna.
- ICRU (1994). *Gamma ray Spectrometry in the Environment*, ICRU Report 53. International Commission On Radiation Units And Measurements, Bethesda, USA.
- Inglis D.R. (1955) *Theories of the Earth's Magnetism Rev. Mod. Physics*. 27, pp. 212–248
- Junner, N. R. (1940). *Geology of the Gold Coast and Western Togoland*. Geological Survey Bulletin No.1
- Kearey P, Brooks M, Hill I (2002), *An introduction to geophysical Exploration* third Edition. TJ international. pp. 2-160
- Keating, P. B. (1995). A simple technique to identify magnetic anomalies due to kimberlite pipes. *Exploration and Mining Geology*, 4(2): pp. 121–125.

- Kenworthy S, Noormohamed K, Stuart H, Hodkiewicz P 2009. Mapping and 3D modelling of structural controls in the Chirano gold deposits, Ghana: keys to better resource delineation and near-mine exploration targeting.
- Kesse, G. O. (1985). The Mineral and Rock Resources of Ghana. A.A. Balkema, Rotterdam.
- Kitson, A.E. 1928. Provisional Geological map of the Gold Coast and Western Togoland, with brief descriptive notes thereon. Gold Coast Geological Survey. Bull.No. 2.
- Koimtsidis A., (2003) Managing Director, Cardinal Resources Limited. Airborne geophysical survey commences +233 (0)26 190 52 20 Skype: Cardinal Archie.
- Kono M. and Schubert G. 2007 Geomagnetism (Treatise on Geophysics) Volume 5.
- Krishnaswami, S. (1999). Thorium encyclopedia of geochemistry, KluwerAcademic Publishers, London pp. 712.
- Langenheim V.E, Duval J.S., Laurie Wirt and Ed Dewitt, 2000. Preliminary Report on Geophysics of the Verde River headwaters region Arizona. Open-File Report 00-403.
- Langmuir, D. and Hermans, J. S. (1980). The mobility of thorium in natural waters at low temperatures. *Geochimica et Cosmochimica Acta*, 44: pp. 1753–1766.
- Leube, A., Hirdes, W., Mauer, R., and Kesse, G. (1990). The early proterozoic birimian supergroup of ghana and some aspects of its associated gold mineralization. *Precambrian Research*, 46: pp.139–165.
- Li, X. (2008). Magnetic reduction-to-the-pole at low latitudes. The Meter Reader, pages Fugro Gravity and Magnetic Services, Houston, USA pp. 990–1002.
- Liu S. and Mackey T. (1998). Using images in a geological interpretation of magnetic data. AGSO Research Newsletter 28
- Lunt, D J, Kirby, E and Ritchie, I C (1995). Design of Gold Projects in Ghana. African Mining '95, Institution of Mining and Metallurgy, London.

- Manu, J. (1993). Gold deposits of Birimian greenstone belts in Ghana: Hydrothermal alteration and thermodynamics. Verlag Mainz, Wissenschaftsverlag, Aachen  
Herstellung: Fotodruck Mainz GmbH Susterfeldstr. 83. 52072 Aachen.
- Mendonça, C. A. and Silva, J. B. C. (1993). A stable truncated series approximation of the reduction-to-the-pole operator. *Geophysics*. 58(No. 8).
- Milesi, J. P., Ledru, P., Feybesse, J. L., Dommangeat, A., and Marcoux, E. (1992). Early proterozoic ore deposits and tectonics of the Birimian orogenic belt, West Africa. *Prec.Res.*, 58: pp. 305–344.
- Milligan, P. R. and Gunn, P. J. (1997). Enhancement and presentation of airborne geophysical data. *AGSO Journal of Australian Geology and Geophysics*, 17(2): pp. 64–774.
- Milsom J, 2003. *Field Geophysics, the geological field guide series*. Third edition. John Wiley & Sons Ltd, The Atrium, Southern Gate, Chichester, pp. 71
- Minty, B. R. S. (1996). The fundamentals of airborne gamma-ray spectrometry. *AGSO Journal of Australian Geology and Geophysics*, 17(2): pp. 39–50.
- Mumin, A. H., Fleet, M. E., and Longstaffe, F. J. (1996). Evolution of hydrothermal fluids in the Ashanti gold belt, Ghana; stable isotope geochemistry of carbonates, graphite, and quartz. *Economic Geology*, 91(1): pp. 135–148.
- Murphy, B. S. R. (2007). Airborne geophysics and the Indian scenario. *J. Ind. Geophysics Union*, 11(1): pp. 1–28.
- Murthy B.S.R 2007, *Airborne Geophysics and the Indian Scenario*
- Nabighian, M. N. (1972). The analytical signal of two-dimensional magnetic bodies with polygonal cross-section: its properties and use for automated anomaly interpretation. *Geophysics*, 37(3): pp. 507–517.
- Nagata, T. (1961). *Rock Magnetism*. Tokyo: Maruzen, 2nd edition.

- Nicolet J.-P. and Erdi-Krausz G. (2003), Guidelines for radioelement mapping using gamma ray spectrometry data
- Ostrovskiy, E. A. (1975). Antagonism of radioactive elements in wellrock alteration fields and its use in aerogamma spectrometric prospecting. *International Geological Review*, 17: pp. 461–8.
- Petersen, N. (1990). Curie temperature. In James, D. E. (ed.), *The Encyclopedia of solid Earth Geophysics*, pp. 166–173. New York: Van Nostrand Reinhold
- Phillips, D. J. (1997). Potential-field geophysical software for the PC, version 2.2.U.S.G.S. Open-File Report 97-725, pp. 34.
- Plumlee, G. S., Smith, K. S., Ficklin, W. H., and Briggs, P. H. (1992). Geological and geochemical controls on the composition of mine drainages and natural drainages in mineralized areas. *Proceedings, 7th International Water-Rock Interaction Conference*. Park City, Utah, July, 1992. pp. 419–422
- Plummer, C. C., McGeary, D., and Carlson, D. H. (2001). *Physical Geology*. New York: McGraw Hill, 8th edition.
- Pohl D.1998 A decade of change mineral exploration in West Africa. *The Journal of the South African Institute of Mining and Metallurgy*.
- Quijano L, Gaspar L, López-Vicente M, Chaparro M A.E., Machín J, Navas A 2011. Soil magnetic susceptibility and Surface topographic characteristics in cultivated Soils pp 1-6.
- Rajagopalan, S. (2003). *Exploration Geophysics*, 34(No. 4): pp. 257–262.
- Reeve W. D. (2010) *Geomagnetism Tutorial*. Reeve Observatory Anchorage, Alaska-USA
- Reeves, C. V. (1989). Aeromagnetic interpretation and rock magnetism. *First Break*, 7: pp. 275–286.
- Reimold W., Koeberl C., Gibson, R., and Dressler, B. 2005. *Economic mineral deposits*

- Remke L. van Dam, Jan M.H. Hendrickx, Bruce Harrison, Brian Borchers, David I. Norman, Samuel Ndur, Chris Jasper, Patrick Niemeyer, Robert Narthey, David Vega, Lucas Calvo and Janet E. Simms (2004). Spatial variability of magnetic soil properties. The International Society for Optical Engineering. 2004;5415(PART 1): pp.665-675.
- Reynolds J. M. (1997) An introduction to Applied and Environmental Geophysics, John Wiley & Ltd. Bann Lane, Chichester. pp. 124-132
- Rivas J. (2009). Gravity and Magnetic Methods. jarivas@lageo.com.sv
- Roest, W. R. and Pilkington, M. (1993). Identifying remanent magnetization effects in magnetic data. *Geophysics*, 58: pp. 653–659.
- Shanks Pat W, C (2010). Hydrothermal Alteration. Volcanogenic massive sulfide occurrence Model (Scientific Investigation Report)
- Shives, R., Charbonneau, B., and Ford, K. (2000). The detection of potassic alteration by gamma-ray spectrometry-recognition of alteration related to mineralization. *Geophysics-Wisconsin The Tulsa-Society Of Exploration Geophysicists*, 65(6): pp. 2001–2011.
- Sillitoe, R. H. (1979). Some thoughts on gold-rich porphyry copper deposits. *Mineralium deposita*. 14: pp. 161–1744.
- Silva, A. M., Pires, A. C. B., McCafferty, A., Moraes, R. A. V., and Xia, H. (2003). Application of airborne geophysical data to mineral exploration in the uneven exposed terrains of the Rio Das Velhas greenstone belt. *Revista Brasileira de Geociências*, 33(2):17–28.
- Smith S. M. and Amanor J 2010. Mineral Resource Estimation Bibiani Gold Mine Western Region Ghana.
- Studemeister, P. A. (1983). The redox state of iron: a powerful indicator of hydrothermal alteration. *Geoscience Canada*, 10: pp. 189–194.

- Tay, C. and Momade, F. (2009). Trace metal contamination in water from abandoned mining and non-mining areas in the northern parts of the Ashanti gold belt, Ghana. *West African Journal of Applied Ecology*, 10(1).
- Telford, W. M., Geldart, L. P., and Sheriff, R. E. (1990). *Applied Geophysics*. Cambridge University Press, second edition.
- Urquhart W.E.S 2003, GeoExplo Ltd, Santiago Chile.
- Van Straaten P. 2002. Rocks for crops: Agrominerals of Sub-Saharan Africa. ICRAF, Nairobi, Kenya, pp. 338.
- Wedepohl, K.K (Exec. Ed) 1978, *Handbook of Geochemistry*, Volume 2, Part 5, Berlin, Heidelberg, New York
- Wemegah, D. D., Menyeh, A., and Danuor, S. K. (2009). Magnetic Susceptibility Characterization of mineralized and non mineralized rocks of the Subenso Concession of Newmont Ghana Gold Limited. In *Ghana Science Association Biennial Conference*, UCC.
- Whitham, K. (1960). Measurement of the geomagnetic elements. In *Methods and techniques in Geophysics 1*, S. K. Runcorn. pp. 134–48.
- Wilford, J. R., Bierwirth, P. N., and Craig, M. A. (1997). Application of Airborne Gamma-ray Spectrometry in Soil/Regolith Mapping and Applied Geomorphology. *AGSO Journal of Australian Geology and Geophysics*, 17(2):201-216.
- Wright, J. B. (1985). *Geology and Mineral Deposits of West Africa*. Allen and Unwin, London, pp. 189.

## APPENDICES

### APPENDIX A

#### Aeromagnetic and Radiometric Images of Chirano Area

##### A.1 TDR and 1VD Images

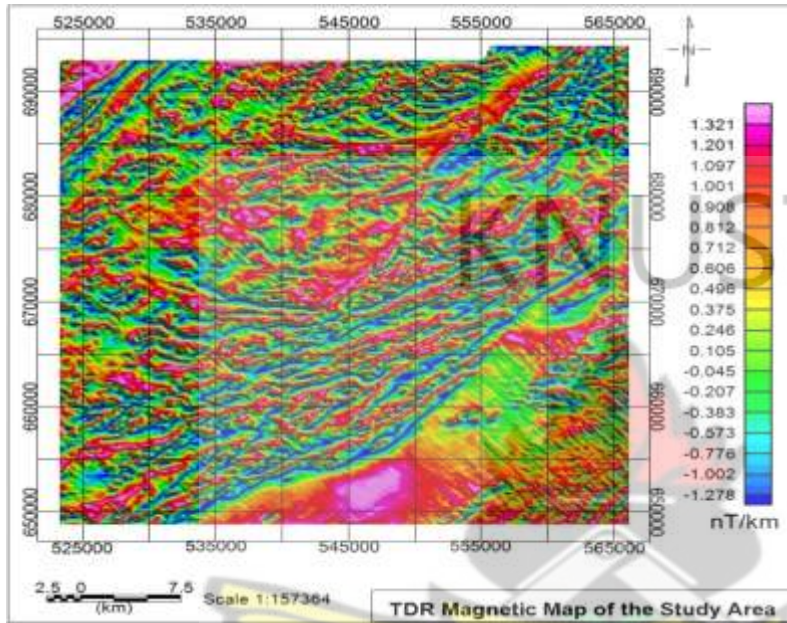


**Figure A.1:** A magnetic TDR map

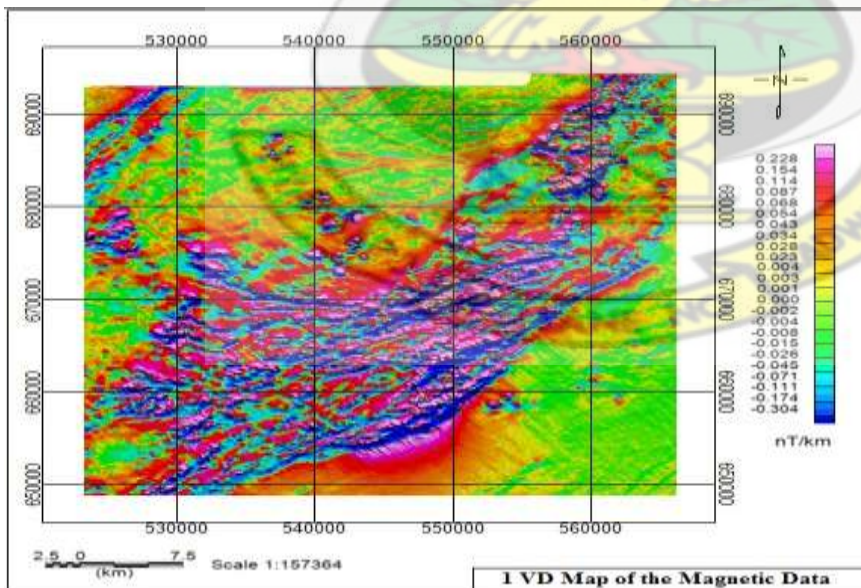


**Figure A.2:** First order vertical derivative map and upward continued to 100 m showing magnetic structures

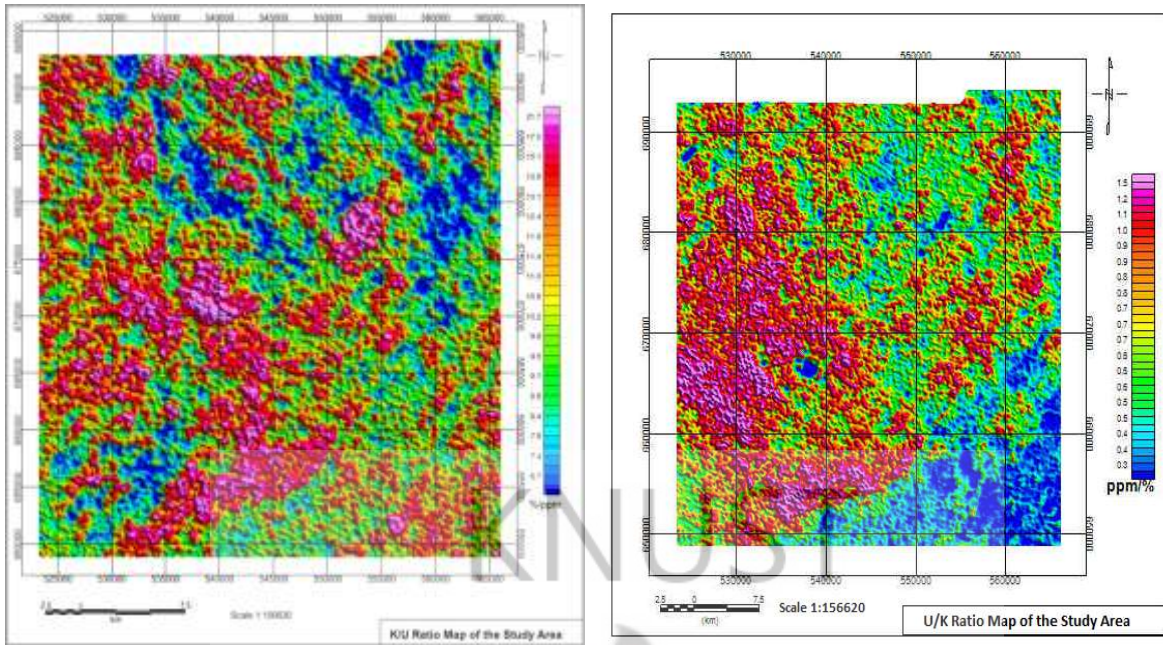


**Figure A.3:** Gamma spectrometric images of the Chirano project area. A) K/U; B) U/K

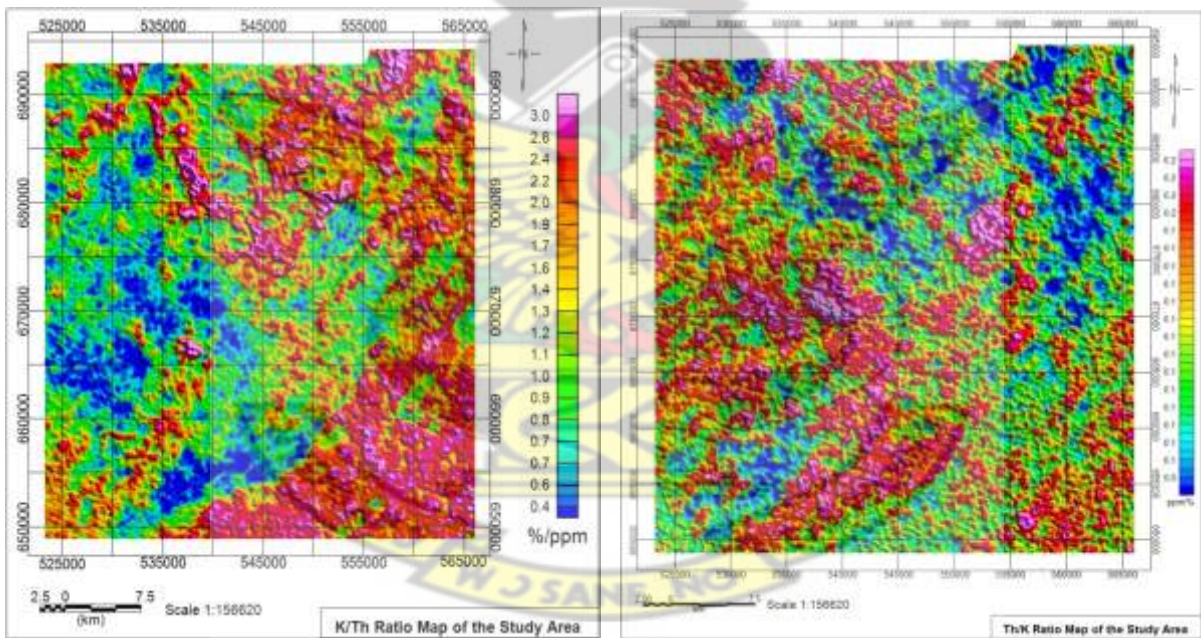


**Figure A.4:** Gamma spectrometric images of the Chirano project area. A) K/Th; B) Th/K

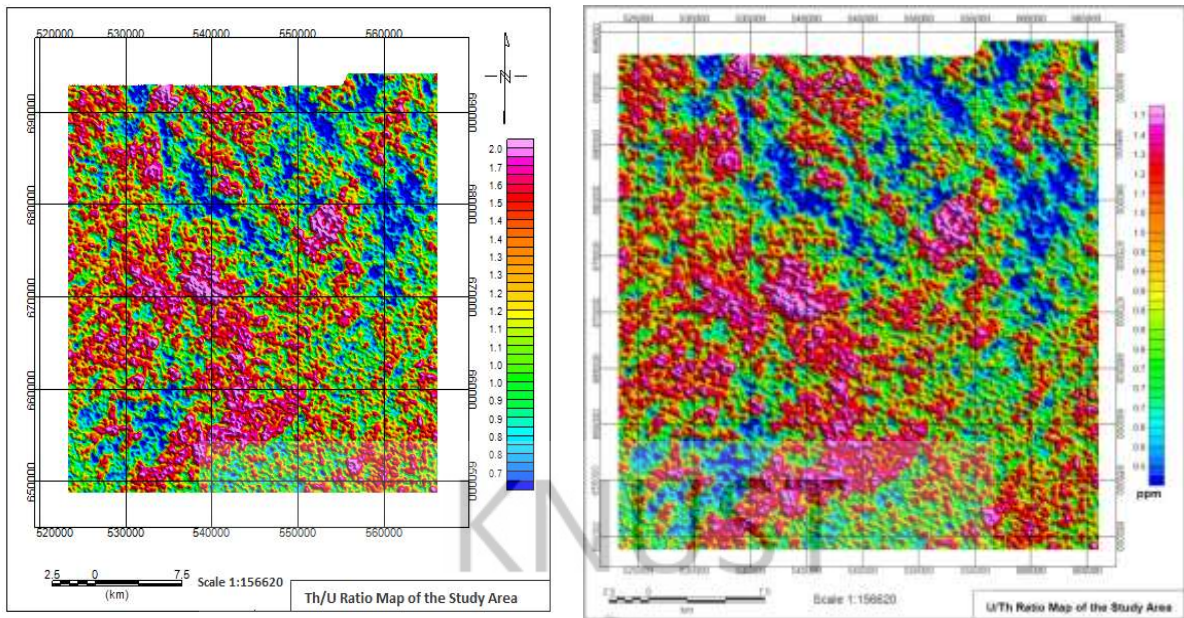
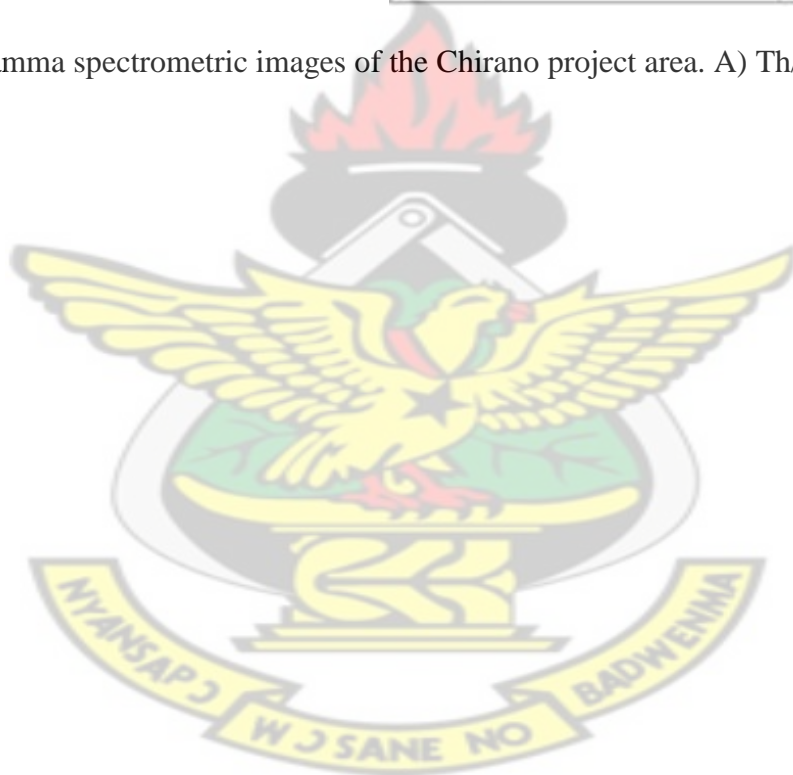


**Figure A.5:** Gamma spectrometric images of the Chirano project area. A) Th/U; B) U/Th



## APPENDIX B

### B.1 Used Softwares

- Microsoft Word (2007): typesetting and layout
- Coral Draw X5: graphics
- Oasis Montaj (Geosoft): data processing and enhancing
- MapInfo 10.5-Discover 11.1: data processing and enhancing

KNUST

